As of 10 June 2016

This GOES-R Level 2+ space weather Algorithm Theoretical Basis Document (ATBD) is preliminary and subject to change as the GOES-R Program prepares for a launch in late 2016.

The NOAA National Centers for Environmental Information (NCEI) is currently developing a demonstration version of the Satellite Product Analysis and Distribution Enterprise System (SPADES) which will host the L2+ algorithms. The operational SPADES will be instantiated by the National Weather Service in FY2017 to serve the needs of the Space Weather Prediction Center (SWPC).

Updated versions of the L2+ ATBDs will periodically be made available and posted to the SPADES website.

Bill Denig
NCEI

http://www.ngdc.noaa.gov/stp/space-weather/online-publications/stp_sii/spades/

NOAA NESDIS CENTER for SATELLITE APPLICATIONS and RESEARCH

GOES-R EXIS EUVS.04
EVENT DETECTION AND CHARACTERIZATION
ALGORITHM THEORETICAL BASIS DOCUMENT
Version 1.2

Hardcopy Uncontrolled

TITLE: EUV EVENT DETECTION AND CHARACTERIZATION ALGORITHM THEORETICAL BASIS DOCUMENT
VERSION 1.2

AUTHORS:
Dr. Steven W. Mueller
Dr. Donald L. Woodraska
S. Dave Bouwer
Dr. W. Kent Tobiska
Dr. Tom N. Woods
Dr. Frank G. Eparvier

APPROVAL SIGNATURES:
_____<Actual Signature Date>
<Name of Technical Approver> Date
Technical Approver
_____<Actual Signature Date>
<Name of Agency Approver> Date
Agency

EUVS.04 ATBD Document Version History

Version	Description	Revised Sections	Date
1.0	Created by Steven Mueller, LASP, from template provided by Don Woodraska	New document	June 8, 2011
1.1	Steven Mueller	New figures and updated text	June 15, 2011
1.2	Steven Mueller	Final version	September 26, 2011

LIST OF FIGURES 7
LIST OF TABLES 8
LIST OF ACRONYMS 9
ABSTRACT 10
1 DOCUMENT SUMMARY 11
1.1 Purpose 11
1.2 Intended Users 11
1.3 Section Outline 11
1.4 Related Documents 13
1.5 Revision History 14
2 ALGORITHM OVERVIEW AND BACKGROUND 15
2.1 Introduction 15
2.2 Observing System Instrument Characteristics 17
2.3 Operational and Scientific Objectives 18
2.3.1 EUV Event Definition and Spectral Line Selection ..... 19~~20~~
2.4 Software Overview ..... 22~~23~~
2.4.1 Development Language ..... 24~~25~~
2.4.2 Application Components ..... 24~~25~~
3 ALGORITHM DESCRIPTION ..... 27~~28~~
3.1 Historical Perspective ..... 27~~28~~
3.1.1 Critical Differences Between XRS Flares and EUV Events ..... 27~~28~~
3.2 EUV Event Terminology ..... 29~~30~~
3.2.1 Algorithm and Event Status Indicators ..... 32~~33~~
An additional optional flag is WATCH, which indicates that a false alarm suppression has occurred. It will appear only if a specific configuration file flag is set. The purpose is to alert the operator that irradiance is increasing at a significant rate, but the algorithm is suppressing an alert until the false alarm threshold has been exceeded. ..... 32~~33~~
3.3 Operational Specifications and Requirements ..... 32~~33~~
3.4 Processing ..... 33~~34~~
3.5 Event Detection and Characterization Logic ..... 38~~39~~
3.5.1 Data Metrics ..... 39~~40~~
3.5.1.1 Simple Difference ..... 41~~42~~
3.5.1.2 Mean Irradiance ..... 41~~42~~
3.5.1.3 Time-Irradiance Slope ..... 41~~42~~
3.5.1.4 Standard Deviation ..... 43~~44~~
3.5.1.5 Monotonic Rank ..... 44~~45~~
3.5.1.6 Monotonic Rank of the Mean ..... 46~~47~~
3.5.1.7 Maximum Relative Increase ..... 47~~48~~
3.5.1.8 Nth Percentile Difference ..... 48~~49~~

3.5.2 Missing/Invalid Input Data ..... 49~~50~~
3.5.3 Event Initiation Logic ..... 50~~51~~
3.5.3.1 Start Time and Pre-event Irradiance ..... 50~~51~~
3.5.3.2 False Alarm Suppression ..... 52~~53~~
3.5.3.3 28.4 nm Spectral Line Event Initiation 55
3.5.3.4 30.4 nm Spectral Line Event Initiation ..... 56~~57~~
3.5.3.5 121.6 nm Spectral Line Event Initiation ..... 57~~58~~
3.5.4 Event Rise and Event Decline Designation Logic ..... 58~~59~~
3.5.5 Event Peak Detection Logic ..... 59~~60~~
3.5.5.1 28.4 nm Event Peak Detection ..... 59~~60~~
3.5.5.2 30.4 nm Event Peak Detection ..... 60~~61~~
3.5.5.3 121.6 nm Event Peak Detection 61
3.5.6 Event Half-Maximum Designation Logic ..... 61~~62~~
3.5.7 Event Termination Logic ..... 61~~62~~
3.5.7.1 28.4 nm Spectral Line Event Termination ..... 62~~63~~
3.5.7.2 30.4 nm Spectral Line Event Termination ..... 63~~64~~
3.5.7.3 121.6 nm Spectral Line Event Termination ..... 65~~66~~
3.6 Input Data ..... 66~~67~~
3.6.1 Data Acquisition ..... 67~~68~~
3.6.2 Data Format ..... 67~~68~~
3.6.3 Validity Indicators ..... 67~~68~~
3.6.4 Data Input Example 68
3.7 Output ..... 68~~69~~
3.7.1 Output Files ..... 68~~69~~
3.7.2 Output Data Content ..... 69~~70~~
3.7.3 Output Data Format ..... 71~~72~~
3.8 Theoretical Considerations 76
4 TESTING ..... 77~~76~~
4.1 Proxy Input Data ..... 77~~76~~
4.2 Software Testing 81
4.2.1 Unit/Regression Testing 82
4.2.2 Integration Testing 82
4.2.3 Performance Testing 82
4.2.4 Memory Testing 83
5 ADDITIONAL CONSIDERATIONS 84
5.1 Risk 84
5.2 Skill Tradeoffs 84
5.3 Configuration Files 87
5.3.1 Main Configuration Parameters 87
5.3.2 Event Detection and Characterization Configuration Parameters 88

5.4 Log Files 88
5.5 Error Checking and Handling 88
6 ASSUMPTIONS AND LIMITATIONS 90
6.1 Assumptions 90
6.2 Limitations 90
7 PRELIMINARY RESULTS 91
7.1 Explanation of Symbols 91
7.2 Simple Events 91
7.3 Complex Events 94
7.4 Algorithm Deficiencies 97
8 ALGORITHM VALIDATION 101
8.1 Data Considerations 101
8.2 Contingency Tables 102
8.3 Skill Scores 102
8.3.1 Probability of Detection 103
8.3.2 False Alarm Ratio 103
8.3.3 Missed Detection Rate 103
8.3.4 Frequency Bias 103
8.3.5 Compound Skill Scores 104
9 REFERENCES 105
APPENDIX A 106
APPENDIX B 107
APPENDIX C 144
APPENDIX D 148
APPENDIX E ..... 151~~152~~

LIST OF FIGURES

Figure 1. EUV irradiance “event” examples 16
Figure 2. GOES-R EUV spectral measurements ..... 17~~18~~
Figure 3. "Non-event" example ..... 21~~22~~
Figure 4. "Non-event" example ..... 22~~23~~
Figure 5. Normalized EUV irradiance with X-ray flares ..... 29~~30~~
Figure 6. Components of an idealized EUV event ..... 31~~32~~
Figure 7. Event statuses schematic ..... 37~~38~~
Figure 8. Simplified event processing flow diagram ..... 38~~39~~
Figure 9. EUV event with different pre- and post-event irradiances ..... 42~~43~~
Figure 10. Example of 15-minute slope data metric ..... 43~~44~~
Figure 11. Example of standard deviation data metric ..... 44~~45~~
Figure 12. Example of monotonic rank data metric ..... 45~~46~~
Figure 13. Example of monotonic rank of 5-min mean ..... 46~~47~~
Figure 14. Example of 10-minute maximum relative increase data metric ..... 47~~48~~
Figure 15. Example of Nth percentile difference data metric 49
Figure 16. Schematic diagram of event start determination ..... 51~~52~~
Figure 17. Relationship between "look back" interval and start determination .. 52~~53~~
Figure 18. Example of false alarm suppression ..... 54~~55~~
Figure 19. Gaussian convolution kernel 77
Figure 20. Convolved SDO/EVE solar spectrum 78
Figure 21. GOES-15 EUV-E measurements with geocoronal absorption 79
Figure 22. Geocoronal absorption correction 80
Figure 23. Corrected GOES-15 EUV-E spectrum 81
Figure 24. False alarm ratio vs detection latency 85
Figure 25. Example of single vs multiple event ambiguity 87
Figure 26. Preliminary algorithm results for 30.4 nm event (Aug 7, 2010). 92
Figure 27. Preliminary algorithm results for 121.6 nm event (Aug 7, 2010) 93
Figure 28. Preliminary algorithm results for 28.4 nm event (Aug 7, 2010) 94
Figure 29. Preliminary algorithm results for 28.4 nm event (Nov 5, 2010) 95
Figure 30. Preliminary algorithm results for 28.4 nm event (Aug 14, 2010) 96
Figure 31. Preliminary algorithm results for 28.4 nm event (Nov 3, 2010) 97
Figure 32. Preliminary algorithm result with possible missed detection 99
Figure 33. Preliminary alorithm result with single/multiple event ambiguity 100

Additional figures are included in Appendix B.

LIST OF TABLES

Table 1. Algorithm and event status indicators. 3233
Table 2. Example of a one-minute update output file. 74
Table 3. Example of a post-event summary output file. 76
Table 4. Validation contingency table 102

LIST OF ACRONYMS

ATBD	Algorithm Theoretical Basis Document
AWG	Algorithm Working Group
CIRES	Cooperative Institute for Research in Environmental Sciences
EUV	Extreme Ultraviolet
EUVS	Extreme Ultraviolet Sensor
EUVS-A	GOES-R sensor for 25.6 nm, 28.4 nm and 30.4 nm EUV emissions
EUVS-B	GOES-R sensor for 117.5 nm, 121.6 nm, 133.6 nm and 140.5 nm EUV emissions
EUVS-C	GOES-R sensor for 275-285 nm EUV emissions
EUVS.04	EUV event detection and characterization algorithm
EXIS	EUV and X-ray Instrument Suite
GOES	Geostationary Operational Environmental Satellite
GOES-R	Next series of GOES satellites
LASP	Laboratory for Atmospheric and Space Physics
NA	Not Applicable
SET	Space Environment Technologies
STAR	Center for Satellite Applications and Research
SWPC	Space Weather Prediction Center
XRS	GOES-R X-ray Sensor

ABSTRACT

This document describes the EUVS.04 EUV event detection and characterization algorithm, which will monitor selected GOES-R EXIS EUV solar irradiance data for potentially geoeffective brightenings. An algorithm overview is presented in which the GOES-R EXIS data products are discussed along with the operational and scientific objectives. The algorithm will monitor the 28.4 nm, 30.4 nm and 121.6 nm spectral lines for EUV events. An event is defined as a 10% or greater irradiance increase within 5 hours or less for the 28.4 nm spectral line, a 3% or greater irradiance increase within 2 hours or less for the 30.4 nm spectral line, and a 3% or greater irradiance increase within 2 hours or less for the 121.6 nm spectral line. Critical differences between X-ray flares and EUV events are examined. Operational requirements and input/output data formats are specified and the algorithm processing logic is described. Graphical representations of algorithm results are presented for twelve test and development days that were selected for each spectral line. The algorithm was evaluated using 476 days of proxy irradiance data beginning with April 30, 2010 and concluding with August 19, 2011. During this period, there were 31 28.4 nm events, 195 30.4 nm events, and 25 121.6 nm events. The algorithm detected 26 28.4 nm events, 193 30.4 nm events, and 25 121.6 nm events. The algorithm missed 5 28.4 nm events, 2 30.4 nm events, and no 121.6 nm events. The algorithm produced 1 false alarm for the 28.4 nm spectral line, 21 false alarms for the 30.4 nm spectral line, and 3 false alarms for the 121.6 nm spectral line. On the basis of these results, it was determined that the probability of detection, false alarm rate, and mean detection latency values are 83.9%, 3.7% and 41.3 minutes for the 28.4 nm spectral line, 99.0%, 9.5% and 18.3 minutes for the 30.4 nm spectral line, and 100.0%, 10.7% and 21.8 minutes for the 121.6 nm spectral line. Probability of detection increases with a more substantial irradiance increase. For example, for 28.4 nm events associated with irradiance increases of 15% or greater and 20% or greater, the probability of detection is 91.7% and 100.0%, respectively.

1 DOCUMENT SUMMARY

1.1 Purpose

The purpose of this document is to provide a detailed description of the requirements, design, development and implementation of the *EUVS*.04 EUV event detection and characterization algorithm. Algorithm inputs and outputs are specified in detail, and preliminary algorithm results are presented.

1.2 Intended Users

This document provides product developers, program reviewers, and application users with a technical description of the GOES-R EXIS extreme ultraviolet event detection and characterization algorithm.

This document will enable staff of the Space Weather Forecast Office and the Research and Customer Requirements Section of the Space Weather Prediction Center to verify that the proposed algorithm will satisfy operational requirements. The ground system contractor should use this document to design, develop, and implement the algorithm.

1.3 Section Outline

Section 2 – ALGORITHM OVERVIEW AND BACKGROUND
This section includes an algorithm introduction, a summary of the EXIS instrument suite and associated measurements that will constitute input to the algorithm, a review of the operational and scientific objectives, a discussion of EUV event definition and spectral line selection, and a software overview.

Section 3 – ALGORITHM DESCRIPTION
This section includes a discussion of the critical differences between X-ray flares and EUV events. The manner in which these differences influence algorithm logic and operational requirements is also addressed. This discussion includes an explanation of why EUV event detection and characterization logic does not closely resemble that of the corresponding X-ray algorithm. The processing logic of EUV event detection and characterization is presented, and the input/output formats are specified.

Section 4 – TEST DATA AND PROCESS
This section describes the proxy data that will be used to develop and validate the algorithm, and outlines the test procedures employed.

Section 5 – ADDITIONAL CONSIDERATIONS
Describes the risks, tradeoffs, configuration and log files, and error checking.

Section 6 – ASSUMPTIONS AND LIMITATIONS
Summarizes critical algorithm assumptions and discusses potential limitations.

Section 7 – ALGORITHM RESULTS
Algorithm results are presented for selected processing days.

Section 8 – ALGORITHM VALIDATION
Discusses the methodologies and skill measures used to quantify algorithm performance.

Section 9 – REFERENCES
List of references.

Appendix A
List of days used for algorithm development and optimization

Appendix B
Graphical representation of algorithm results for the development and optimization days listed in Appendix A.

Appendix C
Algorithm Validation Statistics

Appendix D
Preliminary EUV Event Catalog

1.4 Related Documents

GOES-R EXIS EUVS.04 Test Plan and Results (version 1.0)
GOES-R EXIS EUVS.04 User Guide (version 1.0)
GOES-R EXIS XRS.07 Algorithm Theoretical Basis Document

1.5 Revision History

Version 1.0 June 8, 2011, Steven Mueller, Initial version
Version 1.1 June 15, 2011, Steven Mueller, New figures and updated text
Version 1.2 September 15, 2011, Steven Mueller, Final version

2 ALGORITHM OVERVIEW AND BACKGROUND

2.1 Introduction

The purpose of this algorithm is to automate the detection, characterization and cataloging of potentially geoeffective EUV brightenings or “events” in real-time GOES-R EXIS time series irradiance data.

Detection refers to the ability to recognize that a significant EUV brightening is occurring. *Characterization* refers to the ability to accurately report critical aspects of event evolution, including start time and irradiance, peak time and irradiance, end time and irradiance, event duration, and total integrated energy.

Like X-ray flares, significant EUV events are of considerable scientific interest and may have important space weather implications.

The EUV event detection and characterization algorithm is expected to fulfill a role similar to the X-ray flare detection algorithms that have been previously utilized by the space weather community. Legacy X-ray detection algorithms have been deployed for the dual-purpose of operator notification and flare archival. The EUV event algorithm will be optimized for a limited number of spectral lines chosen on the basis of geoeffective potential (Section 2.3.1).

EUV events do not conform to a simple mathematical description and exhibit a variety of shapes, ranging from relatively simple to quite complex (e.g., Figure 1). Proposed definitions of EUV events for selected spectral lines (Section 2.3.1) form the basis for algorithm development, optimization and validation.

No source of GOES-R EXIS-like EUV data currently exists. Consequently, algorithm development required the creation of proxy input data (Section 4.1). Operational algorithm performance may depend critically on how closely this proxy development data resembles the EUV irradiances that will ultimately be provided by GOES-R EXIS (Section 5.1).

For each spectral line, twelve days of solar irradiance data were selected for algorithm optimization (Appendix A).

The most significant challenges associated with algorithm optimization are prompt event detection, minimization of false alarms, appropriate discrimination between extended duration multi-peak events and a rapid succession of brief single-peak events, and appropriate event termination.

Algorithm output consists of a diagnostic log file, a one-minute algorithm status and/or event progression updates, and single-line post-event summaries. "Tunable" algorithm parameters are specified in configuration files (Section 5.3), and modification of those parameters will require only that the algorithm be restarted (not recompiled).

The algorithm will be prototyped in IDL (Interactive Data Language) and delivered in C++. Basic error checking will be incorporated, but error handling will be the responsibility of the ground system contractor. Optimization, testing and validation was performed to the extent permitted by scheduling constraints.

Algorithm results are presented in this document.

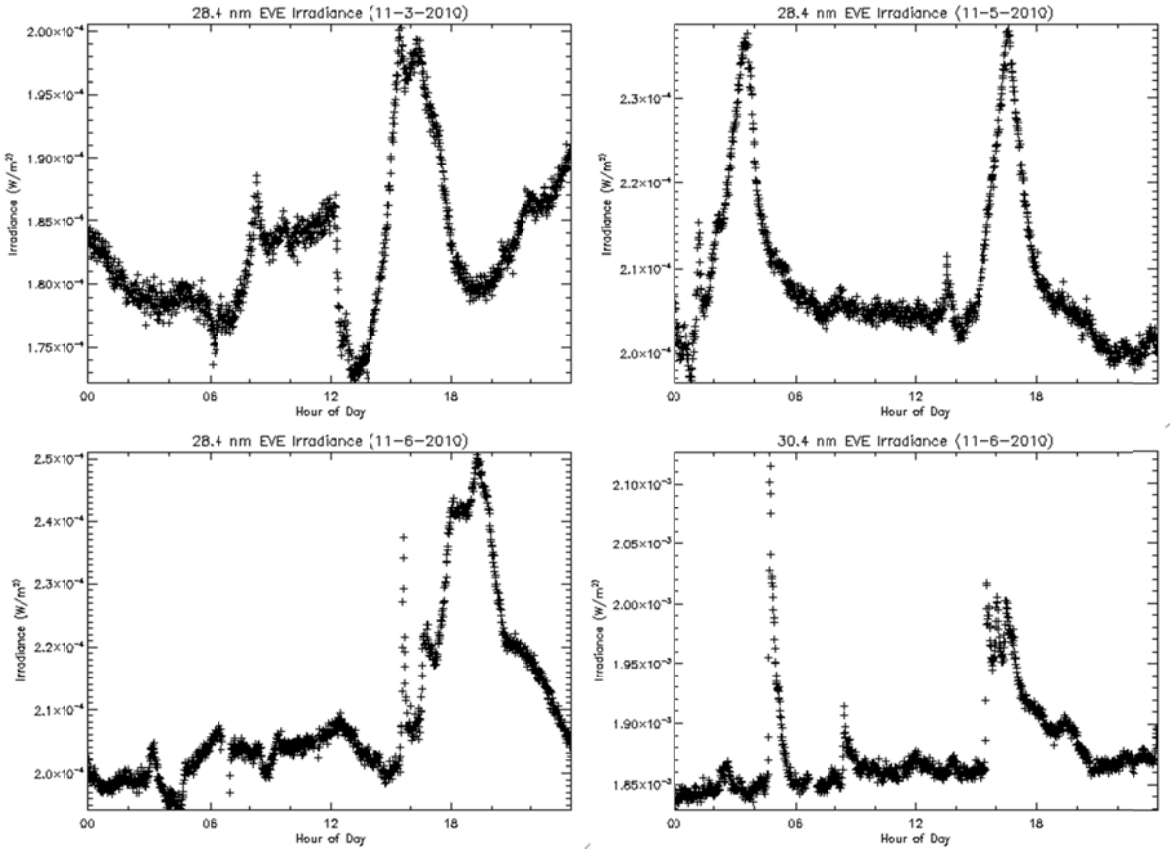

Figure 1. EUV irradiance "event" examples from early November 2010

2.2 Observing System Instrument Characteristics

The GOES-R EXIS instrument suite includes the following irradiance sensors: XRS, EUVS-A, EUVS-B, and EUVS–C.

The XRS sensor consists of X-ray photometers for spectral bands designated A (0.05-0.4 nm) and B (0.1-0.8 nm).

The EUVS instruments are grating spectrographs that measure specific spectral ranges in the extreme ultraviolet (Figure 2). EUVS-A measures selected corona and transition region emission lines in the 22-34 nm range. EUVS-B measures selected transition region and chromosphere emission lines in the 115-141 nm range. EUVS-C measures the Mg II chromosphere and photospheric emission continuum surrounding 280 nm, which is used to calculate the Mg II core-to-wing ratio (Viereck & Puga, 1999; Viereck *et al.*, 2001).

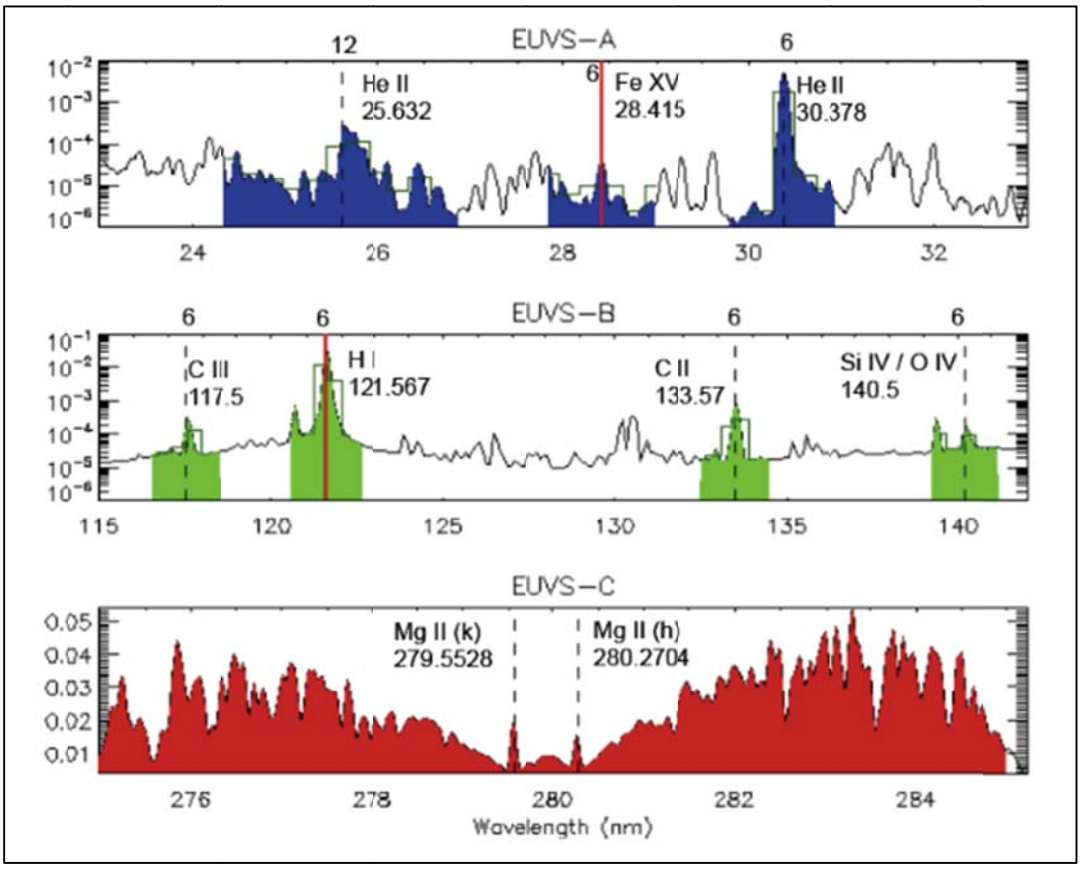

Figure 2. GOES-R EUV Spectral Measurements

EUVS-A, EUVS-B and EUVS-C processed data products are combined to construct a proxy EUV spectrum from 5 to 127 nm.

Only EUVS-A and EUVS-B measurements are relevant to the EUV event detection and characterization algorithm.

The EUVS-A and EUVS-B instruments will produce data at a cadence of once per second and the EUV event detection and characterization algorithm will expect new input data at a rate of once per minute.

2.3 Operational and Scientific Objectives

The EUVS.04 EUV event detection and characterization algorithm will be a new application that is expected to fulfill a role for the extreme ultraviolet that is similar to X-ray flare detection algorithms. The algorithm will be designed to detect, characterize and catalog significant solar EUV brightenings.

This dual-purpose algorithm will alert space weather observers of potentially problematic EUV spikes and catalog the event characteristics for research purposes. As with previously implemented X-ray flare cataloging procedures, it is assumed that the EUV event summaries may be reviewed and/or modified by a human interpreter. Note, however, that a primary objective of algorithm design is to minimize such operator intervention.

EUV eruptions may have significant space weather implications. Geoeffective irradiance spikes may induce ionospheric disturbances that disrupt high-frequency communications and increase drag on low-earth-orbiting satellites. In addition, geoeffective solar emission lines deposit significant amounts of energy directly into the thermosphere.

EUV solar events are also of considerable scientific interest. EUV irradiances are generally elevated for considerably longer periods of time than associated X-ray flares and are responsible for a significantly greater amount of integrated flux. Some EUV variations are associated with coronal mass ejections.

The GOES-R EUVS data product is expected to consist of seven individual emission lines, in addition to the MgII core/wing ratio

1. 25.6 nm (He II)
2. 28.4 nm (Fe XV)
3. 30.4 nm (He II)
4. 117.5 nm (C III)
5. 121.6 nm (H I - Lyman Alpha)
6. 133.6 nm (C II)
7. 140.5 nm (Si IV/O IV)
8. Mg II core/wing ratio

Although the EUV event detection algorithm may be applied to any of the above spectral lines, it will be optimized only for selected lines of known geoeffective potential.

While reliable event detection and characterization will likely be straightforward for “well-behaved” EUV emission lines, the presence of complex patterns of brightening and/or dimming in other emission lines may be problematic. Examples of complexity include variable “shapes” in peaks (brightening) and valleys (dimming), multiple subpeaks, and irregular irradiance background levels. Also, note that, unlike X-ray flares, EUV irradiance variation during enhanced solar activity is not characterized by sudden changes of several orders of magnitude. Increases on the order of 5-25% are more typical of the EUV, and, in some cases, increases as small as 3% may warrant detection. This behavior, combined with the associated detection requirements, is expected to render EUV event detection particularly vulnerable to false alarms.

2.3.1 EUV Event Definition and Spectral Line Selection

X-ray solar flares are characterized by quantitative definitions that have formed the basis for cataloging and analysis for decades (e.g., A-, B-, C-, M- and X-class flares). Unfortunately, there are no comparable definitions for extreme ultraviolet irradiance fluctuations. Moreover, there is no consensus concerning which EUV brightenings qualify as significant “events” and which do not.

Specific details are debatable, but EUV event definition guidelines should embody the following points

- An event must have geoeffective significance.

- Event definitions should be spectral line specific. For example, a 3% increase may be significant for one spectral line and of no consequence for another.
- EUV events must be recognized independent of X-ray flare activity. Although often correlated, the recognition of X-ray flares and EUV events should not depend upon one another.
- Effective definitions must include thresholding to prevent excessive alerts.

One simple approach to event definition is to specify a minimum irradiance increase that must be attained within a specific time period. Definitions based on absolute irradiance levels would be potentially problematic as background levels vary with the solar cycle.

In addition to specifying event definitions, algorithm development requires that specific spectral lines must be designated for processing and monitoring. Given scheduling constraints, it is not practical to develop and algorithm that will efficiently process all EUV irradiance bands. Algorithm development will be limited to the available spectral lines with the most significant geoeffective potential. Each spectral line of interest must be individually optimized for event initiation, event termination, and false alarm suppression.

Including the EUVS-A, EUVS-B and EUVS-C instruments, there are seven spectral lines, plus the *MgII* core/wing ratio, that could potentially be monitored for enhanced irradiance activity.

On the basis of geoeffectiveness, the following emission lines are proposed for event processing

- 28.4 nm, a coronal line from EUVS-A
- 30.4 nm, a transition region line from EUVS-A
- 121.6 nm (Lyman-Alpha), a transition region line from EUVS-B

Subject to revision, the following event definitions are proposed for each of these spectral lines

- 28.4 nm – 10% increase in 5 hours or less
- 30.4 nm – 3% increase in 2 hours or less
- 121.6 nm – 3% increase in 2 hours or less

Note that, on the basis of these definitions, smaller fluctuations, regardless of how sharp or well-defined they may be, will not qualify as true “events” (e.g., Figure 3).

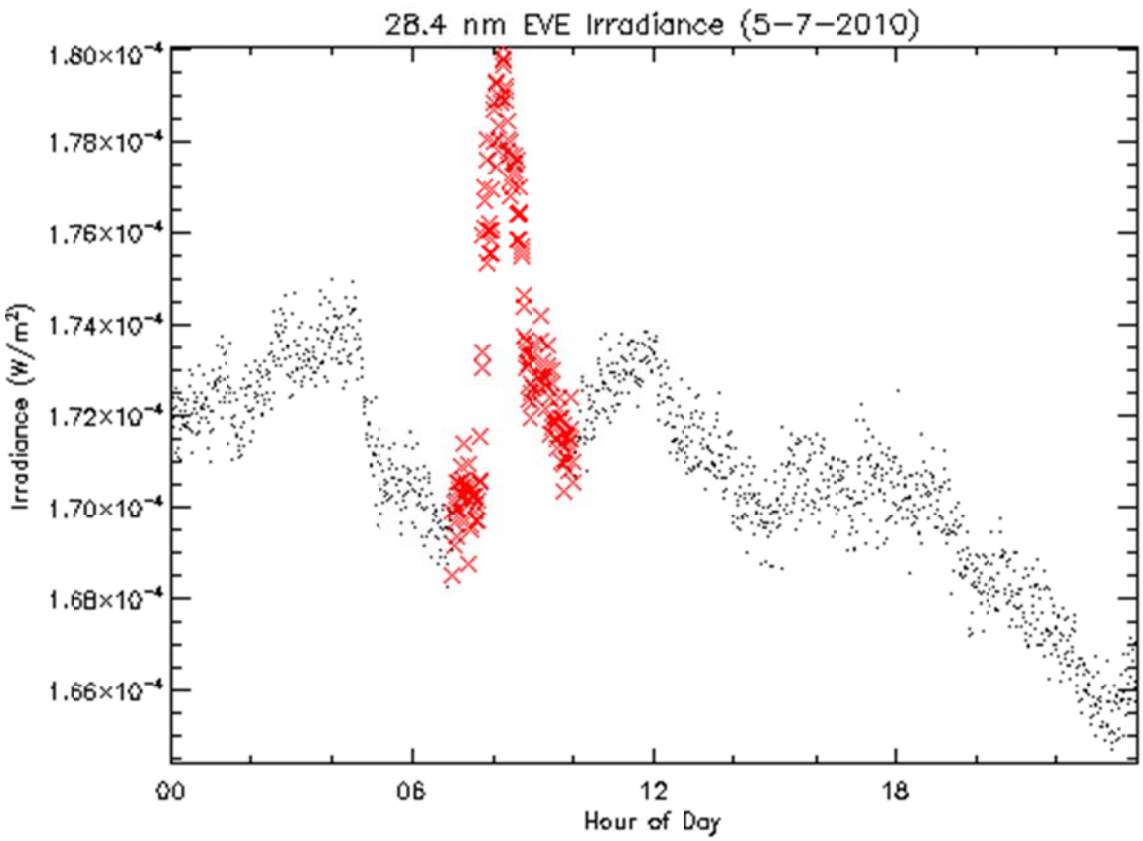

Figure 3. Example of a sharp abrupt irradiance fluctuation that does not qualify as an event on the basis of the 28.4 nm event definition proposed in this document.

Also, because the proposed event definitions are based solely on relative irradiance increases, sustained periods of consistently elevated irradiance will not qualify as events in the absence of sudden upward fluctuations. This may create the appearance of incongruous results. This is illustrated in Figure 4, which depicts 28.4 nm time series irradiance data for August 7, 2010 and March 6, 2011. Although the August 7 irradiance values are consistently lower than the March 6 irradiance values, a portion of the August 7 emissions qualifies as an event, whereas no portion of the considerably greater March 6 emissions qualifies as an event.

Note that the behavioral contrast evident in Figure 4 is not necessarily objectionable. If an absolute irradiance threshold were adopted as a basis for event definition, a potential consequence would be events that persist for days or weeks. During solar maximum conditions, consistently elevated irradiance levels

may qualify as “perpetual events”, and during solar minimum conditions events may be extremely rare.

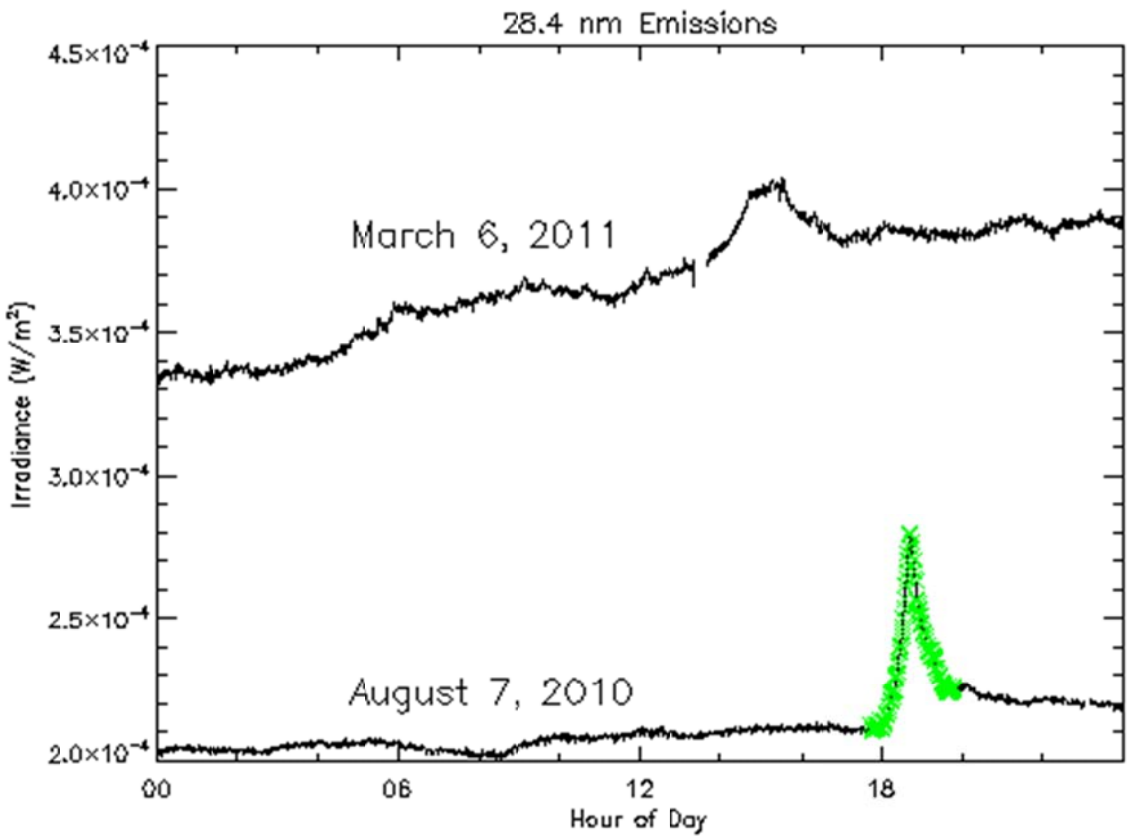

Figure 4. Implication of the independence of the proposed EUV event definition on absolute magnitude. The green portion of the lower irradiance time series qualifies as an event because the relative irradiance increase exceeds 10%. In contrast, although all portions of the upper time series exceed the maximum irradiance associated with the lower event, no portion of the upper time series irradiance qualifies as an event.

2.4 Software Overview

A single algorithm was developed that will simultaneously process three potentially geoeffective spectral lines: 28.4 nm, 30.4 nm, and 121.6 nm. From an operational perspective, a single-algorithm design will simplify delivery, installation and maintenance.

The EUV event detection and characterization algorithm will run continuously in a data-driven mode. In other words, the application will not start when new data is available and stop after that data has been processed. Note that this behavior

implies stringent conditions for memory management (i.e., even relatively small memory leaks will eventually become problematic).

The algorithm will be delivered in C++ (Section 2.4.1), and incorporates only native language features (i.e., without third-party components, such as commercial math libraries, Boost, etc.).

Because there is no currently existing “live” source of GOES-R EXIS EUV irradiance data, the deliverable application was implemented to run in an “archive mode”, which allowed development, testing and optimization to proceed with the proxy data described in Section 4.1. The ground system contractor will be required to re-implement the application in a real-time mode. In the deliverable (archive mode) version of the application, processing is associated with a single input file. In the operational (real-time mode) version, processing will continue indefinitely and the data ingest must be based on the current availability of data.

Input data for all processed spectral lines must be bundled into a single-source that must be updated once per minute (Section 3.6.4).

Three types of output files are produced (Section 3.7.1).

1. A daily log file to record diagnostic information.
2. A daily one-minute update file for each spectral line.
3. A single post-event summary file that will combine information associated with all spectral lines and will expand indefinitely.

Note that the ground system contractor may choose an alternative strategy for the organization of output files, such as monthly post-event summary files.

Key processing parameters are provided in a configuration file (Section 5.3.1).

Each spectral line is associated with independent event detection and characterization parameters specified in individual external configuration files (Section 5.3.2).

Deliverable application components include basic error *checking*. Error *handling* will be the responsibility of the ground system contractor. Refer to Section 5.5 for explanations of error checking and error handling.

2.4.1 Development Language

Although the application was prototyped in ITT/IDL (Interactive Data Language), it was reimplemented, tested and will be delivered in C++. Algorithm logic is, for all practical purposes, nearly identical for both the prototype and deliverable applications.

IDL was preferable for preliminary algorithm development because it provides extensive graphic resources that allow convenient and intuitive analysis of results, which is useful during the initial evaluation of event detection and characterization schemes.

IDL is not an appropriate choice for the deliverable application because it is a commercial product and is not a STAR-compliant development language. Moreover, graphic display capability is not relevant to the final deliverable algorithm.

While the choice of C++ over C (or FORTRAN) is essentially a matter of developer preference, C++ offers several well-known advantages such as improved type safety, larger standard library (including the standard template libraries), convenient string handling, method overloading, and robust type-safe I/O capability.

Although, in principle, the EUV event detection and characterization algorithm could be implemented in an alternative language, it is assumed that the ground system contractor will also implement the algorithm in C++.

2.4.2 Application Components

In this section an overview of major application components is presented.

A class-based application was developed because it allows the bundling of data with relevant functionality. For example, a class representing a spectral line can be used to store irradiance data history along with the methods necessary to detect the initiation of an EUV event.

All non-trivial class methods are listed in Appendix E.

SpectralLine Class

A *SpectralLine* class encapsulates the data and methods associated with the processing of time-series irradiance data. At runtime, there will be three instances of the *SpectralLine* class: one each for the 28.4 nm, 30.4 nm, and 121.6 nm irradiance emissions.

Each *SpectralLine* object will update the relevant data metrics, and store a limited history of irradiance and data metric values for the relevant spectral line.

The *SpectralLine* class includes the event detection and characterization logic and is responsible for the one-minute output file updates.

EuvEventAlgorithm Class

High-level processing is managed by the *EuvEventAlgorithm* class.

The responsibilities of this class include the initialization of algorithm parameters, configuration file processing, log file management, instantiation and updating of *SpectralLine* objects, ingest and validation of input data, and creation and maintenance of the post-event summary file.

This class includes a *run*() method to start the application, is responsible for the ingest and validation of irradiance data, and triggers *SpectralLine* processing for each new valid set of irradiance data.

Event Class

Each EUV event will be represented by a transient instantiation of an *Event* object.

Objects of this class will be instantiated upon event detection and destructed subsequent to event termination. *Event* objects will assemble and update information (as it becomes available) that represents the state of the ongoing event, including detection time, start time and irradiance, peak time and irradiance, end time and irradiance, accumulated energy, duration, and current status. *Event* objects also store diagnostic information, such as detection latency and initiation/termination criteria, that will be recorded in the application log file.

Event objects are responsible for the post-event summary output.

Config Class

A *Config* class was created to facilitate the management of configuration files and configurable parameters. An external configuration file specified in the constructor argument will be parsed during instantiation of the *Config* object. All configurable application content are specified as “keyword = value” strings.

Both parameter keywords and values are stored as strings in a *Standard Template Library* map object. Values are requested by type using the associated key. For example, if the number of one-minute data points retained by the algorithm (i.e., the amount of data history) is specified in the main configuration file as “MAX_NBR_PTS = 500”, this value would be retrieved from a *Config* object, *config*, with the *getIntFromKey*() method as follows

maxNbrPts = *config->getIntFromKey*(“MAX_NBR_PTS”)

Logger Class

Log file output and error handling is implemented with a *Logger* class. A *Logger* object will direct diagnostic output to a consistent destination. If a log file is not specified in the main configuration file, log output will be directed to standard output. The *Logger* class will also insure that all warnings or errors of a specific level will be handled in a consistent manner.

AlgorithmUtilities Library

This custom C++ library includes miscellaneous mathematical, date-time and output formatting functionality.

3 ALGORITHM DESCRIPTION

3.1 Historical Perspective

X-ray solar irradiance monitoring has been a component of the GOES satellite observation suite since program inception. In contrast, monitoring of extreme ultraviolet solar irradiance is a relatively recent (and still evolving) feature of GOES data collection.

Currently, there are no extreme ultraviolet measurements of the spectral and temporal resolution comparable to that expected from GOES-R EXIS. The availability of such measurements will offer the potential to monitor and catalog EUV irradiance fluctuations at an unprecedented level.

As previously discussed, while X-ray flares have quantitative flare class definitions that have been utilized for decades, there are no such definitions specifying which EUV irradiance fluctuations qualify as “events” and which do not.

3.1.1 Critical Differences Between XRS Flares and EUV Events

Considering the longstanding operational use of GOES X-ray detection algorithms, it is useful to discuss the differences between the physical nature of EUV events and X-ray flares, as well as the implications for algorithm design.

A critical difference is that there is no source of EUV irradiance data that matches the temporal and spectral resolution anticipated for GOES-R EXIS. The XRS algorithm can be optimized and validated with extensive volumes of data that closely resemble the data characteristics anticipated for GOES-R EXIS. In contrast, EUV algorithm development must be based on proxy irradiance data (Section 4.1). If the derived proxy data is not sufficiently “EXIS-like”, the algorithm may require reoptimization. This is a potential source of risk.

Given the history of operational X-ray flare detection and characterization algorithms, each updated X-ray algorithm may be evaluated with respect to its predecessor. Because there is no predecessor in the case of the EUV event detection and characterization algorithm, there is no benchmark with which to compare the performance and skill of the algorithm.

Unlike X-ray flares, EUV events, as measured by EXIS, will not spike by orders-of-magnitude. Maximum changes of a few tens of percent are expected. This is a

critical distinction, because it renders EUV detection more susceptible to false alarms.

EUV events may be associated with very complex time series fluctuations and extremely variable durations (i.e., 10's of minutes to more than a half day). There is no single shape or mathematical function to which EUV brightenings consistently conform. Curve-fitting options are therefore of limited utility. There is no "one size fits all" solution for EUV event detection. Instead, a multiple criteria approach is adopted in which more than one condition can trigger both the detection and the termination of an event.

Finally, temporal correlations between X-ray flares and EUV events are complex and do not exhibit a consistent pattern. In many cases, EUV irradiance simply does not increase in response to the physical conditions that generate X-ray flares. When X-ray flares are associated with coronal mass ejections, EUV irradiance may exhibit transient dimming coincident with the flare. Delayed post-flare EUV brightenings are a common observation (Figure 5**Error! Reference source not found.**).

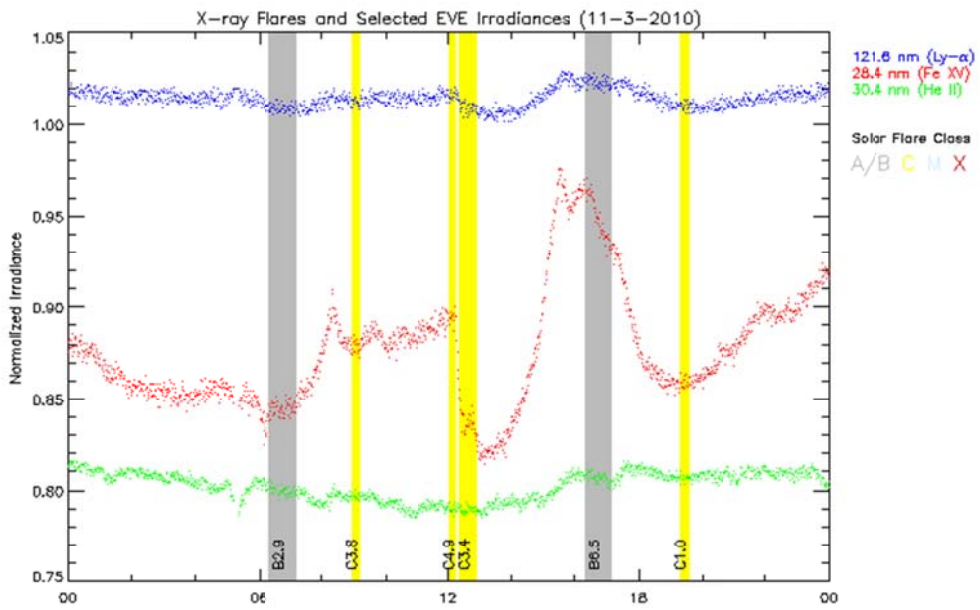

Figure 5. Normalized EUV irradiance variations superimposed on a background of X-ray flares. Color-coded vertical bars represent X-ray flares. EUV irradiances are normalized to allow presentation within a single plot.

3.2 EUV Event Terminology

The significant elements of EUV event evolution are illustrated in Figure 6.

The highly idealized, well-behaved, symmetric, single-peak event depicted is intended solely to define the terminology used throughout this document, and is not representative of a real or typical EUV event.

Rising phase refers to a period when the irradiance is predominantly increasing and *declining phase* refers to a period when the irradiance is predominantly decreasing. A simple single-peak event will consist of a single rising phase followed by a single declining phase. Events characterized by multiple peaks will consist of multiple rising and declining phases.

In the simplified event depicted in Figure 6, the rising phase is the period between the event start and the event peak, and the declining phase is the period between the event peak and the event end.

In Figure 6, X's represent detection times and boxes represent actual times.

The event start is designated by the green box. Note that a distinction between *event start time* and *event detection time* is critical because the event will invariably be detected some time after it actually commences. This difference will be referred to as *detection latency* and is an important parameter in assessing algorithm skill.

The *pre-event irradiance* refers to the irradiance level immediately prior to event initiation. The difference between the maximum event irradiance and the pre-event irradiance is a useful measure of event magnitude. The pre-event irradiance is also used as a reference value during event termination logic.

The *actual peak time* and irradiance are indicated by a blue box, and a blue X indicates the *peak detection time*.

The *actual event end time* is indicated by a red box, and the time at which event termination was detected is represented by a red X.

The *half-maximum point* refers to the time at which the event irradiance initially decreases below the average of the pre-event and peak irradiances. Multi-peak events may be associated with multiple half-maximum points.

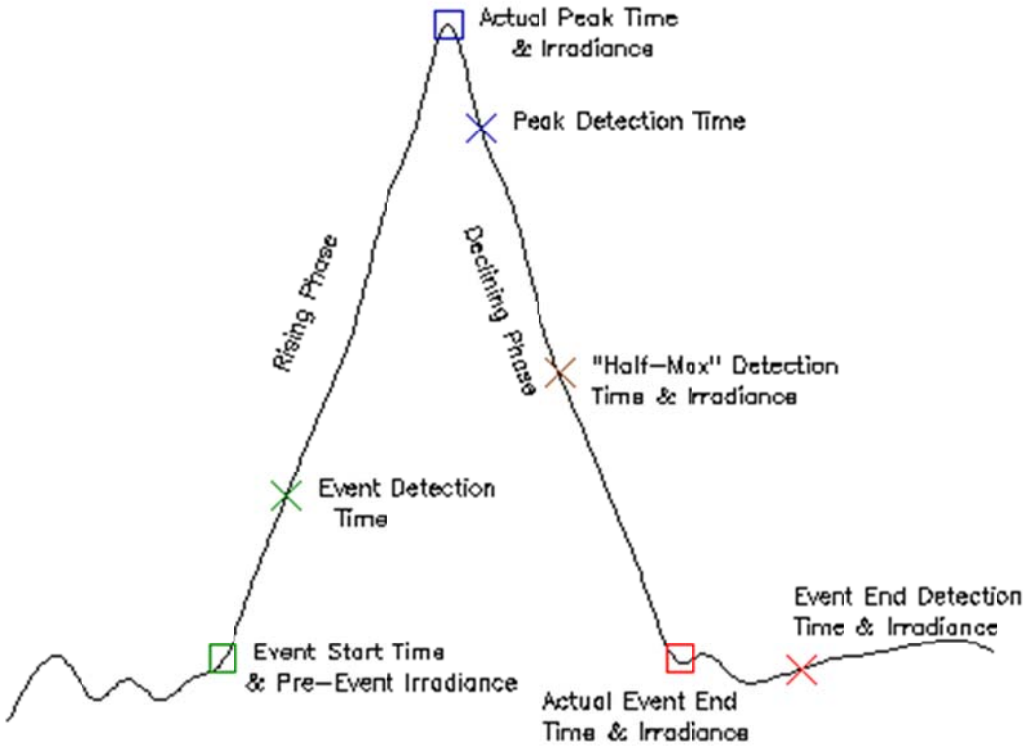

Figure 6. Components of an idealized EUV event.

3.2.1 Algorithm and Event Status Indicators

A summary of algorithm and event status indicators (e.g., Figure 6) is provided in Table 1.

STARTUP	Algorithm impaired due to Insufficient data at startup
MONITORING	No activity
EVENT_START	Event detection
EVENT_RISE	Event irradiance is increasing
EVENT_DECLINE	Event irradiance is decreasing
EVENT_PEAK	Event irradiance has peaked
HALF_MAX	Event irradiance has decreased below half-max
EVENT_END	Event termination
IMPAIRED	Algorithm impaired due to insufficient valid data

Table 1. Algorithm and event status indicators.

An additional optional flag is *WATCH*, which indicates that a false alarm suppression has occurred. It will appear only if a specific configuration file flag is set. The purpose is to alert the operator that irradiance is increasing at a significant rate, but the algorithm is suppressing an alert until the false alarm threshold has been exceeded.

3.3 Operational Specifications and Requirements

The deliverable product is a single operational application that will concurrently process all relevant spectral lines (Section 2.4).

The algorithm will run continuously and processing will be data driven (Section 2.4).

During periods of inactivity (no ongoing EUV event), the algorithm will report the current time and irradiance for each spectral line, and issue an event status of *MONITORING* (Section 3.7.2).

The algorithm will detect EUV events with reasonable latencies, although not at the expense of an unacceptable false alarm rate (Section 5.2). It is required that event detection must occur prior to the event maximum irradiance and certainly before the event end. Excluding missed detections, in the worst-case scenario, the algorithm will detect the event simultaneous with the peak.

During periods of EUV activity, the algorithm will track and report event evolution, including indications of increasing or decreasing irradiance in spectral line-specific

output files (Section 3.7.2). The algorithm will report the event start time and irradiance, event end time and irradiance, and event peak time and irradiance.

At the conclusion of an EUV event, the algorithm will issue a one-line summary of the event to a separate output file (Section 3.7.2).

3.4 Processing

A main executable is provided to start the application. In the deliverable (archive mode) version of the algorithm, an input file must be provided as a command-line argument to main.

Several one-time procedures are performed at startup, including configuration file and parameter processing, initialization of critical variables and state flags, allocation of data arrays, and the instantiation of all component objects, excluding event objects.

Initially, processing is limited to data ingest and the calculation of data metrics (Section 3.5.1). Event detection is deactivated during this *startup period*, which is a configurable interval of time and minimum volume of valid data that must be accumulated and processed to enable a meaningful evaluation of current conditions. Only in extreme circumstances, for example, would it be possible to infer event initiation from less than five data points without the context of recent history. A designated startup period and critical mass of valid irradiance data circumvents this difficulty. An algorithm status of *STARTUP* is reported during this time.

In addition to the startup period, algorithm processing is also suppressed when new data is not received at the expected rate or when excessive amounts of invalid data accumulate within a short period of time.

It is assumed that new input data will be available once per minute, within a configurable set of tolerance limits described in the algorithm user guide. If the lower tolerance limit is violated, a warning will be recorded in the algorithm log file. If the upper tolerance is violated, the algorithm will terminate with a fatal log entry. Note that invalid data indicators represent acceptable algorithm input and, provided that they are updated at an acceptable rate, will not trigger a violation of the input data rate tolerances.

An excessive accumulation of invalid data indicators within a specified period of time will impact algorithm processing in one of two ways. Relatively low rates of invalid data occurrences will simply preclude any modification of algorithm status. In this case, an event cannot be initiated and an ongoing event will retain the most recent valid status (i.e., an event cannot be terminated and an event peak cannot be declared). Relatively high rates of invalid data accumulation will temporarily suspend all processing of the relevant spectral line. In this case, any ongoing event is immediately terminated, and the spectral line status will be *IMPAIRED* and the algorithm returns to startup mode for the affected spectral line. Note that an impaired processing state affects only the relevant spectral line. Provided that valid input data exists, processing of one or both of the remaining spectral lines remains unaffected.

When the algorithm is not in a startup or impaired state, an event status of *MONITORING* is reported during periods of inactivity. When the application is in a monitoring state, each data metric is evaluated to determine if it satisfies any of the event detection criteria. The transition from a monitoring state to an event state may be triggered by multiple criteria. It is possible that one spectral line may enter an event state while other spectral lines remain in a monitoring state. In fact, it is anticipated that spectral line-specific events will be common.

When an event initiation criterion is satisfied, the algorithm “looks back” to estimate the actual start time and pre-event (i.e., background) irradiance of the event (Section 3.5.3.1). This “look back” processing is necessary because the time of event detection will not be equivalent to the time at which the event actually began. Detection of almost any phenomenon will lag the phenomenon itself.

The difference between the irradiance at the time of detection and the pre-event irradiance (see Figure 6) is used to suppress false alarms. If the difference does not exceed a configurable threshold, the algorithm will not initiate event processing. False alarm suppression (Section 3.5.3.2) is critical to prevent the algorithm from excessive event declaration in response to minor irradiance fluctuations that do not qualify as events (Section 2.3.1). If false alarm suppression is not invoked, event initiation occurs and a one-time status of *EVENT_BEGIN* is reported.

A configurable flag can be set that will force the algorithm to report a status of *WATCH* when false alarm suppression occurs. If this flag is not set, the status following a false alarm suppression will remain *MONITORING*.

During an ongoing event, a status of *EVENT_RISE*, *EVENT_DECLINE*, *EVENT_PEAK*, *HALF_MAX* or *IMPAIRED* will be reported each minute. Unless superseded by an event status of *EVENT_PEAK* or *HALF_MAX*, a status of either *EVENT_RISE* or *EVENT_DECLINE* will be reported depending upon whether the irradiance is predominantly increasing or decreasing, respectively. “Coasting” of *EVENT_RISE* and *EVENT_DECLINE* statuses was implemented (Section 3.5.4), which is intended to reduce “thrashing” in which repeatedly alternating statuses of *EVENT_RISE* and *EVENT_DECLINE* are reported in response to local fluctuations associated with noisy data.

Upon event detection, the application begins tracking the maximum event irradiance and associated time. Peak detection logic (Section 3.5.5) is also activated at this point. If peak detection is positive, a status of *EVENT_PEAK* is reported, along with the maximum event irradiance and associated time.

Multiple peaks may be reported during a single EUV event. Note, however, that each peak must be associated with a greater maximum event irradiance. In other words, a local maximum that does not exceed the current maximum event irradiance will not be classified as a peak. If this were not the case, minor upward fluctuations along the declining phase of the event might be designated as additional peaks.

Following detection of the first event peak, the half-maximum detection logic (Section 3.5.6) is activated. Detection of the half-maximum condition is simple. When the current irradiance initially decreases below the average of the pre-event and maximum irradiances, a status of *HALF_MAX* is reported (Figure 6). An event characterized by multiple peaks may also be associated with multiple half-maximum statuses.

The half-maximum designation was introduced because there is an established convention of reporting the half-maximum time and irradiance for X-ray flares.

Preliminary analysis indicated that the ability of the algorithm to distinguish a rapid succession of short-duration events from a single long-duration event characterized by multiple peaks might be problematic. It was discovered that this difficulty is alleviated by the application of a more demanding event termination criteria nearer the event peak and a more relaxed event termination criteria further from the event peak. The point selected to relax some of the event termination criteria is an irradiance reduction of 75% from the maximum event value (Section 3.5.7).

Event termination logic is activated immediately upon event detection. Event termination analysis is entirely independent of the event peak and half-maximum detection process. Once initiated, an event may be terminated at any point at which the relevant criteria are satisfied, regardless of whether or not an intervening peak or half-maximum condition has been detected.

Similar to event initiation, event termination may be triggered by multiple criteria. When the end of the event is detected, a one-time status of *EVENT_END* is reported, and a once-per-minute status reporting of *MONITORING* is resumed. Note that once an *EVENT_START* status has been reported, another *EVENT_START* status cannot occur without an intervening *EVENT_END* status.

Event status designators are graphically depicted in Figure 7. Note that the *EVENT_START*, *EVENT_PEAK* and *EVENT_END* status designations are delayed with respect to the corresponding conditions. These delays result from the fact that the detection of critical points of event evolution will always occur later in time than the related changes.

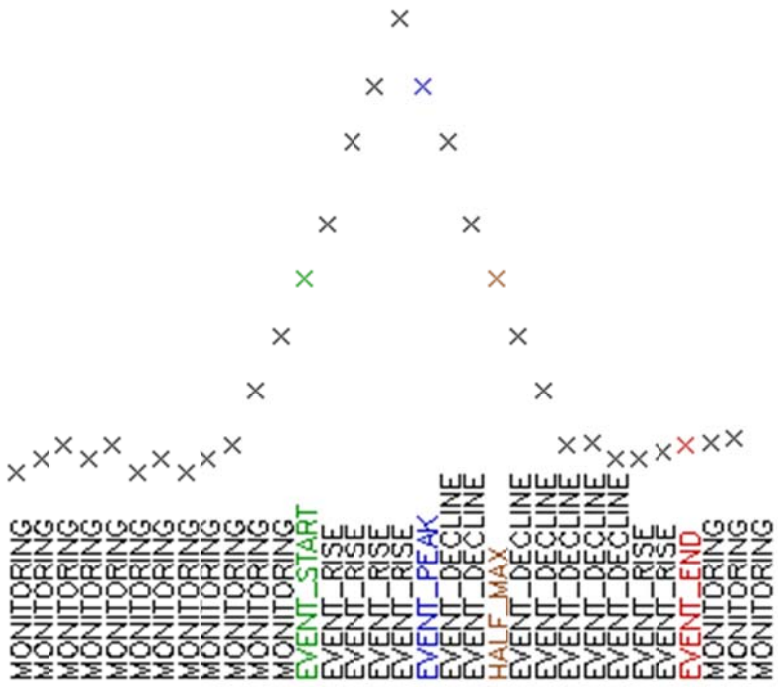

Figure 7. Example of event statuses for an idealized single-peak EUV event.

A simplified representation of algorithm event processing is presented in Figure 8.

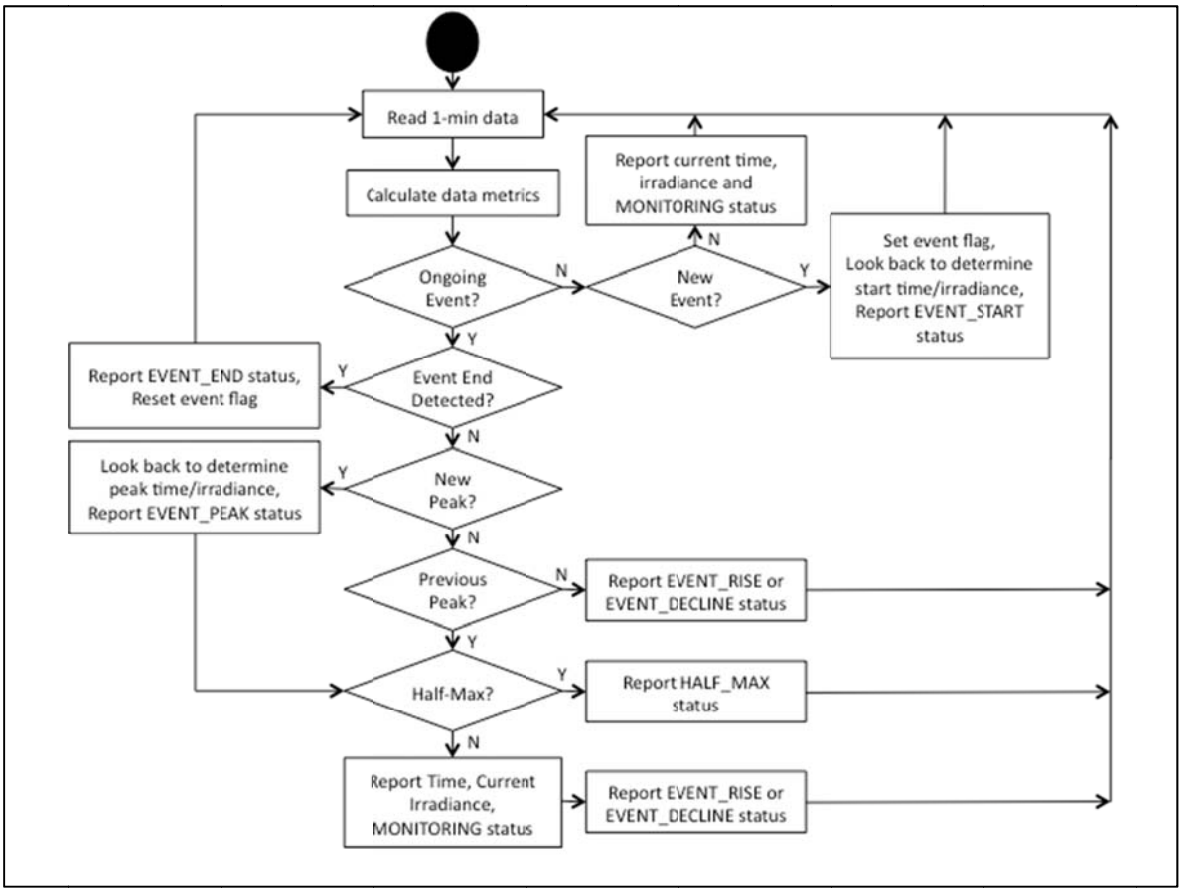

Figure 8. Simplified event processing flow diagram.

3.5 Event Detection and Characterization Logic

In the following discussion, *event initiation* refers to the detection of the start of an EUV event and the initiation of event processing logic. *Event termination* refers to the detection of the end of an EUV event.

Both the initiation and termination of EUV events are based on multiple criteria, which refers to the ability of more than a single condition to trigger the same event status change. In most cases, the detection and termination criteria are represented by *data metrics* (Section 3.5.1), which quantify critical aspects of irradiance evolution.

The advantage of schemes that allow multiple criteria is that additional criteria can be specifically designed to augment the detection and characterization of atypical

events. In the case of event initiation, for example, the mutual independence of metric-based criteria assures that the inclusion of additional criteria can only result in the detection of more, and never fewer, events. This is in sharp contrast to single-criterion event detection methodologies in which a consequence of parameter adjustment is frequently a tradeoff of decreased missed detection rates for one subset of event types and increased missed detection rates for another subset of event types. The primary disadvantage of multiple criteria event detection is that the false alarm rate is potentially increased with the addition of each criterion. For this reason, the number of event initiation criterion is limited to a practical minimum.

Multiple criteria schemes are particularly useful for event termination. If existing criteria prove inadequate at terminating atypical events, additional criteria can be designed to terminate such events without compromising the ability of the algorithm to properly terminate more typical events. The primary disadvantage of a multiple criteria approach to event termination is that additional criteria may result in the premature termination of some events. For this reason, the number of event termination criterion is limited to a practical minimum.

Each new irradiance value triggers the computation of all associated data metrics. The irradiance value and all associated metrics are maintained in data containers of fixed size, which is a configurable parameter that effectively represents the amount of irradiance and data metric “history” retained by the algorithm.

3.5.1 Data Metrics

In this section, data metrics, which embody the elemental components of event detection and characterization logic, are introduced.

Data metrics were chosen solely on the basis of demonstrable effectiveness. Any data metric with unequivocal event detection value was incorporated regardless of counter-arguments based on physical plausibility. In some cases, “intuitively obvious” data metrics that might seem to offer considerable potential were eventually determined to be ineffective.

A new set of data metrics is calculated with each data input (once per minute) and each data metric is stored in a fixed-size data container within the associated *SpectralLine* object (Section 2.4.2).

By intent, all algorithm data metrics are both intuitive and relatively simple to implement. Extremely complex data metrics, such as those derived from curve-fitting or elaborate signal processing models, are avoided because even a preliminary assessment of efficacy would likely require an excessive investment of time and resources with no assurance of improvement. Metrics derived from data mining techniques are excluded for similar reasons.

Most data metrics represent simple direct measures of irradiance state and/or evolution, such as mean, slope, data scatter, or monotonic rank (Section 3.5.1.5).

Many data metric methods have an associated data window that is characterized by a width and end point. The width is the number of data point within the window and the end point is the last data point within the window. The end point is often either the current irradiance data value or the irradiance value that immediately precedes the current value.

The effectiveness of a specific data metric may be critically dependent upon the associated time window. For example, a 5-minute slope leveling may be sufficient for event termination when irradiance levels have decreased to near pre-event levels, but a more robust requirement of 30-minute slope leveling may be a more appropriate event termination criterion if irradiance levels have stagnated near the half-maximum level.

The EUV event detection and characterization algorithm utilizes eight data metrics. Some data metrics are exclusively associated with either event initiation or termination, whereas other data metrics serve multiple purposes, including peak detection. Descriptions of these data metrics are presented below. The precise manner in which each data metric is used in event detection and characterization processing is discussed in Sections 3.5.3 through 3.5.7.

Finally, assessments of even relatively simple data metrics require a substantial analysis effort. A wide variety of candidate metrics are available, including those based on slope, monotonic rank, averages, medians, goodness of fit, etc. For each metric, the optimal data window must be determined. In addition to multiple input combinations, there is no single gauge of algorithm improvement or degradation. Missed detection rates that decrease only at the expense of an increased false alarm rate may not be desirable. Subjective judgments are required, and the evaluation process is resource and time intensive.

3.5.1.1 Simple Difference

This is the most trivial data metric. It is the difference between an irradiance value (or mean irradiance value) and a previous irradiance value (or mean irradiance value). The *simple difference* data metric is used by event termination logic that compares the current irradiance (or a mean of recent irradiance values) to the pre-event irradiance.

Data metric parameters:

- 1st data point (or mean value)
- 2nd data point (or mean value)

3.5.1.2 Mean Irradiance

The *mean irradiance* data metric is the arithmetic mean of irradiance values determined over a specified interval. When consistently less than the pre-event irradiance, the mean irradiance can be an event-terminating criterion.

Data metric parameters:

- Window size (number of data points in mean)
- Window lag (last data point relative to current data point)
- Invalid data tolerance (should increase/decrease with window size)

3.5.1.3 Time-Irradiance Slope

The *time-irradiance slope* is a simple data metric that is useful for the detection of event peaks and event termination. Slope reversals are primarily utilized in peak detection logic. Slope leveling can be an effective criterion to detect event termination when the post-event irradiance level exceeds the pre-event irradiance level (Figure 9).

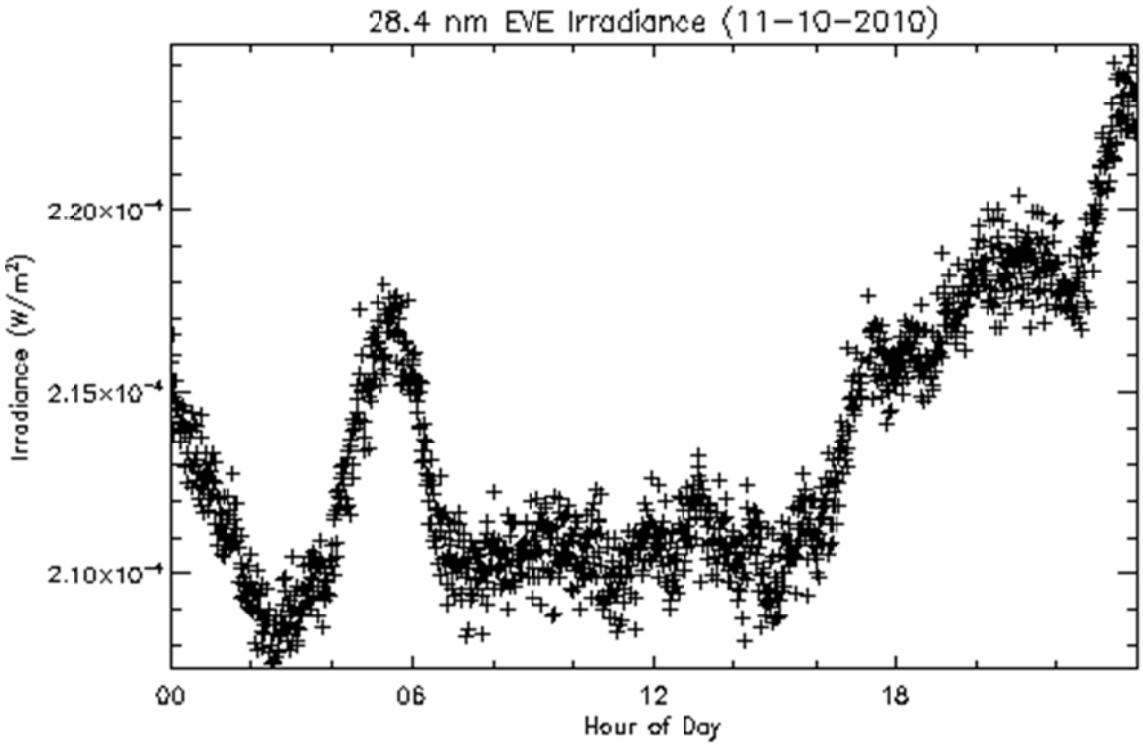

Figure 9. Example of an EUV event in which the post-event irradiance (approximately 7-12 UTC) exceeds the pre-event irradiance (approximately 2.5 UTC) by a non-negligible margin. In such circumstances, slope leveling can be a useful criterion for detecting event termination.

The slope is determined from a specified data interval that is defined by a width (i.e., number of data points) and an end point, which is usually the most recent irradiance value. The slope is that of the linear regression line determined by performing a least-squares best-fit through the specified data interval. The fifteen-minute slope data metric corresponding to the irradiance data in Figure 9 is presented in Figure 10. Although characterized by considerable scatter, note that the immediate post-event slope values are centered on zero with a reduced noise level. The degree of noise evident in the bottom panel of Figure 10 is fairly typical and illustrates why slope determinations alone are generally insufficient to reliably detect event termination.

Data metric parameters:

- Window size (number of data points in mean)
- Window lag (last data point relative to current data point)
- Invalid data tolerance (should increase/decrease with window size)

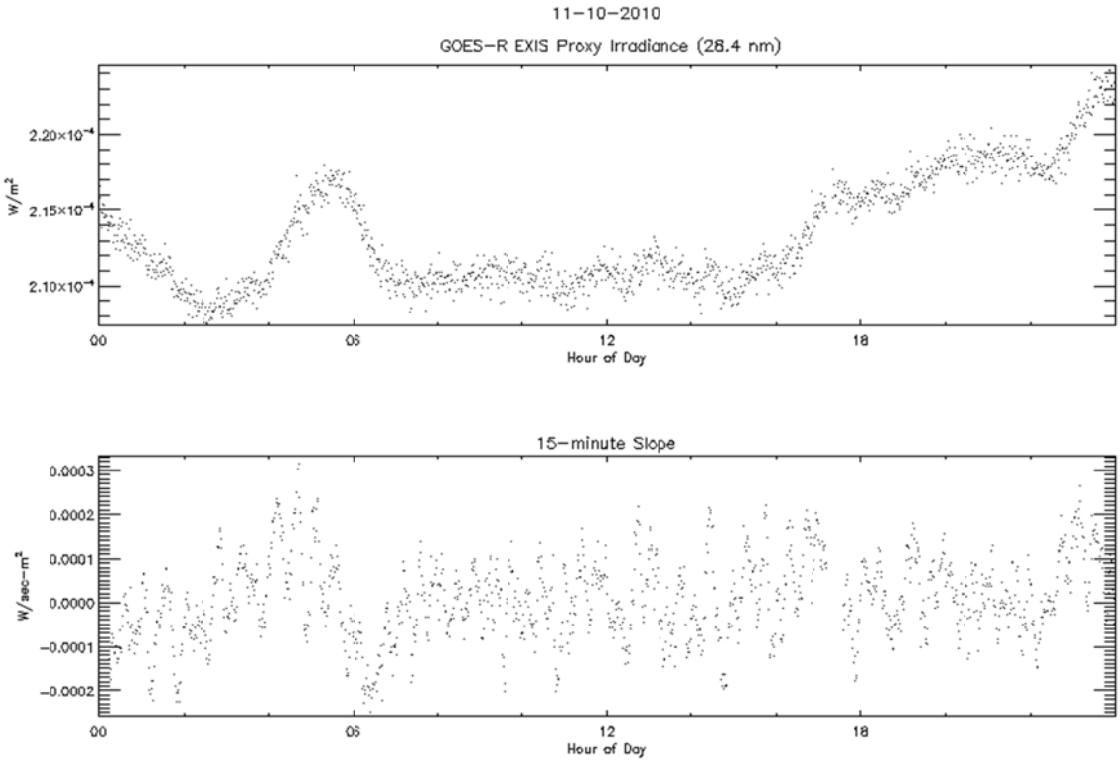

Figure 10. Example of the 15-minute slope data metric corresponding to the data in Figure 9. Top panel, time-series irradiance data. Bottom panel, 15-minute slope.

3.5.1.4 Standard Deviation

Standard deviation is an effective measure of data scatter that can be used as a baseline to assess the significance of a single irradiance variation. Standard deviation is used in conjunction with slope leveling to detect event termination when the post-event irradiance exceeds the pre-event irradiance. A near-zero slope combined with minimal data scatter may be an indication that irradiance fluctuations have “settled down” and the event has concluded.

Data metric parameters:

- Window size (number of data points in mean)
- Window lag (last data point relative to current data point)
- Invalid data tolerance (should increase/decrease with window size)

An example of the standard deviation data metric is shown in Figure 11.

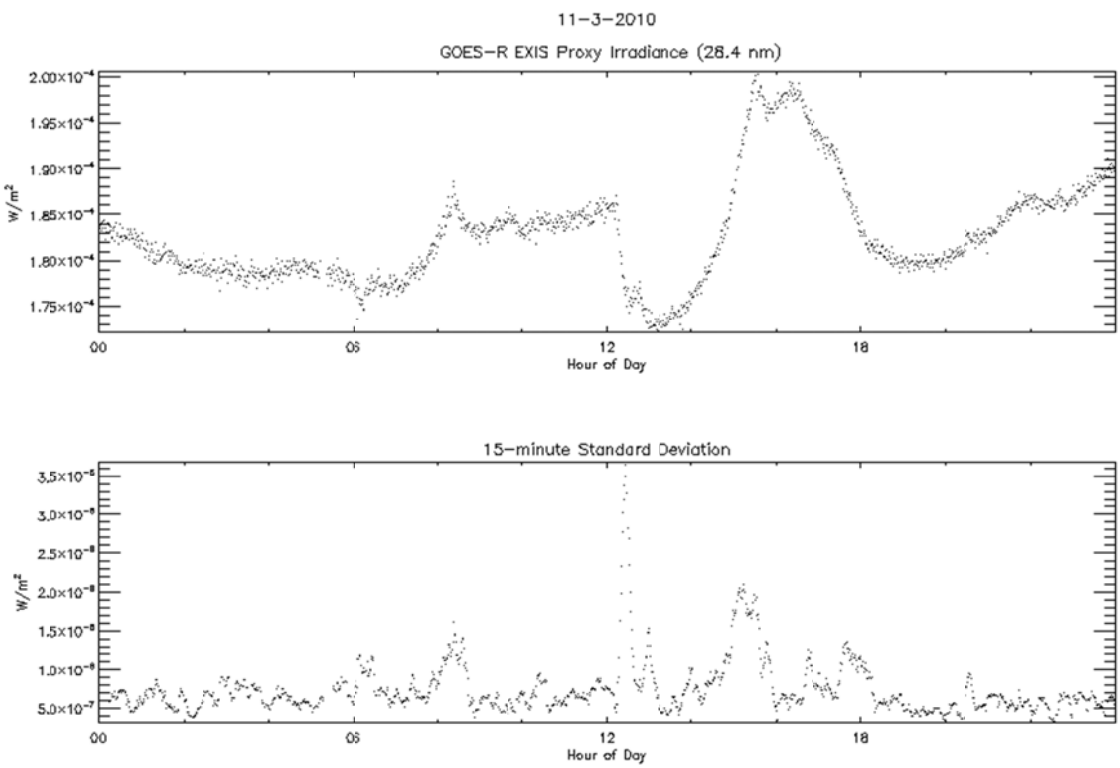

Figure 11. Example of the standard deviation for a 15-minute data interval that concludes with the current irradiance value. Top panel, time-series irradiance data. Bottom panel, the 15-minute standard deviation.

3.5.1.5 Monotonic Rank

Monotonic rank refers to the number of consecutive increases or decreases of the irradiance level. For example, if the current data point represents the third successive increase in irradiance, the associated monotonic rank is +3. If the current data point represents the fourth successive decrease in irradiance, the associated monotonic rank is -4. If the current data point represents the first

increase following any number of successive decreases, the monotonic rank is +1. Monotonic rank can be an effective event termination criterion.

Figure 12 illustrates the monotonic rank for a period of enhanced solar activity.

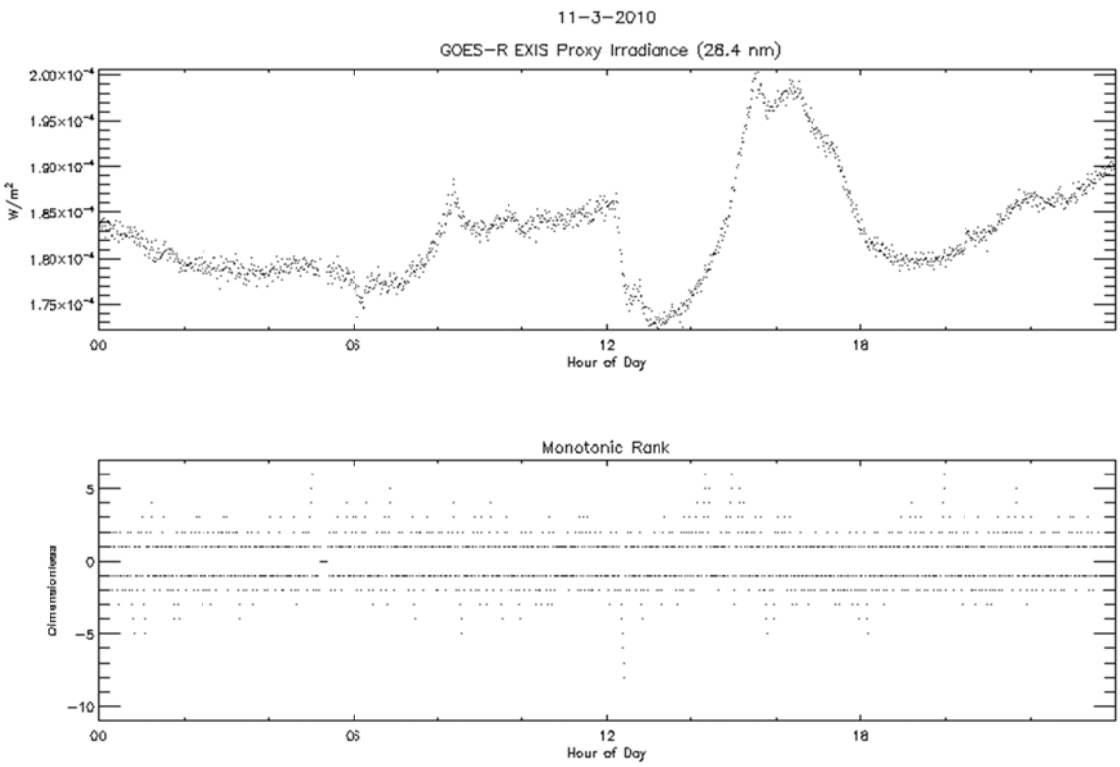

Figure 12. Example of the monotonic rank data metric. Top panel, time-series irradiance data. Bottom panel, the dimensionless monotonic rank. The period of zero monotonic rank corresponds to an interval of contiguous invalid data.

3.5.1.6 Monotonic Rank of the Mean

The effectiveness of monotonic rank in event termination may be enhanced when applied to filtered irradiance data. Preliminary filtering reduces the influence of minor data fluctuations.

Figure 13 illustrates the *monotonic rank of the mean* irradiance for the same period represented in Figure 12. It is evident that the monotonic rank derived from filtered data is more sensitive to event termination (e.g., 12 and 17.5 UTC) than the monotonic rank derived from unfiltered data.

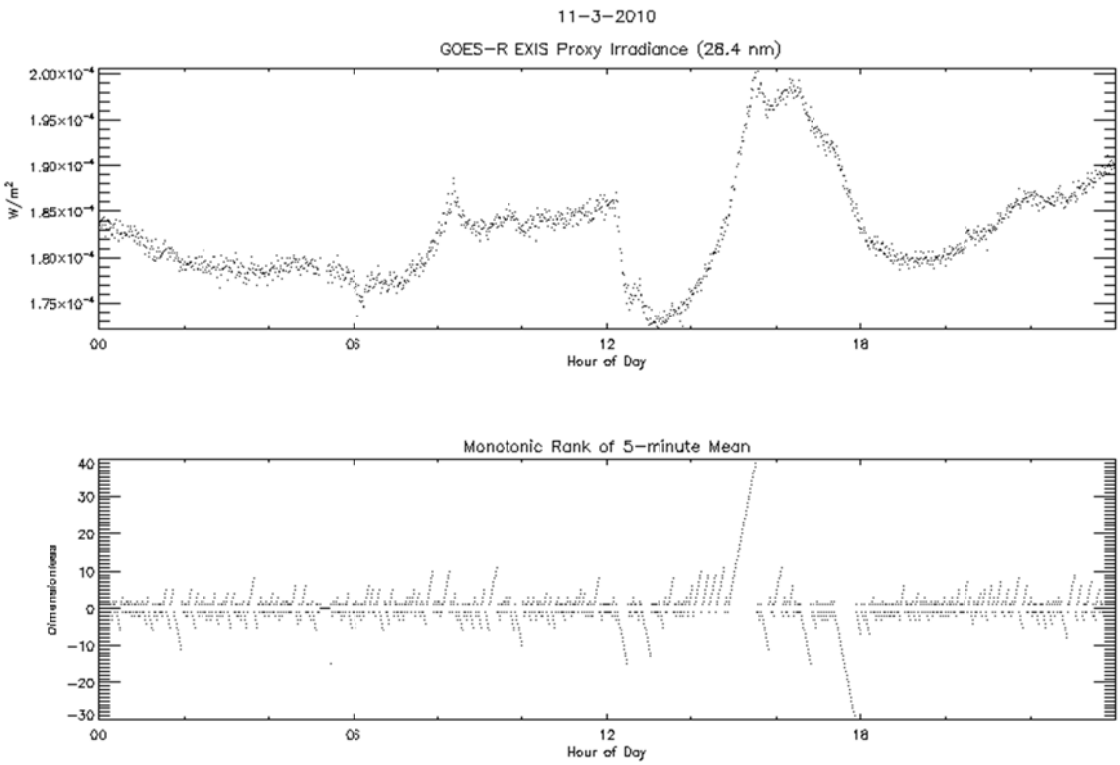

Figure 13. Example of the monotonic rank of 5-min mean irradiance data. In this case, monotonic rank was determined from the results of a five-minute mean filter applied to the irradiance data. Top panel, time-series irradiance data. Bottom panel, the dimensionless monotonic rank of the 5-min mean data.

3.5.1.7 Maximum Relative Increase

A relative irradiance increase that exceeds a critical threshold within a specified time limit has been determined to be an effective trigger for event initiation.

For this reason, a data metric is included that represents the maximum increase of the current irradiance relative to all previous irradiances within a specified data interval. This data metric is determined from the difference of the current irradiance and the minimum irradiance contained within the preceding data interval. The difference is divided by the minimum irradiance.

Figure 14 provides an example of the *maximum relative increase* data metric.

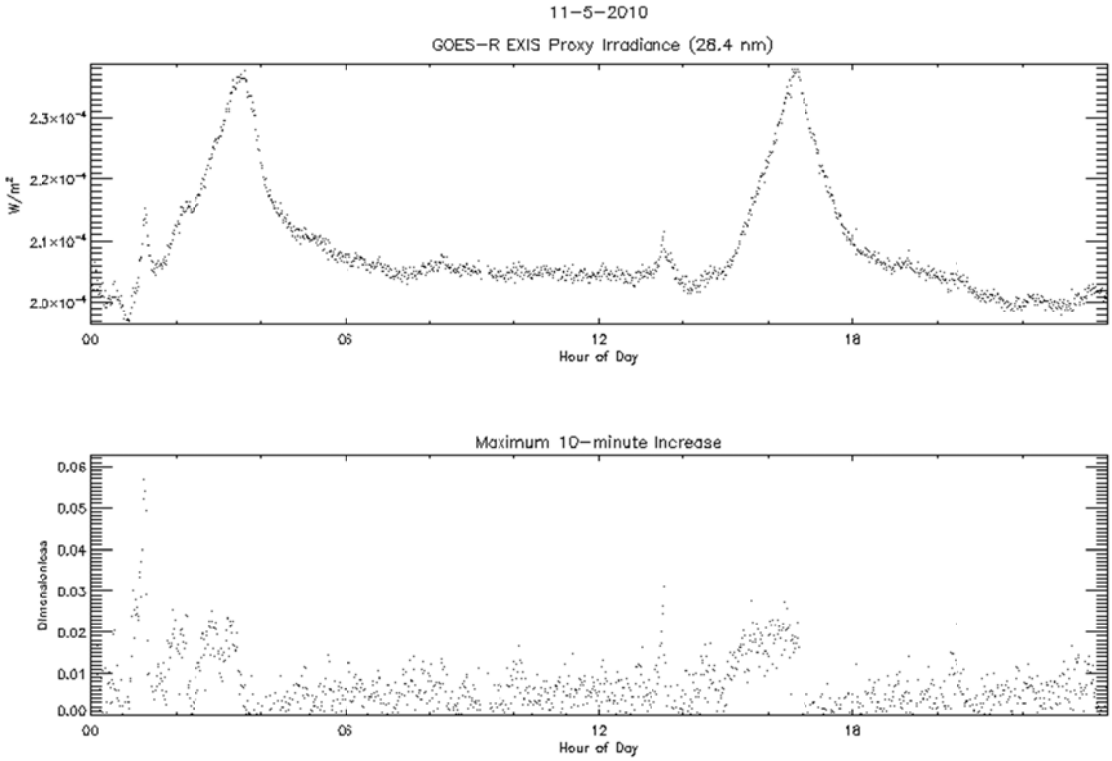

Figure 14. Example of 10-minute maximum relative increase data metric. Top panel, time-series irradiance. Bottom panel, maximum relative increase data metric.

The maximum relative increase is highly sensitive to the low-magnitude events (1 and 13.5 UTC) due to the sudden escalation of irradiance. Notice, however, that

this data metric also increases, although not as dramatically, during the ascending phase of the less abrupt high-magnitude events (2-5 and 15-18 UTC).

Data metric parameters:

- Window size (number of data points in mean)
- Window lag (last data point relative to current data point)
- Invalid data tolerance (should increase/decrease with window size)

3.5.1.8 Nth Percentile Difference

Although impulsively initiated events are readily detected with the *maximum relative increase* data metric (Section 3.5.1.7), slowly escalating events that may proceed erratically require an alternative detection strategy.

The *Nth percentile difference* data metric (Figure 15) represents the difference between an irradiance (usually the current value) and the nth percentile of irradiances over a specified range.

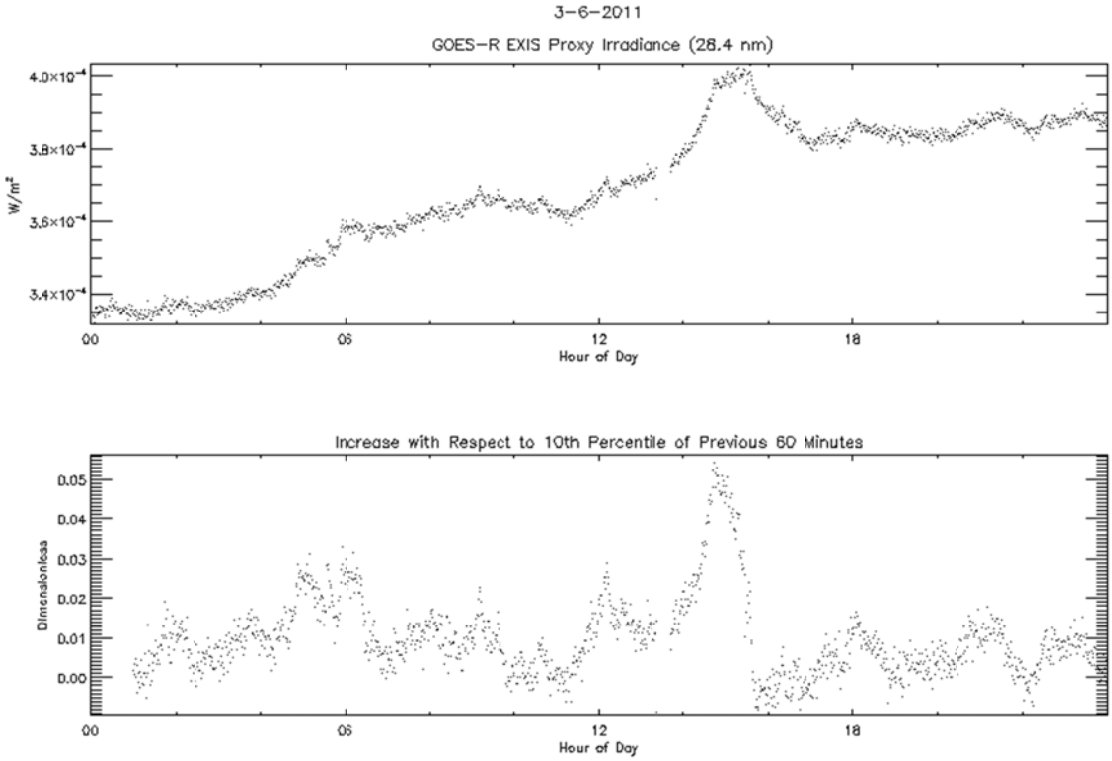

Figure 15. Example of the Nth percentile difference data metric for the 10th percentile of the preceding 60-minute data interval. Top panel, time series irradiance. Bottom panel, Nth percentile difference data metric.

Data metric parameters:

- Percentile
- Window size (number of data points in mean)
- Window lag (last data point relative to current data point)
- Invalid data tolerance (should increase/decrease with window size)

3.5.2 Missing/Invalid Input Data

All calculations of interval-based data metrics (basically all data metrics except simple difference and monotonic rank) include a parameter indicating the maximum number of invalid (bad or missing) irradiance values allowable.

Methods that calculate interval-based data metrics initially retrieve all relevant irradiance values within the specified time window. If the number of invalid irradiance values exceeds a configurable time-based limit, no calculations will be performed and the method will return an invalid indicator. An invalid data metric value cannot trigger an event initiation, termination or any other status modification (Section 3.4).

The algorithm continuously monitors accumulations of invalid data (Section 3.4). Three data outage tolerances are specified in the main configuration file. The first tolerance is the maximum number of consecutive invalid irradiance values allowed. The second and third tolerances are the maximum number of invalid irradiance values permitted within thirty-minute and sixty-minute intervals, respectively. Dual time-dependent tolerances allow the algorithm to respond to a lower level of difficulty if a data outage is persistent.

When any invalid data tolerance is exceeded, the algorithm enters an impaired state for the associated spectral line and a status of *IMPAIRED* is reported until a sufficient amount of valid data accumulates to allow recovery (same criteria for the startup mode – Section 3.4). When the algorithm enters an impaired state, any ongoing event is immediately terminated (with appropriate output file updates) and new events cannot be initiated until algorithm recovery.

Note that it is possible for the algorithm to be in an impaired state for one spectral line and fully functional for another spectral line.

3.5.3 Event Initiation Logic

Data metrics are calculated with each new input data value. At a given time, both the current set of data metrics is available, as well as a limited history of recent data metrics. The size of this “limited history” is a configurable algorithm parameter (Section 5.3.1).

The data metrics used to detect event initiation are the maximum relative increase (Section 3.5.1.7) and the Nth percentile difference (Section 3.5.1.8). Because the first of these data metrics is particularly sensitive to an abrupt irradiance increase, *false alarm suppression* (Section 3.5.3.2) is performed as a check on event initiation.

3.5.3.1 Start Time and Pre-event Irradiance

When a potentially significant irradiance increase is detected, the algorithm will search the recent irradiance history for a local minimum to estimate the actual start time and irradiance, which is referred to in this document as the pre-event irradiance (e.g., Figure 6). This process is necessary because detection time will invariably occur later than the actual start time.

The procedure for determining the actual start time is relatively simple. The mean irradiance is determined for a succession of past data intervals of configurable size N. If the current irradiance index is designated i, then the first mean irradiance corresponds to the interval i-N : i-1 the second mean irradiance corresponds to the interval i-2N : i-(N +1), etc. Note that the intervals do not overlap.

This process is illustrated schematically for a five-point (i.e., five-minute) data interval in Figure 16. The green X represents the detection time and irradiance, and the green box represents the actual start time and pre-event irradiance as determined by the algorithm. The first horizontal bar to the left of the detection point represents the mean irradiance for the five values that immediately precede detection. The second horizontal bar represents the mean irradiance for the preceding five data values and so on.

In the example presented in Figure 16, the five-minute mean “bottoms out” with the fourth data interval that precedes detection. The event start time is assigned the mid-point of the interval and pre-event irradiance is assigned the mean irradiance within the interval.

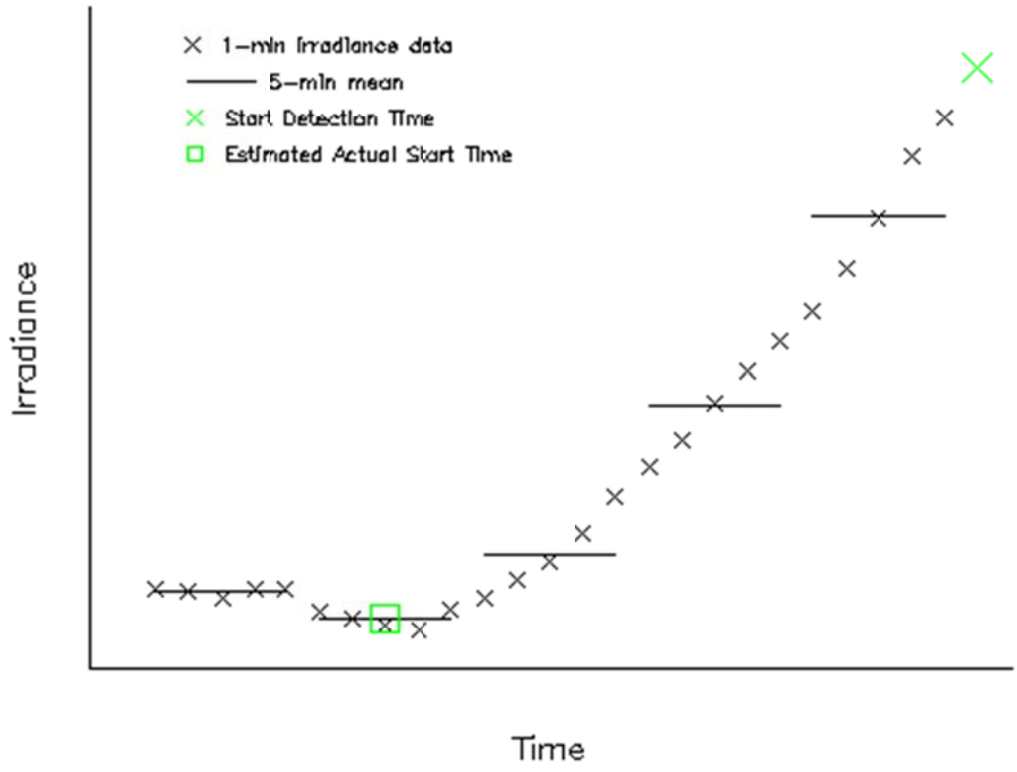

Figure 16. Schematic diagram of the "look back" processing used to determine the event start time and pre-event irradiance level. An interval of five data points is used in this example. The green X indicates the detection time and irradiance, and the green box indicates the estimated start time and irradiance. Horizontal bars represent the five-minute mean irradiance values for each corresponding data interval.

Careful consideration must be given to the data interval size used to determine the event start time and pre-event irradiance. If the interval is too small, the algorithm will have a tendency to identify minor departures from the predominant irradiance trend as the start time and irradiance. If the interval is too large, the algorithm may be relatively insensitive to the precise location of the start time and irradiance. A component of algorithm optimization should include an assessment of the ideal “look back” data interval size. The possible complications are illustrated schematically in Figure 17. Results presented in this document assume a “look back” interval of seven minutes.

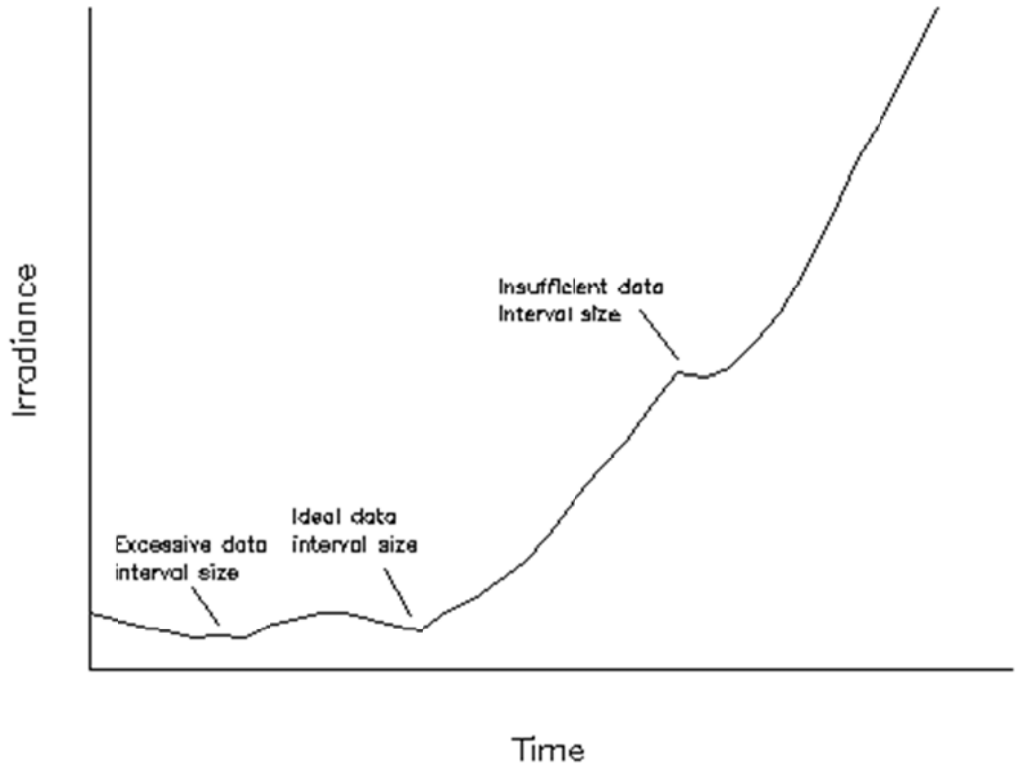

Figure 17. Schematic diagram illustrating how "look back" interval size may affect event start determination. An insufficient interval size will render the algorithm overly sensitive to minor departures from the predominant irradiance trend and result in a start time that is too late. An excessive data interval size may desensitize the algorithm to the actual event start and result in a start time that is too early.

Event start time and pre-event irradiance will have a critical influence on the assessment of detection latency, false alarm suppression (Section 3.5.3.2), half-maximum designation (Section 3.5.6), and event termination (Section 3.5.7).

3.5.3.2 False Alarm Suppression

False alarm suppression is the requirement that an irradiance increase at the time of potential event detection must exceed the estimated pre-event irradiance by a configurable threshold. The pre-event irradiance is determined by the post-detection “look back” processing discussed in Section 3.5.3.1. The false alarm suppression threshold for each spectral line is specified in the spectral line-specific parameter files.

For the results presented in this document (e.g., Appendix B), the false alarm suppression thresholds are set to 9.0% for the 28.4 nm spectral line, and 2.7% for both the 30.4 nm and 121.6 nm spectral lines.

When a data metric indicates a potentially significant irradiance increase, the pre-event irradiance is determined (Section 3.5.3.1). The relative difference between the current irradiance and the pre-event irradiance is compared to the configurable false alarm suppression threshold associated with the spectral line. If the irradiance difference does not exceed the threshold, false alarm suppression is invoked and event initiation is prevented. If the threshold is exceeded, event initiation occurs.

The irradiance difference threshold that modulates false alarm suppression may have a significant impact on detection latencies, particularly for non-impulsive events. Higher thresholds will prove more effective at false alarm suppression, but will also increase detection latencies. In some instances the delay between event start and event detection may exceed one hour. Note, however, that event detection usually occurs well before the event peak. In extreme cases, event detection will coincide with the event peak.

A useful way in which to consider false alarm suppression is that the algorithm “knows” that something is happening, but continues to monitor the irradiance increase until event initiation can be declared with a greater degree of confidence. In general, the minimum irradiance increase associated with a false alarm should be roughly equivalent to the false alarm suppression threshold. For example, if the false alarm suppression threshold is set to 9% for the 28.4 nm spectral line, nearly all 28.4 nm false alarms should be associated with irradiance increases greater than 9% and less than 10% (if the increase exceeds 10%, it is, by definition, not a false alarm).

Without false alarm suppression, the false alarm rate, which is the percentage of “detections” that do not correspond to true events (Section 2.3.1), would likely range from 75-90%, percentages that are clearly unacceptable. Figure 18 illustrates a series of false alarms (red data symbols) that are avoided by setting the suppression threshold to 5% or greater. Detection of the single true event is postponed by 21 minutes with a 9% false alarm suppression threshold (45 minute latency vs 24 minute latency with no suppression).

If a specific flag is set in the main configuration file, false alarm suppressions will be indicated in the one-minute updates with a status of WATCH.

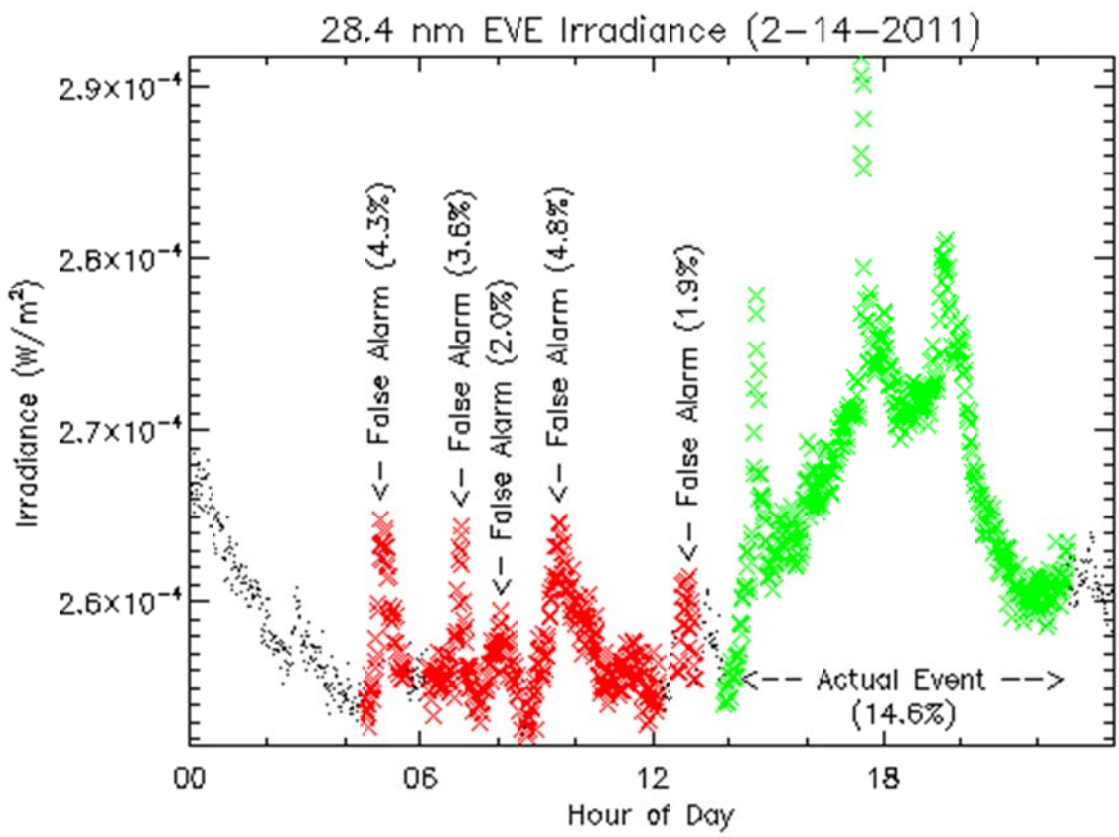

Figure 18. Example of false alarm suppression. Red represents false alarms that result from either no suppression or a suppression threshold that is less than 5%. Green represents the single true event. Percentages indicate the magnitude of the irradiance increase with respect to the pre-event irradiance.

False alarms may be eliminated entirely by setting the false alarm suppression threshold to the event definition threshold (3% for the 30.4 nm and 121.6 nm spectral lines, and 10% for the 28.4 nm spectral line). In this case, there will be an almost negligible detection latency penalty for the 30.4 nm line, a small detection latency penalty for the 121.6 nm spectral line, and a moderate detection latency penalty for the 28.4 nm spectral line.

3.5.3.3 28.4 nm Spectral Line Event Initiation

The following conditions will trigger event initiation for the 28.4 nm spectral line.

Event Initiation Condition 1
Single Data Metric: Maximum Relative Increase

The sole requirement of this condition is that the maximum relative increase within the most recent 10 minutes exceeds 0.025 (2.5 %).

If this condition is satisfied and false alarm suppression is not invoked, the algorithm will trigger an event initiation.

Event initiation criteria:

- Data metric: Maximum Relative Increase
- Data metric window size: 10
- Data metric window lag: 1
- Data metric invalid data tolerance: 2
- Data metric threshold: 2.5%
- False alarm suppression threshold: 9.0%

Event Initiation Condition 2
Single Data Metric: Nth Percentile Difference

Because the definition of an event for the 28.4 nm spectral line is a 10% increase in 5 hours or less, it may be assumed that an irradiance increase that will satisfy the definition must increase at a rate of at least 2% per hour at some point during the rising phase.

The sole requirement of the second condition is that the relative difference between the current irradiance value and the 10th percentile irradiance of the most recent 60 minutes exceeds 0.02 (2%).

If this condition is satisfied and false alarm suppression is not invoked, the algorithm will trigger an event initiation.

Event initiation criteria:

- Data metric: Nth Percentile Difference
- Data metric percentile: 10th
- Data metric window size: 60
- Data metric window lag: 1

- Data metric invalid data tolerance: 10
- Data metric threshold: 2.0%
- False alarm suppression threshold: 9.0%

3.5.3.4 30.4 nm Spectral Line Event Initiation

The following condition will trigger event initiation for the 30.4 nm spectral line.

<u>Event Initiation Condition 1</u>
Single Data Metric: Maximum Relative Increase

The sole requirement of this condition is that the maximum relative increase within the most recent 10 minutes exceeds 0.015 (1.5%).

If this condition is satisfied and false alarm suppression is not invoked, the algorithm will trigger an event initiation.

Event initiation criteria:

- Data metric: Maximum Relative Increase
- Data metric window size: 10
- Data metric window lag: 1
- Data metric invalid data tolerance: 2
- Data metric threshold: 1.5%
- False alarm suppression threshold: 2.7%

<u>Event Initiation Condition 2</u>
Single Data Metric: Nth Percentile Difference

Because the definition of an event for the 30.4 nm spectral line is a 3% increase in 2 hours or less, it may be assumed that an irradiance increase that will satisfy the definition must increase at a rate of at least 1.5% per hour at some point during the rising phase.

The sole requirement of the second condition is that the difference between the current irradiance value and the 10th percentile irradiance of the most recent 60 minutes exceeds 0.015 (1.5%).

If this condition is satisfied and false alarm suppression is not invoked, the algorithm will trigger an event initiation.

Event initiation criteria:

- Data metric: Nth Percentile Difference
- Data metric percentile: 10th
- Data metric window size: 60
- Data metric window lag: 1
- Data metric invalid data tolerance: 10
- Data metric threshold: 1.5%
- False alarm suppression threshold: 2.7%

3.5.3.5 121.6 nm Spectral Line Event Initiation

The following condition will trigger event initiation for the 28.4 nm spectral line.

<u>Event Initiation Condition 1</u>
Single Data Metric: Maximum Relative Increase

The sole requirement of this condition is that the maximum relative increase within the most recent 10 minutes exceeds 0.03 (3%).

If this condition is satisfied, the algorithm will trigger an event initiation.

Event initiation criteria:

- Data metric: Maximum Relative Increase
- Data metric window size: 10
- Data metric window lag: 1
- Data metric invalid data tolerance: 2
- Data metric threshold: 3.0%
- False alarm suppression threshold: 2.7%

<u>Event Initiation Condition 2</u>
Single Data Metric: Nth Percentile Difference

Because the definition of an event for the 121.6 nm spectral line is a 3% increase in 2 hours or less, it may be assumed that an irradiance increase that will satisfy the definition must increase at a rate of at least 1.5% per hour at some point during the rising phase.

The sole requirement of the second condition is that the difference between the current irradiance value and the 10th percentile irradiance of the most recent 60 minutes exceeds 0.015 (1.5%).

If this condition is satisfied and false alarm suppression is not invoked, the algorithm will trigger an event initiation.

Event initiation criteria:

- Data metric: Nth Percentile Difference
- Data metric percentile: 10th
- Data metric window size: 60
- Data metric window lag: 1
- Data metric invalid data tolerance: 10
- Data metric threshold: 1.5%
- False alarm suppression threshold: 2.7%

3.5.4 Event Rise and Event Decline Designation Logic

Between event initiation and event termination, every event status designator will be either *EVENT_RISE* or *EVENT_DECLINE*, unless superseded by a status of *EVENT_PEAK* or *HALF_MAX*.

The first status immediately following event initiation will be set to *EVENT_RISE*, regardless of the irradiance trend. After this initial *EVENT_RISE* status assignment, the event rise/decline designation logic will determine which status is assigned.

Unless superseded by an event termination, the first status immediately following event peak detection will be set to *EVENT_DECLINE*, regardless of the irradiance trend. After this initial *EVENT_DECLINE* status assignment, the event rise/decline designation logic will determine which status is assigned.

Event rise/decline logic includes a limited degree of “coasting”, which refers to the requirement that a trend reversal (i.e., transition from *EVENT_RISE* to *EVENT_DECLINE*, or vice versa) cannot occur in response to a single irradiance value. The purpose of coasting is to avoid “thrashing” of rise/decline status designators in response to noisy data.

The coasting requirement is that the *N* most recent irradiance values must oppose the existing trend if that trend is to be reversed. The results presented in this

document adopt a coasting parameter of 3. For example, if the current status is *EVENT_RISE*, a minimum of 3 consecutive irradiance decreases must occur to modify the status to *EVENT_DECLINE*. *N* is a configurable parameter.

With the exception of the requirement that an *EVENT_START* status is always followed by at least one *EVENT_RISE* status and an *EVENT_PEAK* status is always followed by at least one *EVENT_DECLINE* status, the event rise/decline status indicators are entirely independent of all other status indicators. For example, although the transition from *EVENT_RISE* to *EVENT_DECLINE* will often include a single intervening status of *EVENT_PEAK*, there is no requirement that a peak must separate the two statuses. Similarly, although a status of *EVENT_END* will often be immediately preceded by a status of *EVENT_DECLINE*, status coasting combined with event termination criteria may result in a direct transition from *EVENT_RISE* to *EVENT_END*.

3.5.5 Event Peak Detection Logic

The maximum irradiance of an event is monitored and updated throughout the duration of the event (Section 3.4) and is available as an input to algorithm logic at any point.

For all spectral lines, peak detection processing is activated only when the maximum event irradiance has not increased for a specified number of minutes or when a significant drop in irradiance has been detected (both configurable parameters).

The justification for this delay is to reduce repetitive peak detections and reporting triggered by fluctuations in noisy data. When this condition has been satisfied, peak detection analysis is performed with each new data point received unless the maximum event irradiance increases once again, at which point peak detection processing is suspended for at least the minimum designated period of time.

3.5.5.1 28.4 nm Event Peak Detection

Peak detection for the 28.4 nm spectral line is triggered by a single condition.

The time-irradiance slope is determined using a 5-minute window with no lag (i.e., the current irradiance represents the final data value) and an invalid data tolerance of 1. The peak detection requirement, as determined from proxy data, is that the current 5-minute slope is less than -2.3×10^{-9} W/m^2-sec.

The slope condition is not tested unless the maximum event irradiance is at least 3 minutes old or the irradiance has decreased by at least 20% from the peak value (relative to the pre-event irradiance).

Event peak criteria:

- At least 3 minutes since event maximum
- Data metric: Time-Irradiance Slope
- Data metric window size: 5
- Data metric window lag: 0
- Data metric invalid data tolerance: 1
- Data metric threshold: -2.3 x10^{-9} W/m^2-sec

3.5.5.2 30.4 nm Event Peak Detection

Peak detection for the 30.4 nm spectral line is triggered by a single condition.

The time-irradiance slope is determined using a 5-minute window with no lag (i.e., the current irradiance represents the final data value) and an invalid data tolerance of 1. The peak detection requirement is that the current 5-minute slope is less than -1.16 x10^{-8} W/m^2-sec.

The slope condition is not tested unless the maximum event irradiance is at least 3 minutes old or the irradiance has decreased by at least 20% from the peak value (relative to the pre-event irradiance).

Event peak criteria:

- At least 3 minutes since event maximum or 20% irradiance decrease
- Data metric: Time-Irradiance Slope
- Data metric window size: 5
- Data metric window lag: 0
- Data metric invalid data tolerance: 1
- Data metric threshold: -1.16 x10^{-8} W/m^2-sec

3.5.5.3 121.6 nm Event Peak Detection

Peak detection for the 121.6 nm spectral line is triggered by a single condition.

The time-irradiance slope is determined using a 5-minute window with no lag (i.e., the current irradiance represents the final data value) and an invalid data tolerance of 1. The peak detection requirement is that the current 5-minute slope is less than -1.16×10^{-8} W/m^2-sec.

The slope condition is not tested unless the maximum event irradiance is at least 3 minutes old or the irradiance has decreased by at least 20% from the peak value (relative to the pre-event irradiance).

Event peak criteria:

- At least 3 minutes since event maximum or 20% irradiance decrease
- Data metric: Time-Irradiance Slope
- Data metric window size: 5
- Data metric window lag: 0
- Data metric invalid data tolerance: 1
- Data metric threshold: -1.16×10^{-8} W/m^2-sec

3.5.6 Event Half-Maximum Designation Logic

The half-maximum condition requires that the current irradiance must be less than the average of the pre-event irradiance and the maximum event irradiance.

Algorithm logic for half-maximum detection is initiated only subsequent to the detection of the first event peak.

After a half-maximum condition has been reported, the algorithm will not attempt to detect a new half-maximum condition unless a new (and greater) peak is detected.

3.5.7 Event Termination Logic

Regardless of data metric-based analysis of event evolution, if an event exceeds the configurable duration limit, the event will be immediately terminated. Note that this limit may be deactivated (see the *EUVS04 User Guide*).

A more common event termination criterion is the difference between the current irradiance and the pre-event irradiance (Figure 6). Alternatively, slope-based data

metrics are effective at establishing event termination when the post-event irradiance background level exceeds the pre-event irradiance background level (e.g., Figure 9). In this case, a “leveling criterion” must be adopted to identify a reasonable end point of an EUV event. Every spectral line must include at least one termination criterion based on “slope leveling” to prevent “runaway event processing” associated with post-event irradiance levels that exceed pre-event irradiance levels.

Some event termination criteria are applied only when the irradiance has decreased below 25% of the maximum (relative to the pre-event irradiance, not zero). Event termination criteria are more stringent nearer the event peak and more relaxed following the decrease below 25% maximum irradiance. This allows the algorithm to more effectively discriminate between a rapid succession of multiple short-lived events and an extended duration event with multiple peaks.

When event termination is triggered, an algorithm status of *MONITORING* is resumed and all flags and counters are reset to pre-event values.

3.5.7.1 28.4 nm Spectral Line Event Termination

Three conditions can trigger event termination in the 28.4 nm spectral line.

<u>Event Termination Condition 1</u>
Two Data Metrics: Monotonic Rank and Mean

The monotonic rank of the 5-minute mean irradiance must be greater than or equal to 4. This relatively mild condition for event termination is only applied after the irradiance has decreased below 25% of the maximum event irradiance.

If this condition is satisfied, the algorithm will trigger event termination.

Event termination criteria:

- Irradiance: <25% maximum
- Data metric: Monotonic Rank of the 5-min Mean
- Data metric window size: 5
- Data metric window lag: 0
- Data metric invalid data tolerance: 1
- Data metric threshold: 4

<u>Event Termination Condition 2</u>

One Data Metric: Mean Irradiance

The mean irradiance is determined using a 5-minute window with no lag (i.e., the current irradiance represents the final data value) and an invalid data tolerance of 1. The requirement is that the 5-minute mean is less than the pre-event irradiance.

If this condition is satisfied, the algorithm will trigger event termination.

Event termination criteria:

- Data metric: Mean
- Data metric window size: 5
- Data metric window lag: 0
- Data metric invalid data tolerance: 1
- Data metric threshold: < Pre-event irradiance

<u>Event Termination Condition 3</u>
Two Data Metrics: Time-Irradiance Slope and Standard Deviation

The slope is determined using a 10-minute window with no lag (i.e., the current irradiance represents the final data value) and an invalid data tolerance of 2. The requirement is that the absolute value of the 10-minute slope is less than 5.2×10^{-10} W/m^2-sec.

The standard deviation is determined using a 30-minute window with no lag (i.e., the current irradiance represents the final data value) and an invalid data tolerance of 5. The requirement is that standard deviation is less than 1.75×10^{-7} W/m^2.

If both conditions are satisfied, the algorithm will trigger event termination.

Event termination criteria:

- Data metrics: Time-irradiance Slope and Standard Deviation
- Data metric window sizes: 10 (slope) and 30 (σ)
- Data metric window lags: Both 0
- Data metric invalid data tolerances: 2 (slope) and 5 (σ)
- Data metric thresholds: 5.2×10^{-10} W/m^2-sec (slope) and 1.75×10^{-7} W/m^2 (σ)

3.5.7.2 30.4 nm Spectral Line Event Termination

Three conditions can trigger event termination in the 30.4 nm spectral line.

Event Termination Condition 1
Two Data Metrics: Monotonic Rank and Mean

The monotonic rank of the 5-minute mean irradiance must be greater than or equal to 4. This relatively mild condition for event termination is only applied after the irradiance has decreased below 25% of the maximum event irradiance.

If this condition is satisfied, the algorithm will trigger event termination.

Event termination criteria:

- Irradiance: <25% maximum
- Data metric: Monotonic Rank of the 5-min Mean
- Data metric window size: 5
- Data metric window lag: 0
- Data metric invalid data tolerance: 1
- Data metric threshold: 4

Event Termination Condition 2
One Data Metric: Simple difference

At least 4 of the most recent 5 irradiance values must be less than the pre-event irradiance.

If this condition is satisfied, the algorithm will trigger event termination.

Event termination criteria:

- Data metric: Simple Difference
- Data metric window size: 5
- Data metric window lag: 0
- Data metric invalid data tolerance: 0
- Data metric threshold: At least 4 must be less than the pre-event irradiance

Event Termination Condition 3
Two Data Metrics: Time-Irradiance Slope and Standard Deviation

The slope is determined using a 10-minute window with no lag (i.e., the current irradiance represents the final data value) and an invalid data tolerance of 2. The requirement is that the absolute value of the 10-minute slope is less than 5.8×10^{-10} W/m^2-sec.

The standard deviation is determined using a 10-minute window with no lag (i.e., the current irradiance represents the final data value) and an invalid data tolerance of 2. The requirement is that standard deviation is less than 5.0 x10^{-7} W/m^2.

If both conditions are satisfied, the algorithm will trigger event termination.

Event termination criteria:

- Data metrics: Time-irradiance Slope and Standard Deviation
- Data metric window sizes: Both 10
- Data metric window lags: Both 0
- Data metric invalid data tolerances: Both 2
- Data metric thresholds: 5.8 x10^{-10} W/m^2-sec (slope) and 5.0 x10^{-7} W/m^2 (σ)

3.5.7.3 121.6 nm Spectral Line Event Termination

Three conditions can trigger event termination in the 121.6 nm spectral line.

<u>Event Termination Condition 1</u>
Two Data Metrics: Monotonic Rank and Mean

The monotonic rank of the 5-minute mean irradiance must be greater than or equal to 4. This relatively mild condition for event termination is only applied after the irradiance has decreased below 25% of the maximum event irradiance.

If this condition is satisfied, the algorithm will trigger event termination.

Event termination criteria:

- Irradiance: <25% maximum
- Data metric: Monotonic Rank of the 5-min Mean
- Data metric window size: 5
- Data metric window lag: 0
- Data metric invalid data tolerance: 1
- Data metric threshold: 4

<u>Event Termination Condition 2</u>
One Data Metric: Simple difference

At least 4 of the most recent 5 irradiance values must be less than the pre-event irradiance.

If this condition is satisfied, the algorithm will trigger event termination.

Event termination criteria:

- Data metric: Simple Difference
- Data metric window size: 5
- Data metric window lag: 0
- Data metric invalid data tolerance: 0
- Data metric threshold: At least 4 must be less than the pre-event irradiance

<u>Event Termination Condition 3</u>
Two Data Metrics: Time-Irradiance Slope and Standard Deviation

The slope is determined using a 10-minute window with no lag (i.e., the current irradiance represents the final data value) and an invalid data tolerance of 2. The requirement is that the absolute value of the 10-minute slope is less than 5.8×10^{-10} W/m^2-sec.

The standard deviation is determined using a 10-minute window with no lag (i.e., the current irradiance represents the final data value) and an invalid data tolerance of 2. The requirement is that standard deviation is less than 5.0×10^{-7} W/m^2.

If both conditions are satisfied, the algorithm will trigger event termination.

Event termination criteria:

- Data metrics: Time-irradiance Slope and Standard Deviation
- Data metric window sizes: Both 10
- Data metric window lags: Both 0
- Data metric invalid data tolerances: Both 2
- Data metric thresholds: 5.8×10^{-10} W/m^2-sec (slope) and 5.0×10^{-7} W/m^2 (σ)

3.6 Input Data

This section specifies the content, format and temporal requirements of the algorithm input data. Note that it does not address the data ingest process, which is not a deliverable algorithm component and, unless specifically designated as a future Algorithm Working Group task, is solely the responsibility of the ground system contractor.

Input data consists of one-minute averages of the 28.4 nm, 30.4 nm and 121.6 nm irradiances. All input data lines must be of identical length. If this is not the case, the data ingestor will not function properly.

An external script or application will be necessary to reformat the GOES-R EXIS output into the expected format for the EUV event detection and characterization algorithm. *External* refers to the fact that the script will not be part of either the GOES-R EXIS Level 1B processing or the EUV event detection and characterization algorithm.

3.6.1 Data Acquisition

Input data shall be available at a rate of once per minute. Given the temporal resolution of GOES-R EXIS output, this is a reasonable requirement.

3.6.2 Data Format

Each input data line shall consist of a fractional Julian Date (which also represents time) and three irradiance values, one for the 28.4 nm spectral line, one for the 30.4 nm spectral line, and one for the 121.6 nm spectral line. Each value will be delimited by white space.

It is assumed that the date-time value will be represented by the Julian Date in fixed decimal (non-scientific notation) format with a minimum of six significant post-decimal figures.

It is assumed that valid irradiance values will be represented in W/m^2 using scientific notation that includes four significant post-decimal figures.

All input data lines must be of identical length. If this is not the case, the data ingestor will not function properly.

3.6.3 Validity Indicators

Invalid (bad or missing) input irradiance values shall be indicated as -1.0000e+05.

3.6.4 Data Input Example

An example of the input data format is shown. The first column represents time, the second column represents the 28.4 nm irradiance, the third column represents the 30.4 nm irradiance, and the fourth column represents the 121.6 nm irradiance.

```
...
2455406.502083   2.0336e-04   1.8991e-03   7.2016e-03
2455406.502778   2.0281e-04   1.9022e-03   7.2413e-03
2455406.503472   2.0264e-04   1.8973e-03   7.2544e-03
2455406.504167   2.0268e-04   1.9006e-03  -1.0000e+05
2455406.504861   2.0247e-04   1.9114e-03  -1.0000e+05
2455406.505556   2.0323e-04   1.8991e-03  -1.0000e+05
2455406.506250   2.0274e-04   1.9064e-03   7.2225e-03
2455406.506944   2.0344e-04   1.8980e-03   7.2292e-03
2455406.507639   2.0359e-04   1.8985e-03   7.2250e-03
...
```

3.7 Output

Algorithm output will be in the form of human-readable fixed-format ASCII text files that can be parsed to provide input for post-processing applications, such as a user display.

Note that applications to parse algorithm output files and/or display algorithm results are not deliverable components of this algorithm. Unless specifically designated as a future Algorithm Working Group task, it is assumed that the ground system contractor will be solely responsible for these items.

3.7.1 Output Files

The algorithm will produce three output file types: log files, one-minute update files, and post-event summary files.

<u>Log File</u>
A log file will be created to provide diagnostic information, such as event detection latencies or the specific criterion that triggered a status change (e.g., event termination was triggered by the dual 10-slope leveling and 10-minute standard deviation reduction criterion). Log file inspection is not intended for casual users.

<u>One-minute Update Files</u>

One-minute update files will be produced for each spectral line. These will be daily files that are opened at the start of the UTC day and closed at the end of the UTC day. During inactive periods, minimal output consisting of a date-time stamp, the current irradiance, and a system status of *MONITORING* will be issued once each minute. Additional information describing various aspects of event evolution will be reported at one-minute intervals during periods of EUV activity.

Output will be produced at a rate of once per minute, regardless of the level of solar activity. Each archived one-minute update file should have 1440 entries. Three one-minute update files are produced – one for each spectral line.

Post-event Summary Files
A file containing one-line post-event summaries will also be produced. This file will not be daily, but will continually grow and be of indefinite length. It will combine summaries of events from all spectral lines.

3.7.2 Output Data Content

Log Files
Log files will include diagnostic information not intended for the casual user. Log file information will primarily be useful for assessing algorithm skill and/or the re-optimization of algorithm parameters.

For each event detected, the log file will record, at minimum, the event initiation criteria (Section 3.5.3), the detection latency, the event termination criteria (Section 3.5.7), and the event duration.

Errors, warnings and algorithm failure diagnostics, as well as data outages (i.e., IMPAIRED status), will also be recorded in the log file.

There will be three types of log file entries

- DIAGNOSTIC for algorithm processing details
- WARNING for non-fatal algorithm problems
- ERROR for algorithm-terminating violations

One-minute Update Files
During periods of inactivity, excluding startup and impaired periods (Section 3.4), when there is no ongoing EUV event, minimal output will be produced each minute consisting of a spectral line identifier, date-time information, and the most recent irradiance measurement. A status of *MONITORING* will also be reported to

indicate a lack of significant activity and as confirmation that that the application continues to monitor solar irradiance input data.

When an event is detected, a series of event descriptors will be output for the duration of the event, beginning with a single event initiation indicator (*EVENT_START*) and concluding with a single event termination indicator (*EVENT_END*).

Event status will be updated each minute and all updates will include the current time and irradiance.

In general, when the current event irradiance is trending upward, an event status of *EVENT_RISE* is reported. When the opposite condition exists, an event status of *EVENT_DECLINE* is reported. When a local maximum is detected, an event status of *EVENT_PEAK* is reported, provided that the associated maximum exceeds all previous maximum values measured during the event.

See Figure 7 for a schematic diagram illustrating one-minute updates.

When an event is detected, the algorithm will attempt to determine an appropriate pre-event irradiance level for the event (Section 3.5.3.1). The most recent interval during which the seven-minute average was at a local minimum is used to identify the actual start period of the event (i.e., start time as opposed to detection time). The mean irradiance and mid-point time from this period will be selected as the pre-event irradiance and actual start time.

To clarify, the pre-event irradiance level is not simply the irradiance at the time of event detection. The pre-event irradiance represents the last period at which the irradiance could be considered “normal”, and will represent a time prior to event detection. In nearly all cases, detection time irradiance will exceed the pre-event irradiance.

Peak irradiance will be tracked and reported throughout the event duration. The peak irradiance represents the greatest irradiance value thus far measured during the event. The peak irradiance is expected to increase progressively until a peak is attained, at which point it will remain constant until either the event is terminated or a greater peak is attained and reported.

Whenever the current irradiance value during an ongoing event decreases below the average of the pre-event and maximum event irradiances, a half-maximum

irradiance indicator (*HALF_MAX*) is reported. As discussed previously (Section 3.4), the half-maximum irradiance status is included for consistency with legacy X-ray flare detection and characterization algorithms.

When event termination is detected, a one-time status of *EVENT_END* is reported, after which the status returns to *MONITORING* to indicate an absence of activity.

Post-event Summary Files
Single-line post-event summaries will consist of a spectral line identifier, start time/irradiance, peak time/irradiance, and end time/irradiance, as well as the mean event irradiance, the event duration in minutes, the total integrated irradiance, and the maximum irradiance increase as a percentage. The rate at which entries will be appended to this file will vary depending upon the rate at which new events are detected.

3.7.3 Output Data Format

One-minute Update Files
Data columns will be fixed format and delimited by white space. A configurable parameter can be set that will force the inclusion of a descriptive header at the top of each file.

The first output column will consist of one of the following spectral line identifiers: “28.4nm”, “30.4nm”, or “121.6nm”. Because the one-minute update files are spectral line-specific, the first-column value will be repeated identically throughout the entire file.

The second output column will indicate the date in conventional (*YYYYMMDD*) format. This will always be represented as an eight-digit integer value, and the month and/or day value will be padded with a leading zero when necessary. Because the one-minute update files are organized by day, the second-column value will be repeated identically throughout the entire file.

The third output column will contain a four-digit integer representing the hour and minute of the corresponding irradiance value. The format will be *HHMM* and the hour and/or minute value will be padded with a leading zero when necessary.

The fourth output column will represent the fractional Julian Date, which includes time, associated with the irradiance value. It will be expressed as a fixed decimal (non-scientific notation) format with six significant post-decimal figures.

When relevant, the fifth output column will indicate the actual start time of an ongoing event as a fractional Julian date. Note that this time is not equivalent to the event detection time, which will always be later than the actual start time of the event. The event start time will be represented by a fixed decimal (non-scientific notation) format with six significant post-decimal figures. Because there can only be a single event start time, this value will remain constant throughout the event duration. In the absence of an ongoing event, this column will contain -1.0.

The sixth output column will always indicate the current (i.e., most recently reported) irradiance value, regardless of whether or not an event is in progress. The current irradiance will be represented in W/m^2 using scientific notation that includes three significant post-decimal figures.

When relevant, the seventh output column will indicate the pre-event irradiance associated with an ongoing EUV event. This is the irradiance that is associated with the actual start time of the event, not the event detection time. The pre-event irradiance will be represented in W/m^2 using scientific notation that includes three significant post-decimal figures. Because there can only be a single event pre-event irradiance, this value will remain constant throughout the event duration. In the absence of an ongoing event, this column will contain -1.000e+05.

When relevant, the eighth output column will indicate the maximum irradiance thus far associated with an ongoing EUV event. This value will be updated each time a greater maximum event irradiance is detected, and will be represented in W/m^2 using scientific notation that includes three significant post-decimal figures. In the absence of an ongoing event, this column will contain -1.000e+05.

When relevant, the ninth output column will contain the time associated with the maximum event irradiance as a fractional Julian date. This time will be that associated with the time of the actual maximum irradiance value and not the subsequent time at which the peak was detected. The maximum irradiance time will be updated each time the corresponding maximum irradiance value is updated, and will be represented by a fixed decimal (non-scientific notation) format with six significant post-decimal figures. In the absence of an ongoing event, this column will contain -1.0.

The tenth output column will consist of one of the event status indicators described in Section 3.2.1.

The following are selected one-minute updates extracted from output associated with a single 28.4 nm event that occurred on November 5, 2010. Note that inclusion of the descriptive file header is a configurable option.

```
# UNITS: Time (Julian Date), Irradiance (W/m^2)
#
# Line   Current                        Start           Current     Pre-event   Maximum     Max Irradiance  Event
# ID     YYYYMMDD HHMM Time             Time            Irradiance  Irradiance  Irradiance  Time            Status
# ------ -------- ---- --------------   --------------  ----------  ----------  ----------  --------------- ----------
...
28.4nm   20101105 1544 2455506.155556 -1.0             2.175e-04  -1.000e+05  -1.000e+05  -1.0             MONITORING
28.4nm   20101105 1545 2455506.156250  2455506.090278  2.187e-04   2.021e-04   2.187e-04   2455506.156250  EVENT_START
28.4nm   20101105 1546 2455506.156944  2455506.090278  2.185e-04   2.021e-04   2.187e-04   2455506.156250  EVENT_RISE
28.4nm   20101105 1547 2455506.157639  2455506.090278  2.196e-04   2.021e-04   2.196e-04   2455506.157639  EVENT_RISE
28.4nm   20101105 1548 2455506.158333  2455506.090278  2.206e-04   2.021e-04   2.206e-04   2455506.158333  EVENT_RISE
28.4nm   20101105 1549 2455506.159028  2455506.090278  2.203e-04   2.021e-04   2.206e-04   2455506.158333  EVENT_RISE
28.4nm   20101105 1550 2455506.159722  2455506.090278  2.204e-04   2.021e-04   2.206e-04   2455506.158333  EVENT_RISE
28.4nm   20101105 1551 2455506.160417  2455506.090278  2.209e-04   2.021e-04   2.209e-04   2455506.160417  EVENT_RISE
28.4nm   20101105 1552 2455506.161111  2455506.090278  2.207e-04   2.021e-04   2.209e-04   2455506.160417  EVENT_RISE
...
28.4nm   20101105 1640 2455506.194444  2455506.090278  2.386e-04   2.021e-04   2.386e-04   2455506.194444  EVENT_RISE
28.4nm   20101105 1641 2455506.195139  2455506.090278  2.373e-04   2.021e-04   2.386e-04   2455506.194444  EVENT_RISE
28.4nm   20101105 1642 2455506.195833  2455506.090278  2.365e-04   2.021e-04   2.386e-04   2455506.194444  EVENT_RISE
28.4nm   20101105 1643 2455506.196528  2455506.090278  2.361e-04   2.021e-04   2.386e-04   2455506.194444  EVENT_PEAK
28.4nm   20101105 1644 2455506.197222  2455506.090278  2.361e-04   2.021e-04   2.386e-04   2455506.194444  EVENT_DECLINE
28.4nm   20101105 1645 2455506.197917  2455506.090278  2.341e-04   2.021e-04   2.386e-04   2455506.194444  EVENT_DECLINE
28.4nm   20101105 1646 2455506.198611  2455506.090278  2.341e-04   2.021e-04   2.386e-04   2455506.194444  EVENT_DECLINE
...
28.4nm   20101105 1718 2455506.220833  2455506.090278  2.214e-04   2.021e-04   2.386e-04   2455506.194444  EVENT_DECLINE
28.4nm   20101105 1719 2455506.221528  2455506.090278  2.211e-04   2.021e-04   2.386e-04   2455506.194444  EVENT_DECLINE
28.4nm   20101105 1720 2455506.222222  2455506.090278  2.203e-04   2.021e-04   2.386e-04   2455506.194444  HALF_MAX
28.4nm   20101105 1721 2455506.222917  2455506.090278  2.206e-04   2.021e-04   2.386e-04   2455506.194444  EVENT_DECLINE
28.4nm   20101105 1722 2455506.223611  2455506.090278  2.206e-04   2.021e-04   2.386e-04   2455506.194444  EVENT_DECLINE
...
28.4nm   20101105 1855 2455506.288194  2455506.090278  2.054e-04   2.021e-04   2.386e-04   2455506.194444  EVENT_DECLINE
28.4nm   20101105 1856 2455506.288889  2455506.090278  2.056e-04   2.021e-04   2.386e-04   2455506.194444  EVENT_DECLINE
28.4nm   20101105 1857 2455506.289583  2455506.090278  2.059e-04   2.021e-04   2.386e-04   2455506.194444  EVENT_RISE
28.4nm   20101105 1858 2455506.290278  2455506.090278  2.052e-04   2.021e-04   2.386e-04   2455506.194444  EVENT_RISE
28.4nm   20101105 1859 2455506.290972  2455506.090278  2.061e-04   2.021e-04   2.386e-04   2455506.194444  EVENT_RISE
28.4nm   20101105 1900 2455506.291667  2455506.090278  2.062e-04   2.021e-04   2.386e-04   2455506.194444  EVENT_RISE
28.4nm   20101105 1901 2455506.292361  2455506.090278  2.062e-04   2.021e-04   2.386e-04   2455506.194444  EVENT_RISE
28.4nm   20101105 1902 2455506.293056  2455506.090278  2.067e-04   2.021e-04   2.386e-04   2455506.194444  EVENT_END
28.4nm   20101105 1903 2455506.293750 -1.0             2.062e-04  -1.000e+05  -1.000e+05  -1.0             MONITORING
...
```

Table 2. Example of a one-minute update output file.

Post-event Summary Files

Data columns will be fixed format and delimited by white space. A configurable parameter can be set that will force the inclusion of a descriptive header at the top of each file.

The first output column will consist of one of the following spectral line identifiers: “28.4nm”, “30.4nm”, or “121.6nm”.

The second output column will represent the event start date and time in conventional (*YYYYMMDDHHMM*) format. This will always be represented as a twelve-digit integer value. The month, day, hour and minute values will be padded with a leading zero when necessary.

The third output column will indicate the event start irradiance value, which will be represented in W/m^2 using scientific notation that includes three significant post-decimal figures.

The fourth output column will represent the event peak date and time in conventional (*YYYYMMDDHHMM*) format. This will always be represented as a twelve-digit integer value. The month, day, hour and minute values will be padded with a leading zero when necessary.

The fifth output column will indicate the event peak irradiance value, which will be represented in W/m^2 using scientific notation that includes three significant post-decimal figures.

The sixth output column will represent the event termination date and time in conventional (*YYYYMMDDHHMM*) format. This will always be represented as a twelve-digit integer value. The month, day, hour and minute values will be padded with a leading zero when necessary.

The seventh output column will indicate the event termination irradiance value, which will be represented in W/m^2 using scientific notation that includes three significant post-decimal figures.

The eighth output column will indicate the mean event irradiance value, which will be represented in W/m^2 using scientific notation that includes three significant post-decimal figures. The mean event irradiance is only calculated if all event irradiance values are valid, if this is not the case, the mean event irradiance is set to -9.999e+03.

The ninth output column will represent the event duration in minutes.

The tenth output column will represent the integrated event flux, which will be represented in W/m^2 using scientific notation that includes three significant post-decimal figures. The integrated flux is only calculated if all event irradiance values are valid, if this is not the case, the integrated flux is set to -9.999e+03.

The eleventh output column will represent the maximum irradiance increase as a percentage of the pre-event irradiance.

An example of algorithm post-event summary output for events detected from November 2010 irradiance data are presented below. Note that inclusion of the descriptive file header is a configurable option.

```
# UNITS: Irradiance (W/m^2), Energy (J/m^2), Duration (minutes)
#
# Line    Start         Start      Peak          Peak        End           End         Mean        Event     Total       Max Irradiance
# ID      YYYYMMDDHHMM  Irradiance YYYYMMDDHHMM  Irradiance  YYYYMMDDHHMM  Irradiance  Irradiance  Duration  Energy      Increase (%)
# ------  ------------  ---------- ------------  ----------  ------------  ----------  ----------  --------- ----------  ---------------
28.4nm    201011031341  1.741e-04  201011031531  2.005e-04   201011031856  1.798e-04   1.135e-02   315       3.574e+00             15.22
28.4nm    201011050049  1.974e-04  201011050338  2.375e-04   201011050553  2.080e-04   1.296e-02   303       3.926e+00             20.32
```

28.4nm	201011051410	2.021e-04	201011051640	2.386e-04	201011051856	2.056e-04	1.318e-02	285	3.757e+00	18.05
30.4nm	201011060430	1.848e-03	201011060444	2.126e-03	201011060602	1.851e-03	1.145e-01	92	1.054e+01	15.07
121.6nm	201011060431	6.231e-03	201011060444	6.613e-03	201011060615	6.274e-03	4.639e-01	105	4.871e+01	6.12
30.4nm	201011060817	1.851e-03	201011060828	1.914e-03	201011060911	1.863e-03	1.125e-01	54	6.073e+00	3.45
28.4nm	201011061452	1.994e-04	201011061541	2.374e-04	201011061600	2.072e-04	1.483e-02	69	1.024e+00	19.02
30.4nm	201011061521	1.861e-03	201011061535	2.017e-03	201011061851	1.893e-03	1.268e-01	210	2.663e+01	8.40
121.6nm	201011061515	6.299e-03	201011061640	6.589e-03	201011062041	6.288e-03	3.865e-01	326	1.260e+02	4.60
28.4nm	201011061606	2.070e-04	201011061918	2.510e-04	201011062212	2.176e-04	1.371e-02	366	5.017e+00	21.28
30.4nm	201011062341	1.870e-03	201011070006	1.921e-03	201011070041	1.878e-03	1.173e-01	59	6.922e+00	2.72
121.6nm	201011070127	6.339e-03	201011070140	6.580e-03	201011070224	6.342e-03	3.843e-01	57	2.190e+01	3.79
30.4nm	201011070119	1.871e-03	201011070140	2.058e-03	201011070336	1.884e-03	1.315e-01	137	1.802e+01	10.05
30.4nm	201011110155	1.910e-03	201011110213	1.958e-03	201011110250	1.916e-03	1.257e-01	55	6.911e+00	2.52
30.4nm	201011110456	1.912e-03	201011110517	1.986e-03	201011110608	1.918e-03	1.348e-01	72	9.705e+00	3.89
30.4nm	201011110708	1.901e-03	201011110723	2.010e-03	201011110804	1.897e-03	1.159e-01	56	6.489e+00	5.70
30.4nm	201011111548	1.905e-03	201011111614	1.978e-03	201011111707	1.909e-03	1.156e-01	78	9.014e+00	3.81
30.4nm	201011112034	1.909e-03	201011112052	1.959e-03	201011112119	1.911e-03	1.403e-01	45	6.313e+00	2.61
30.4nm	201011120114	1.893e-03	201011120134	2.078e-03	201011120201	1.897e-03	1.202e-01	47	5.651e+00	9.77
121.6nm	201011120122	6.449e-03	201011120135	6.696e-03	201011120215	6.447e-03	3.896e-01	53	2.065e+01	3.83
30.4nm	201011160243	1.912e-03	201011160301	1.966e-03	201011160340	1.917e-03	-9.999e+03	57	-9.999e+03	2.83
30.4nm	201011170426	1.917e-03	201011170439	1.988e-03	201011170453	1.914e-03	1.161e-01	27	3.133e+00	3.70
121.6nm	201011190902	6.347e-03	201011190920	6.507e-03	201011190935	6.337e-03	3.826e-01	32	1.224e+01	2.53

Table 3. Example of a post-event summary output file.

3.8 Theoretical Considerations

There are no relevant theoretical considerations. The detection and characterization methodologies employed are entirely empirical.

4 TESTING

This section describes the proxy input data that will be used for algorithm development, optimization and validation, and briefly outlines the software testing methodologies that will be employed. A separate test plan document will be provided with final algorithm delivery.

4.1 Proxy Input Data

Currently, there is no source of 28.4 nm, 30.4 nm or 121.6 nm solar irradiance data of the temporal and spectral resolution expected of the GOES-R EXIS instrument. Although SDO/EVE produces higher resolution, both temporally and spectrally, these data only extend back to May 2010.

High-resolution SDO/EVE data was convolved with a 1 nm Gaussian distribution (Figure 19) to produce a dataset comparable to the detector plane slit function of the GOES-R EXIS EUVS-A sensor (Figure 20).

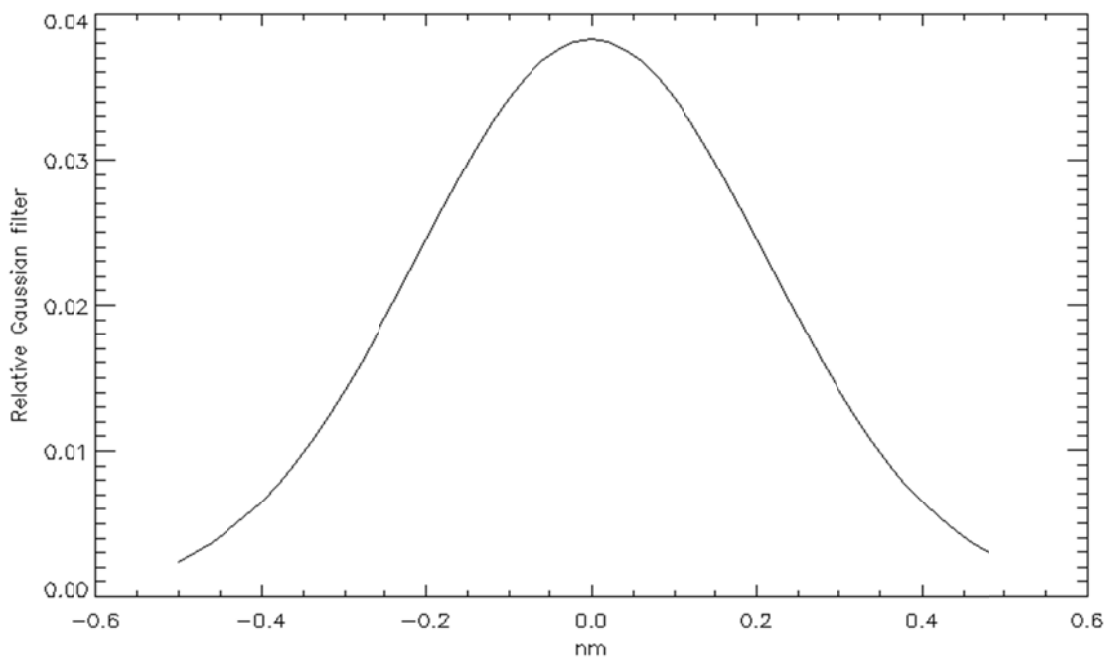

Figure 19. Gaussian convolution kernel used to modify SDO/EVE data to simulate GOES-R EUVS-A data.

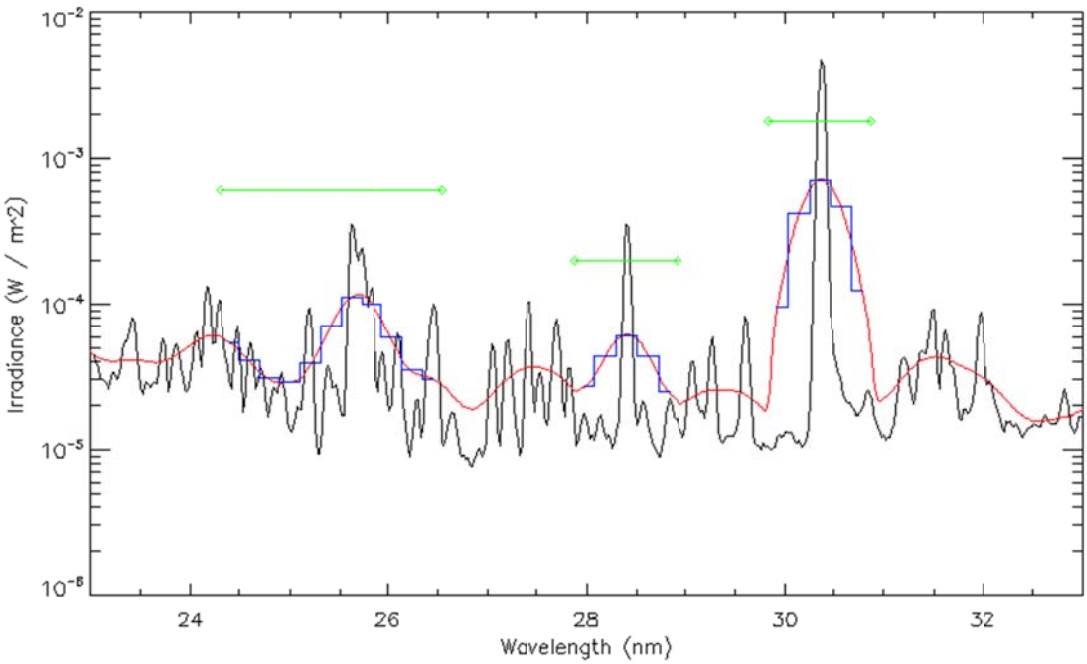

Figure 20. SDO/EVE solar spectrum (black) convolved with the approximate EXIS Gaussian slit function (red). Blue represents the approximate EXIS diode values and green is the sum of the EXIS diodes over the EUVS-A bands.

The physical packaging of the diodes introduces an inter-diode gap of about 0.037 nm in wavelength. Each diode spans approximately 0.171 nm in wavelength. In an effort to faithfully reproduce the anticipated GOES-R behavior, the effective diode irradiance measurements are summed to create an irradiance estimate for the solar emission.

In this manner, estimates for the diode irradiances, as well as the associated spectral line irradiances were produced from the EVE version 2 dataset. This includes the He II 30.4 and the Fe XV 28.4 nm emissions. However, the H I 121.6 nm emission will not be measured by EUVS-A.

In the case of the H I 121.6 nm spectral line, high-cadence measurements are produced by the operational GOES-15 satellite. These measurements have two major problems. First, the long-term trend (months) is not consistent with high-precision measured trend of SORCE SOLSTICE. This problem is resolved by restricting data to a relatively short time frame in which the measurements are not very dissimilar in magnitude. The second problem is the short-term daily geocoronal absorption effect.

A detailed examination of high-cadence GOES-15 data was performed for the period November 2-10, 2010 (Figure 21), and was used to generate a short-term correction for geocoronal absorption.

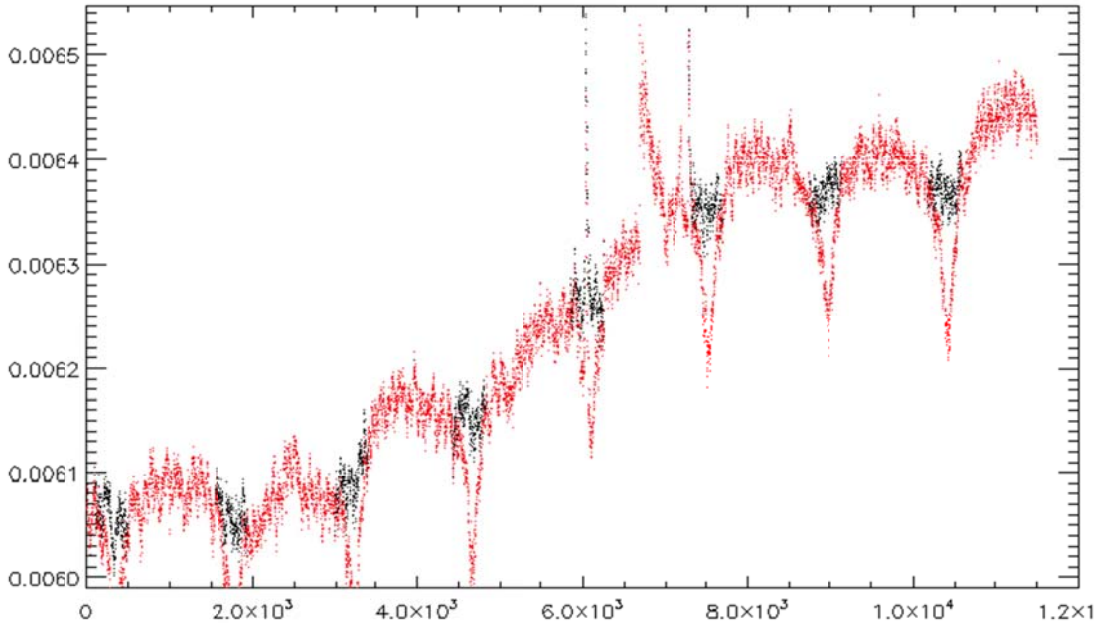

Figure 21. GOES-15 EUV-E measurements (red) from Nov 2-10, 2010. Black represents the geocoronal absorption correction. The vertical axis represents irradiance in W/m^2, and the horizontal axis represents the number of minutes since Nov 2, 0:00 UTC.

An example of geocoronal absorption correction is presented in Figure 22. Irradiance is normalized to the first hour of the day, and an average over each minute of the day is smoothed by 59 minutes to determine the correction (a divisor).

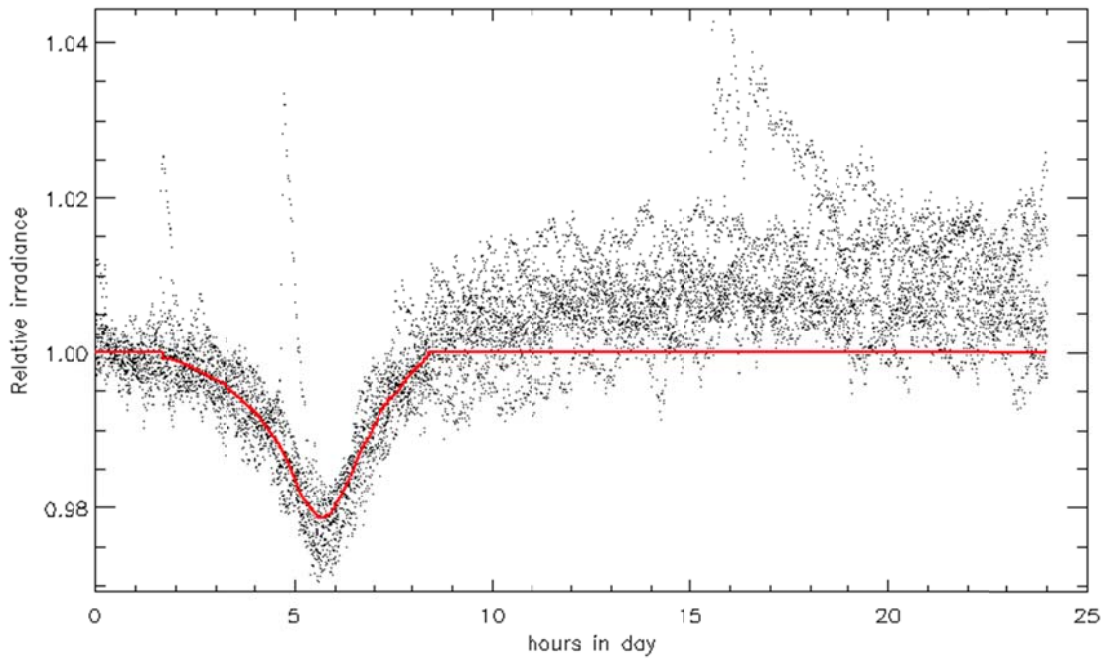

Figure 22. Example of the geocoronal absorption correction divisor for GOES EUV-E (red).

Correlations were performed to determine the portion of the EVE spectrum that is most similar to the corrected GOES-15 EUV-E measurements. The EVE He II 25.6 line (sum of 3 EVE wavelengths bins at the peak) exhibits a 96.3% correlation over this time interval. The He II 25.6 nm spectral line appears to lead the H I 121.6 nm spectral line for low activity, but the impulsive behavior during flares agrees very well. The model used to create a long-term proxy data set for H I is a simple linear function of the peak of the EVE 25.6 nm spectral line, which is not affected by geocoronal absorption.

Figure 23 provides validation of the Lyman-Alpha model.

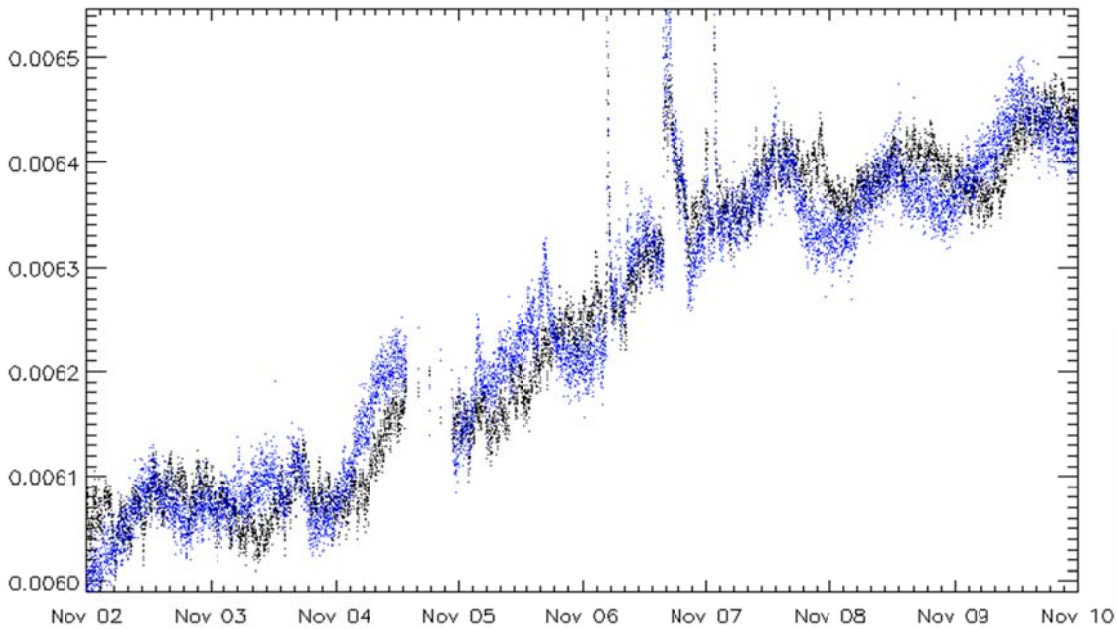

Figure 23. Corrected GOES-15 EUV-E (black) and the EVE model derived from He II 25.6 nm (blue) in W/m^2.

Finally, it is not possible to precisely reproduce the anticipated noise characteristics of EXIS irradiance data because the instrument has not yet been built. Although it is reasonable to assume that EXIS irradiance noise characteristics will be comparable to EVE, improved particle shielding may result in greater noise reduction for GOES-R measurements. This is important because, if the proxy development and validation data is not sufficiently similar to GOES-R irradiance data, the algorithm will not perform in an optimal manner.

4.2 Software Testing

Multiple levels of testing are essential to the development and delivery of functional and reliable software. This section briefly describes the software testing procedures incorporated into algorithm development. Software testing refers specifically to the determination that the processing and logical components of the application are performing as intended. Algorithm validation, which refers to the skill of the application in event detection and characterization, is discussed in Section 8.

A separate test plan document will be delivered with the final algorithm (*GOES-R EXIS EUVS.04 Test Plan and Results*).

4.2.1 Unit/Regression Testing

Unit tests are used to verify that the individual components of an application, typically methods, are functionally compliant. Clearly, if the individual components do not behave as intended, the integrated application must be flawed. Regression tests, which are closely related to unit tests, are employed to verify that previously functional code has not been inadvertently corrupted during continued development.

Once successful, a unit test is generally incorporated into a regression test suite. Although the initial purpose of a unit test is to establish functionality of a newly produced component, the same test is subsequently used repeatedly to verify continued functionality of that component.

Although the extent of unit/regression testing will depend upon schedule constraints, critical and high-risk algorithm components will be tested.

4.2.2 Integration Testing

The purpose of integration testing is to verify that individual application components interact as intended.

Integration testing of the EUV event detection and characterization algorithm will only be applied to the end-to-end application. Given current scheduling constraints, it is neither realistic nor desirable to rigorously test all possible intermediate groupings of software component interaction.

Integration test inputs, execution scripts, and expected results will be included with final algorithm delivery and may be used by the ground system contractor to verify proper implementation.

4.2.3 Performance Testing

Performance testing is used to verify that algorithm processing time is within acceptable limits given expected input data rates.

Although performance testing will be performed, considering that the primary performance requirement of the algorithm is limited to the simultaneous processing of three once-a-minute spectral line inputs, performance issues are not anticipated.

4.2.4 Memory Testing

Because the EUV event detection and characterization algorithm will be designed and implemented to run continuously, as opposed to starting and stopping in a data-driven manner, it is critical that processing-related memory leaks do not exist. Testing will be performed to insure that memory-related problems do not exist.

5 ADDITIONAL CONSIDERATIONS

5.1 Risk

Dependencies on proxy data for algorithm development represent the most significant recognized risk.

If the proxy data does not sufficiently resemble the actual EXIS EUV irradiance data, the degradation of algorithm performance could be significant. In the worst-case scenario, it will be necessary to re-optimize the algorithm with actual EXIS EUV irradiance data once such data is available.

Because the proxy data is based on SDO/EVE measurements, it is also possible that algorithm optimization will be biased toward the portion of the solar cycle for which EVE data is available. It is possible that algorithm performance may deteriorate during other portions of the solar cycle.

As discussed in the following section, compromises involving false alarms and detection latencies are anticipated for the 28.4 nm emission line. False alarms rates can be reduced, but, in the case of non-impulsive events, such reductions are typically at the expense of late detections, or in extreme cases, missed detections, of legitimate EUV events.

Finally, the complex nature of EUV irradiance brightenings may preclude the development of a detection and characterization algorithm that intuitively satisfies all reviewers. The determination of which EUV brightenings represent “events” and which do not is a subjective assessment and disagreement must be anticipated. Additional disagreement concerning the appropriate assignment of event start and/or end times may exist. Assessment of algorithm performance may be highly subjective and differences of opinion may not be easily reconciled.

5.2 Skill Tradeoffs

As previously discussed (Sections 3.5.3 and 5.1), there is a potentially significant tradeoff between the minimization of false alarm rates and that of event detection latency.

The ideal EUV event detection algorithm would be characterized by minimal missed detections, minimal detection latencies, and minimal false alarms. Unfortunately, such an ideal application may not exist because it is not possible to

simultaneously optimize the algorithm for the minimization of both false alarms and event detection latency.

Optimizations that enhance algorithm "sensitivity" will decrease incidences of missed events and increase the promptness of event detection, but will also increase the number of false alarms. As illustrated in Figure 24, this relationship is primarily relevant to non-impulsive events (i.e., "slow risers"), which are most often associated with the 28.4 nm spectral line.

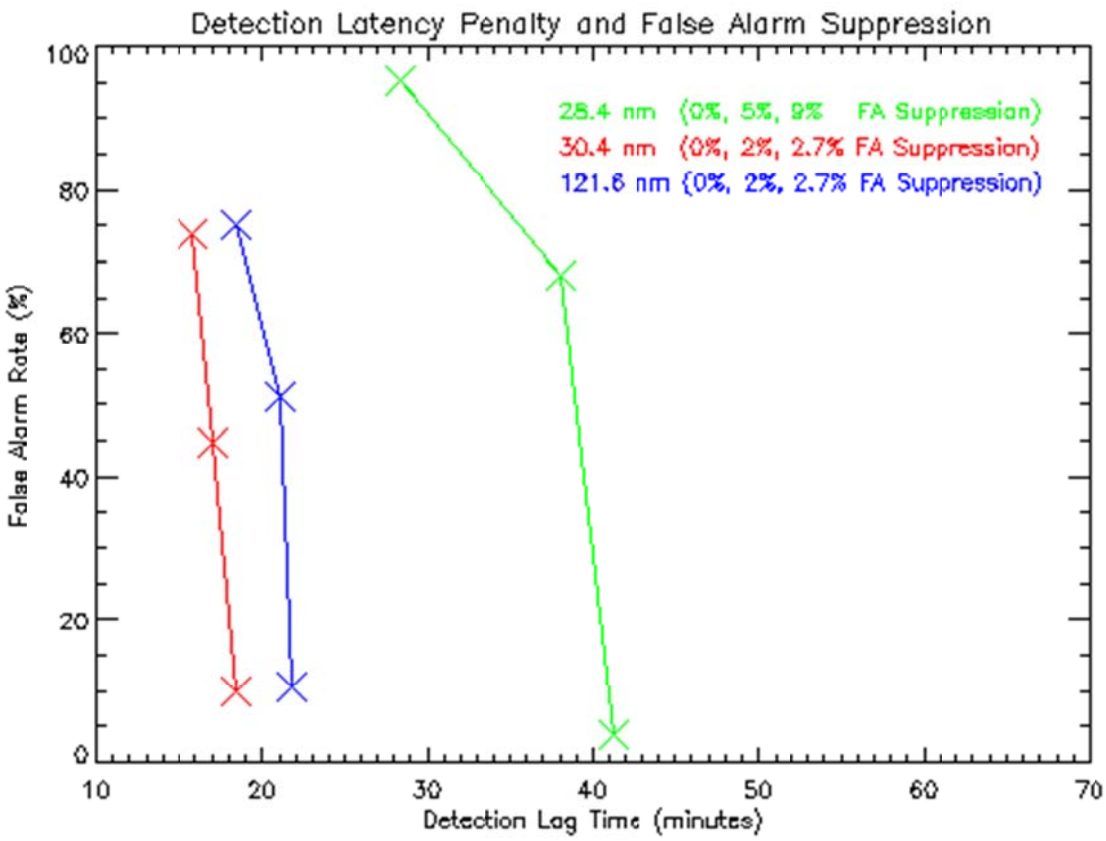

Figure 24. False alarm rate vs detection latency for various false alarm suppression thresholds. The penalty associated with false alarm suppression is indicated by how strongly the line migrates to the right (increased detection latency) for smaller false alarm rates.

In this figure, the near vertical lines associated with the 30.4 nm and 121.6 nm emissions indicate negligible detection latency penalty with decreasing false alarm rate (Section 8.3.2), which is the percent of "event detections" that actually represent false alarms. For both the 30.4 nm (red) and 121.6 nm (blue) lines,

detection latencies do not increase significantly with greater degrees of false alarm suppression. In contrast, the detection latency for the 28.4 nm spectral line initially increases from 28 minutes to 38 minutes as the false alarm suppression threshold increases from 0% to 5%. The detection latency penalty associated with additional increases in the false alarm suppression threshold is minor. As indicated in Figure 24, increasing the false alarm suppression threshold from 5% to 9% increases the mean event detection latency by only three minutes. This is because 28.4 nm events tend to become relatively impulsive above a 5% irradiance increase.

Although the tradeoff between prompt event detection and false alarm rate is the most critical, additional compromises are anticipated. Prompt event termination may conflict with the proficiency of the algorithm in discriminating between a rapid succession of individual events and an extended duration multi-peak single event. Greater sensitivity to event termination increases the probability that extended duration events characterized by multiple peaks will be classified as a series of shorter events. Even human interpreters may find it difficult to objectively discriminate between multiple brief events and a single long-duration multi-peak event (e.g., Figure 25).**Error! Reference source not found.**

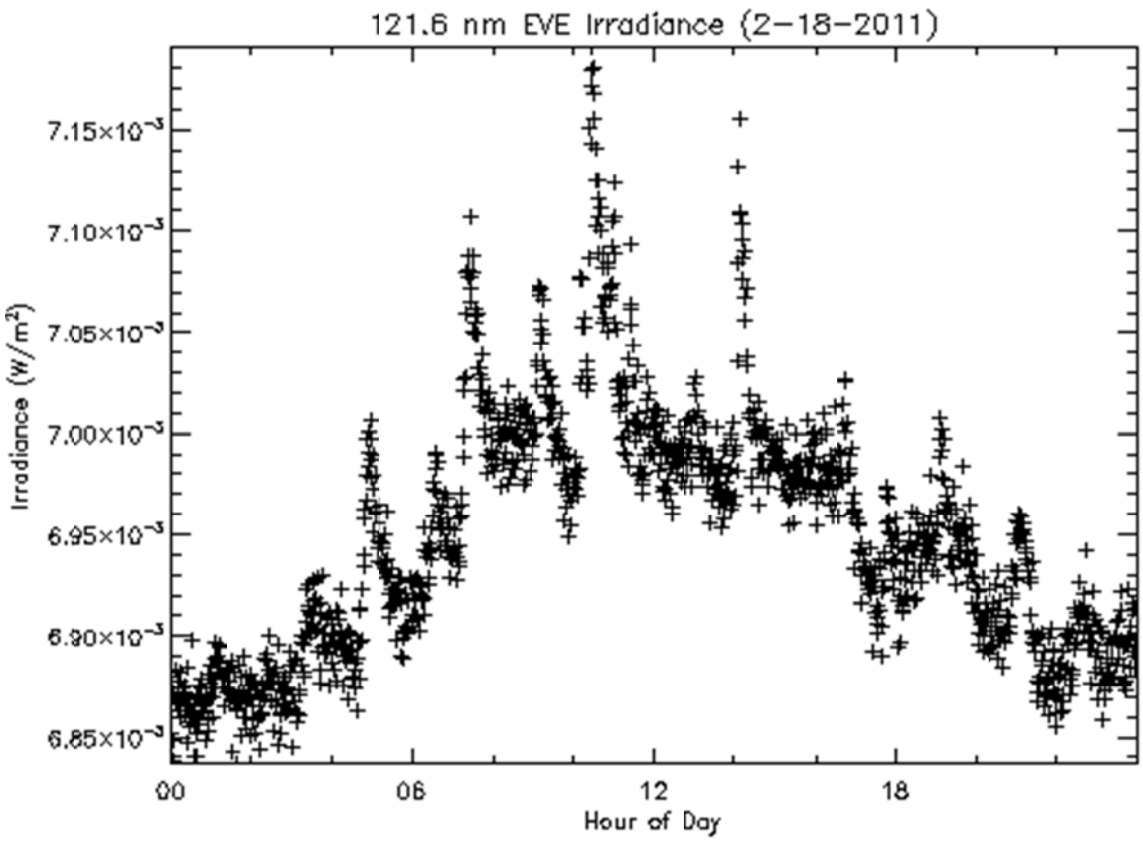

Figure 25. Example of the ambiguity inherent in discriminating between a series of short-duration events and a single long-duration event.

5.3 Configuration Files

Key application parameters will be configurable, meaning that, if they are modified, the application will simply need to be restarted, not recompiled. In addition to a main configuration file, there will be separate configuration files to optimize the event detection and characterization parameters for each spectral line. Refer to the *EUVS04 User Guide* for configuration file details.

5.3.1 Main Configuration Parameters

Primary configuration parameters will be specified as “keyword = value” pairs in an external parameter file named *main.config*. The name and location of this configuration file is specified as a command-line argument to the *main()* function.

Only parameters that are reasonable candidates for user modification are configurable. Modifications that imply a substantive understanding of algorithm processing or logic should be discouraged and, as such, will require source code editing and a recompilation of the application.

Examples of configurable items include the minimum amount of startup data required to initiate event detection logic, the length of the irradiance data and data metric history that is retained, the locations and naming conventions for input and output files, and a log file indicator.

Examples of non-configurable items include the number of spectral lines processed and the expected input data rate.

Refer to the *EUVS.04 User Guide* for a complete list and explanation of all configurable application parameters.

5.3.2 Event Detection and Characterization Configuration Parameters

Configurable event detection and characterization parameters will be specified in spectral line-specific files located in a *config* subdirectory and named *28.4nm.config*, *30.4nm.config* and *121.6nm.config*.

Refer to the *EUVS.04 User Guide* for a complete list and explanation of all configurable application parameters.

5.4 Log Files

Optional log file output will be implemented. If a log file name and directory path are specified in the main configuration file, all processing messages will be written to the specified file. Otherwise, all errors, warnings and diagnostic information will be directed to standard output.

5.5 Error Checking and Handling

In the following discussion, *checking* refers exclusively to testing for software failures of input/output operations or internal logic, such as the inability to open a file, the detection of corrupt input, or an occurrence of an invalid numeric result. *Handling* refers to the application processing that occurs in response to the detection of an error condition.

Because the deliverable application will be developed and tested exclusively on archived data of established validity, it will be assumed that all errors encountered during development and testing are an indication of flawed application logic. Consequently, all such error conditions will result in the immediate termination of the application with a diagnostic log output that will allow the error to be identified and addressed via source code modification.

Operational implementation of the application may require more sophisticated error and exception handling that might, for example, permit processing to continue under recoverable error conditions. Such error/exception handling, which will likely be implementation- and/or operating system-specific, will be the responsibility of the ground system contractor.

6 ASSUMPTIONS AND LIMITATIONS

This section summarizes the assumptions associated with algorithm design and implementation, and the limitations of the operational algorithm.

6.1 Assumptions

Input data will be updated once per minute and will be consistent with the format specified in Section 3.6.2. Invalid data flags are legitimate representations of data.

6.2 Limitations

As delivered, the algorithm will function in archive mode only.

The potential for either an unacceptably high false alarm rate or detection latency must be considered, particularly for the 28.4 nm spectral line.

7 PRELIMINARY RESULTS

In this section, selected results of the EUV event detection and characterization algorithm are presented.

Graphical representation of results, with limited commentary, are presented in Appendix B.

7.1 Explanation of Symbols

In the figures presented in this section, X's represent detection times and boxes represent post-detection estimates of event characteristics (e.g., Figure 6).

To elaborate, a green X represents the time that an event was detected and a green square represents the post-detection estimate of the actual event start time and pre-event irradiance (e.g., Figure 26**Error! Reference source not found.**).

In the plots that follow, actual times (squares) always precede the associated detection time (X's), but in real-time algorithm processing X is always the first to be determined. Equivalently, X's represent the times at which an operator would be notified of event initiation or status modification. All square symbols indicate event characteristics that are determined subsequent to detection.

7.2 Simple Events

Figure 26 depicts the prototype algorithm results for a simple isolated brightening associated with the 30.4 nm emission line. The 10.8% irradiance increase is relatively dramatic and of sudden onset, and the signal is clearly distinguishable from the background trend and noise. This is an example of an unusually simple and "well behaved" event.

Detection latency is 17 minutes and the event duration is 128 minutes.

Regarding event characterization, the post-detection estimate of the actual start time and pre-event irradiance (green square) is appropriate and event termination seems reasonable. The peak detection latency was only a few minutes (blue X) and the post-detection determination of the actual peak time and irradiance (blue square) is exact.

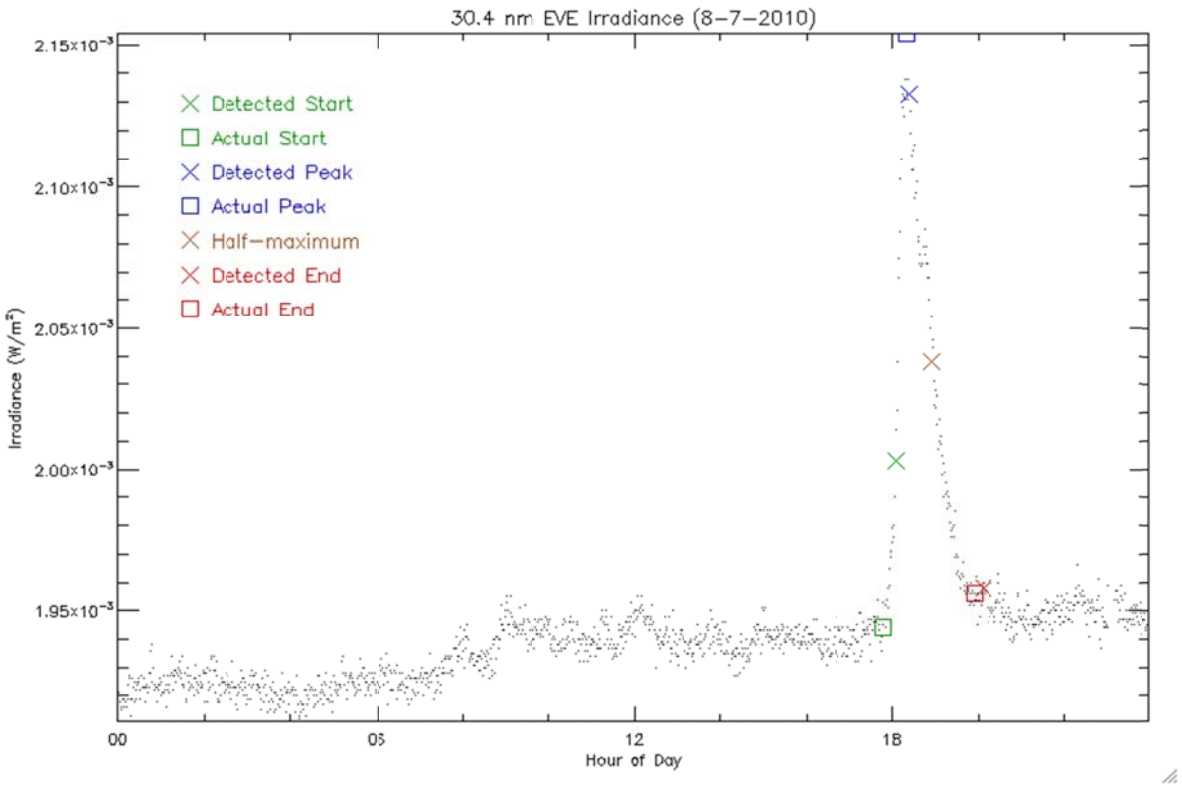

Figure 26. Preliminary algorithm results for a simple 30.4 nm event (Aug 7, 2010).

Figure 27 represents the 121.6 nm irradiance time series data corresponding to the same day depicted in Figure 26. Like the equivalent 30.4 nm results, the irradiance increase is relatively dramatic (4.5%) and of sudden onset, and the signal is clearly distinguishable from the background trend and noise.

Detection latency is 31 minutes and the event duration is 129 minutes.

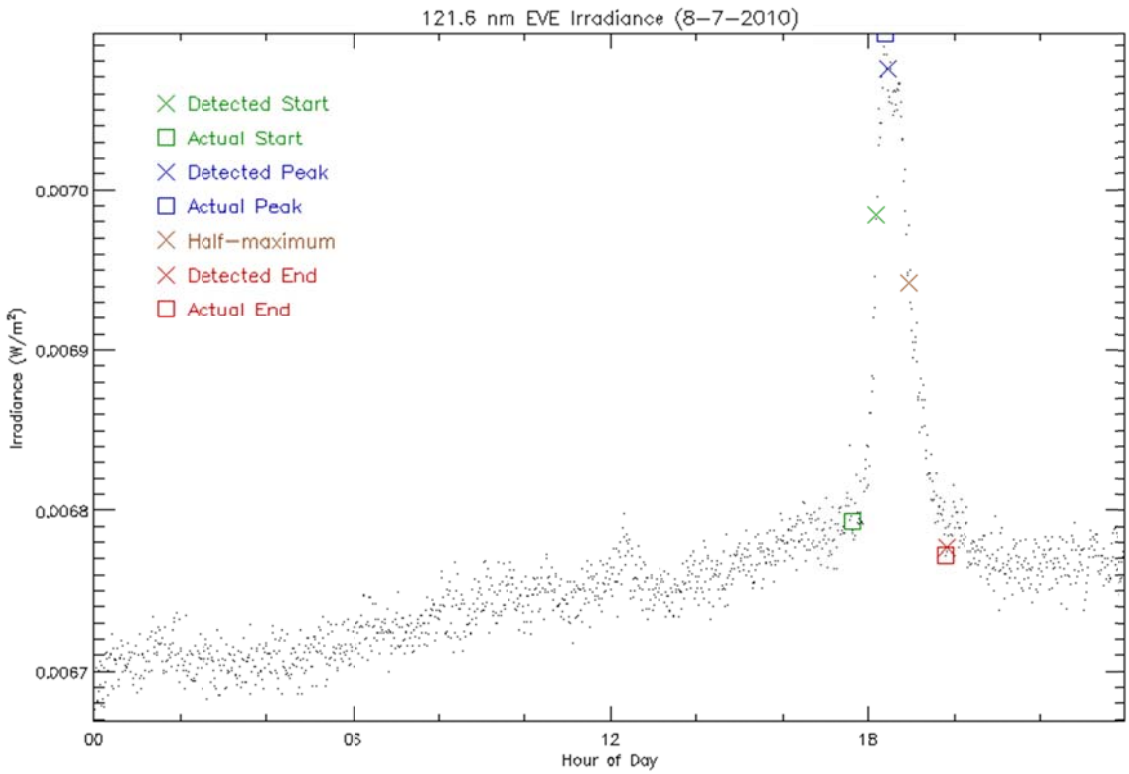

Figure 27. Preliminary algorithm results for a simple 121.6 nm event (Aug 7, 2010).

If all EUV events were as simple as those depicted in Figure 26 and Figure 27 the development of the event detection and characterization algorithm would be relatively simple. Unfortunately, this is not the case.

Figure 28 represents the 28.4 nm irradiance time series data corresponding to the same day depicted in Figure 26. The 32.3% irradiance increase is also relatively abrupt and well defined, but with the slight complication that the post-event irradiance exceeds the pre-event irradiance. Figure 28 demonstrates the reason that a resumption of pre-event irradiance levels cannot represent the sole criterion for event termination.

The 32-minute detection latency is a consequence of the 9% false alarm suppression threshold applied. The post-detection estimate of the actual start time and pre-event irradiance (green square) is appropriate. The peak detection latency was only a few minutes (blue X) and the post-detection determination of the actual peak time and irradiance (blue square) is exact. Although the precise time of event termination is somewhat subjective, the algorithm assigned the event end to

coincide with a point where the irradiance exhibits a dramatic change in slope and a slight reversal in trend.

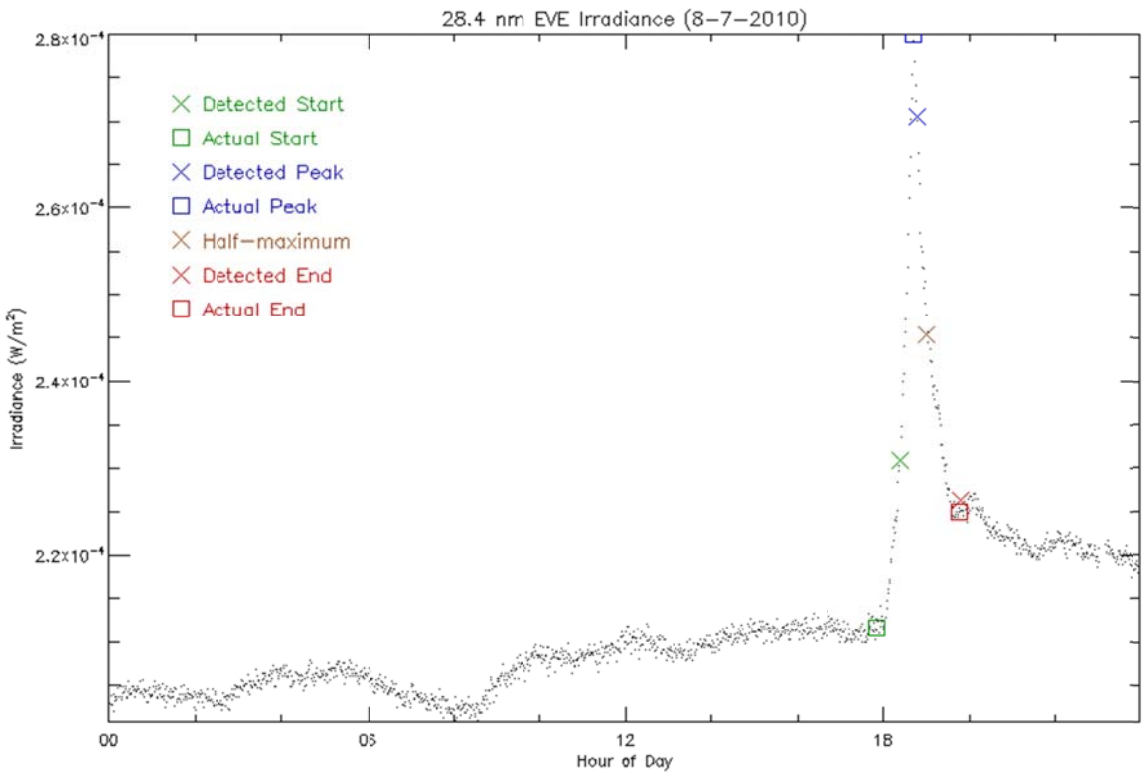

Figure 28. Preliminary algorithm results for a relatively simple 28.4 nm event (Aug 7, 2010).

7.3 Complex Events

In this section, preliminary algorithm results are presented for more complex event types.

In many EUV events, the initial irradiance increase is unremarkable and may progress erratically. When complicated by coronal mass ejections, brightening may be preceded by pronounced dimming. It is also not uncommon for events to “fade away” through a gradual reduction in irradiance slope that does not feature a single well-defined break that unambiguously represents event termination.

In Figure 29, two major 28.4 nm brightenings (20.5% and18.0%) are preceded by less significant brightenings. In the first case, the algorithm treats the precursory

spike as a component of the larger subsequent event. In the second case, the smaller precursory spike is simply ignored.

Detection latencies are 24 minutes for the first event and 101 minutes for the second event. The second event has a greater detection latency because it rises more slowly and the 9% minimum irradiance increase demanded by the false alarm suppression requires longer to attain.

For both events, the pre-event times and irradiances, as well as the event terminations, are appropriately assigned.

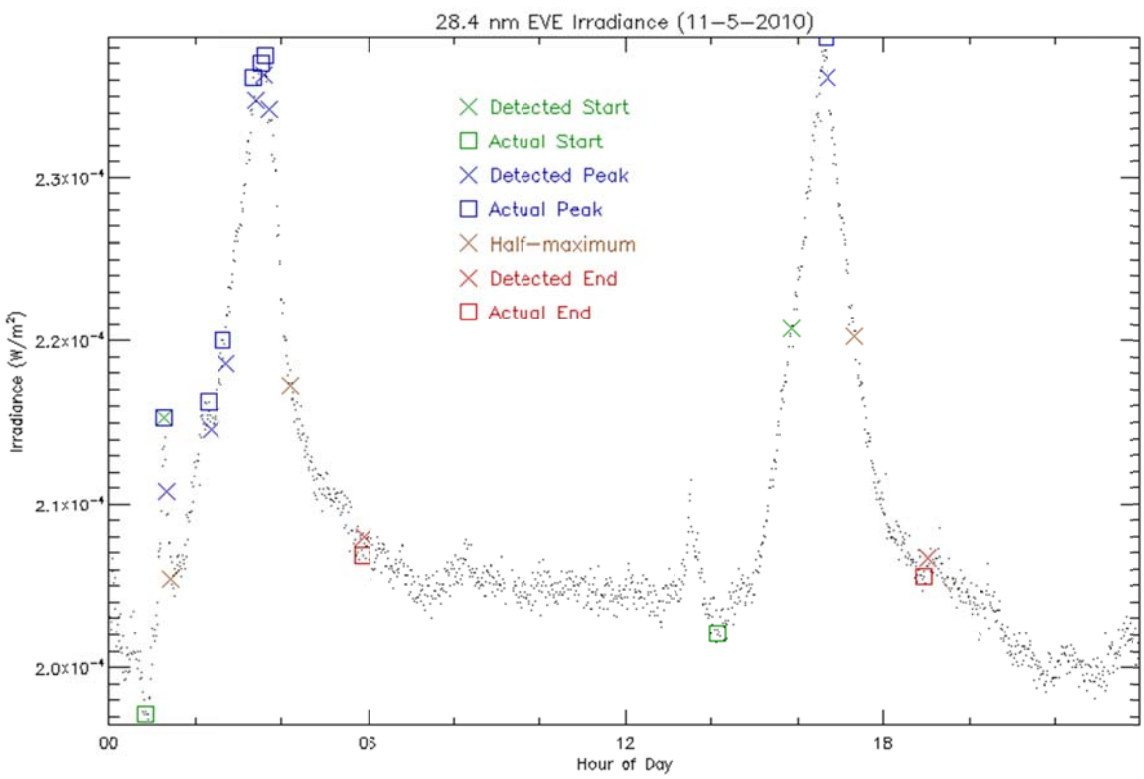

Figure 29. Preliminary algorithm results for a 28.4 nm irradiance event of slight complexity (November 5, 2010).

Error! Reference source not found. Figure 30 presents algorithm results for a 28.4 nm irradiance event (11.3% irradiance increase) of somewhat greater complexity. In this case, the event is superimposed on a marked secular trend of increasing irradiance. As a result of this trend, the pre-event background level is

not re-established subsequent to event termination. Nevertheless, the algorithm performs impressively in its determination that the event has ended.

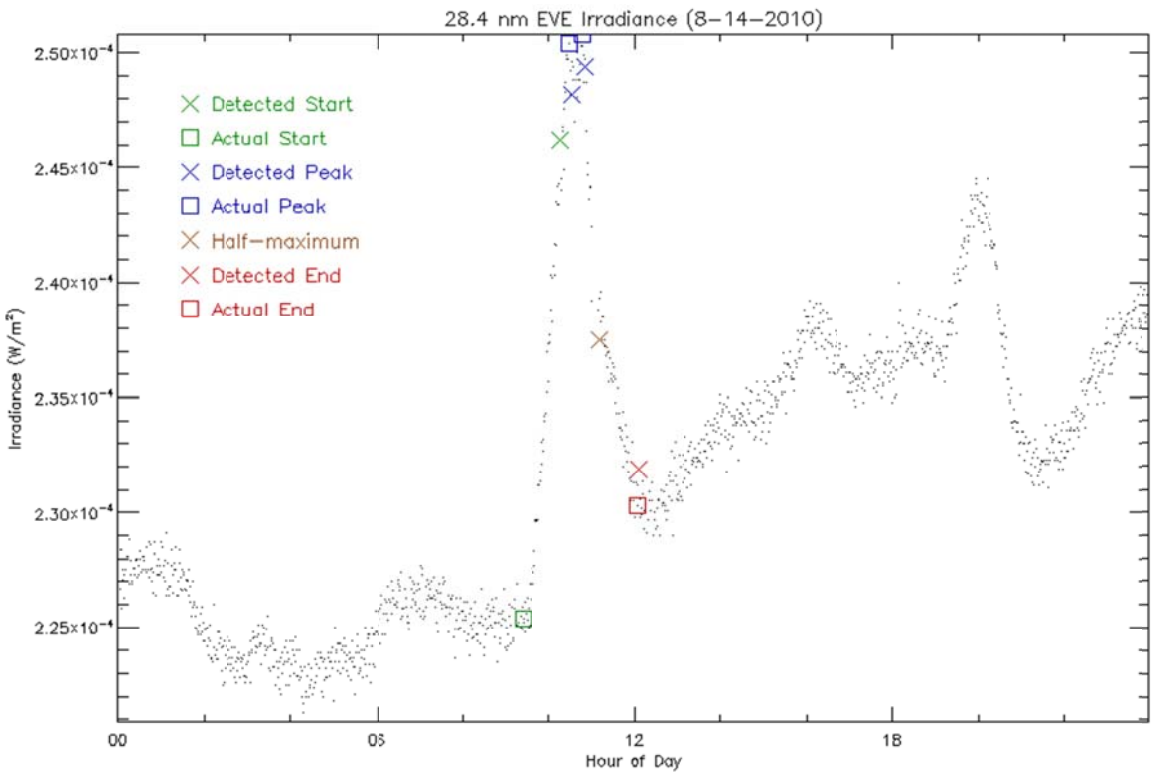

Figure 30. Preliminary algorithm results for 28.4 nm irradiance data of moderate complexity (August 14, 2010).

The detection latency of 52 minutes reflects the amount of time required for the irradiance increase to attain the 9% false alarm suppression threshold assigned to the 28.4 nm spectral line.

Note the dual peaks associated with the event depicted in Figure 30. Two peaks were reported because the second peak slightly exceeded the magnitude of the first peak.

Figure 31**Error! Reference source not found.** depicts prototype algorithm results for a 28.4 nm event during a period of considerable complexity that includes a highly variable background and pre-event dimming associated with coronal mass ejection. From trough to peak, the event irradiance increase is 15.2%. Although the event detection latency of 81 minutes may appear excessive, detection precedes the event peak.

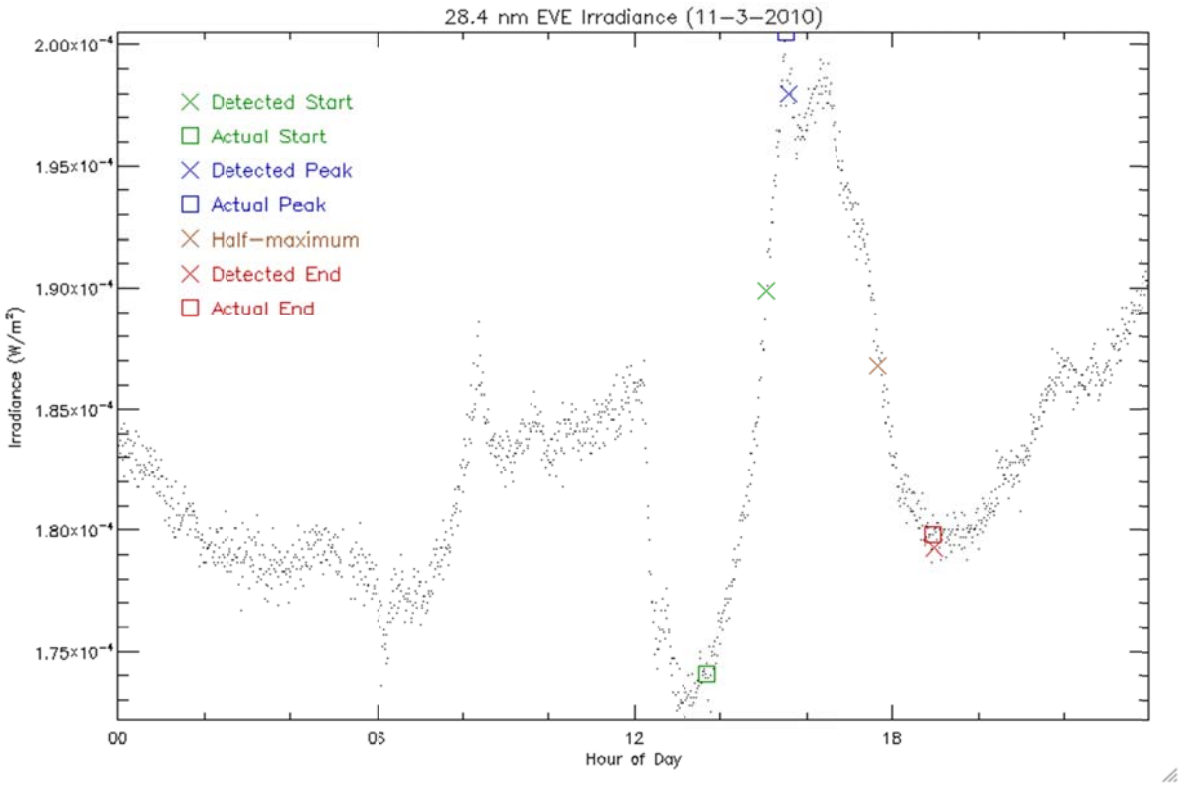

Figure 31. Preliminary algorithm results for 28.4 nm irradiance data of considerable complexity (November 3, 2010).

7.4 Algorithm Deficiencies

Individual cases remain in which the event detection and/or characterization skill of the prototype algorithm is relatively poor.

Potential algorithm deficiencies include

- Excessive detection latencies, particularly for 28.4 nm emissions
- Reliable differentiation between a rapid succession of brief events of short duration and a single extended duration event with multiple peaks
- False alarms for irradiance increases that fall slightly short of event qualification
- Missed detections

Event detection latency is the difference between the time of event detection and the time at which the event actually began. Algorithm validation results (Appendix C) based on 476 days of available GOES-R proxy data (Section 4.1) suggest that detection latencies for the 30.4 nm and 121.6 nm spectral lines will likely be on the order of 20 minutes for the highest levels of false alarm suppression, and that event detection latencies associated with the 28.4 nm spectral line will be approximately double that value.

It is useful to compare these projected event detection latencies to mean event durations, which are 318 minutes for 28.4 nm events, 77 minutes for 30.4 nm events, and 159 minutes for 121.6 nm events (Appendix D).

In addition to event detection latency, missed detections may also be a problem. Figure 32 illustrates a missed detection associated with an 11.0% irradiance increase in the 28.4 nm emissions that occurred on March 8, 2011.

The cause of this missed detection is likely the brief accelerated spike that occurred on the rising limb. The 9% false alarm suppression likely precluded event initiation prior to this spike, which peaked at approximately 7.7%. Subsequent to the spike it is likely that the “look back” processing utilized to determine the actual start time and pre-event irradiance (Section 3.5.3.1) was “misled” by the local minimum that immediately followed the decay of the spike and thus estimated the pre-event irradiance at approximately $4.13e^{-04}$ W/m^2 as opposed to a more appropriate value of approximately $3.92e^{-04}$ W/m^2. The excessive estimate of the pre-event irradiance prevented the false alarm suppression threshold from being satisfied.

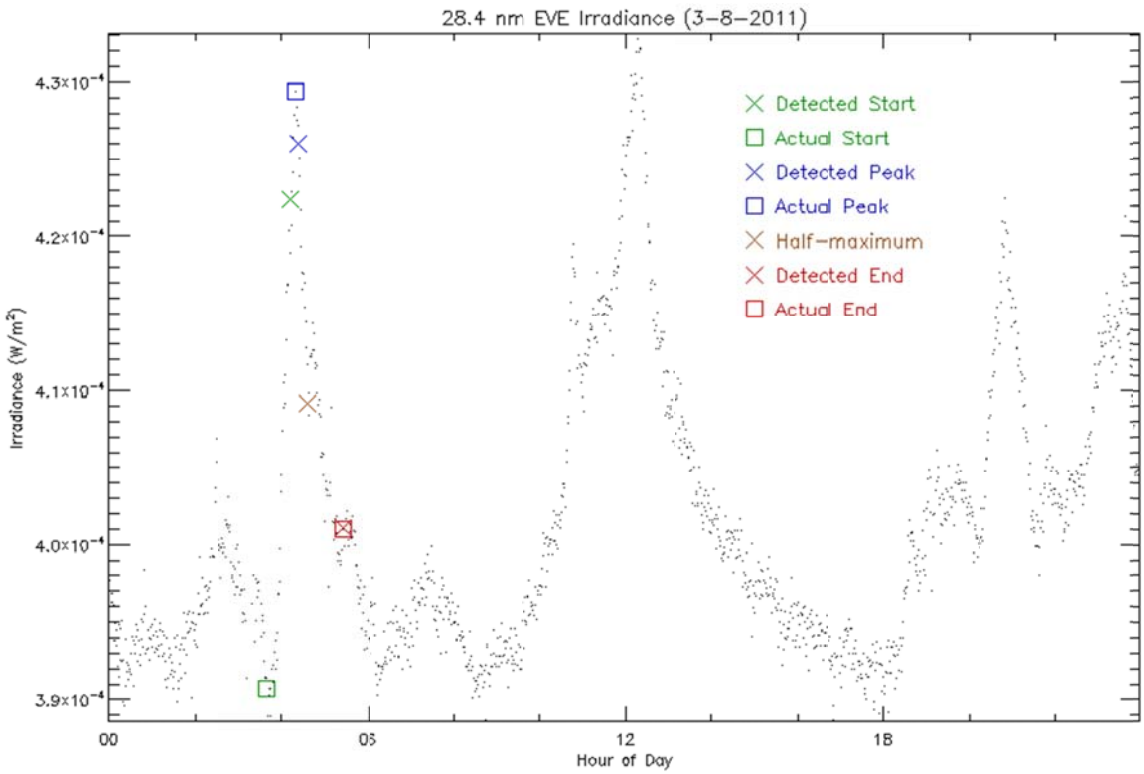

Figure 32. Example of a missed detection associated with an 11.0% irradiance increase in 28.4 nm emissions on March 8, 2011.

Finally, the prototype algorithm does not always distinguish between long duration multi-peak events and a rapid succession of single-peak events in an intuitive manner.

This is illustrated in Figure 33, in which a visual inspection of the irradiance data might suggest to some interpreters to represent an extended event of approximately one-day duration that is punctuated by multiple peaks. The algorithm only identified the greatest peak as a single event.

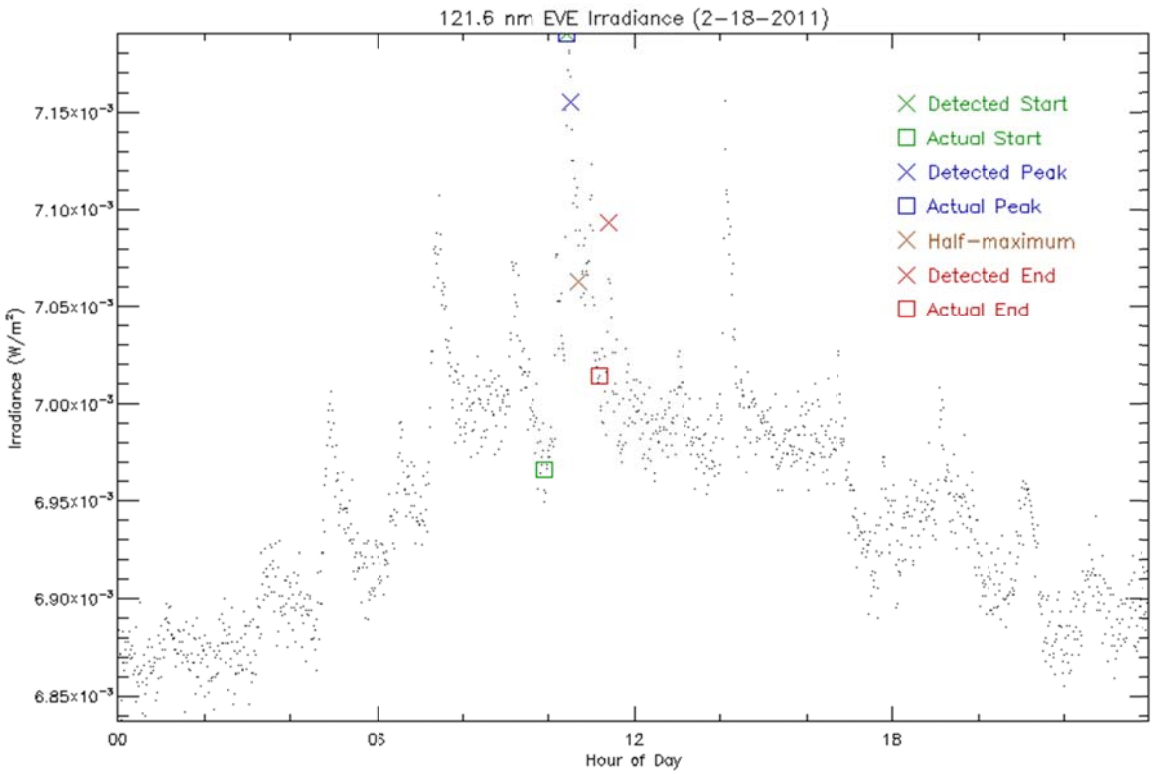

Figure 33. Example of discriminating between extended duration multi-peak event and a rapid succession of brief sharp individual events.

8 ALGORITHM VALIDATION

Validation refers to an assessment of algorithm skill, and should not be confused with testing, which refers to the verification of proper (bug-free) functioning of the individual and integrated software components. This section addresses algorithm validation. Algorithm testing is discussed in Section 4.

Simple visual verification of algorithm results, which is often based on a relatively small number of “cherry-picked” data intervals, cannot constitute a statistical basis sufficient to predict operational algorithm performance. Moreover, such an approach is likely to be influenced by interpretative bias and unlikely to be representative of algorithm behavior, particularly if the data set used for visual verification is a subset of the data set used for algorithm optimization (i.e., “training data bias”). Meaningful statements regarding future algorithm performance can only be derived from statistical validation methodologies.

Although an assessment of mean event detection latency will be performed, rigorous statistical validation will primarily be limited to event detection.

Note that the greatest priorities of EUV event detection and characterization algorithm development are optimization, documentation and testing. Although validation was not budgeted into the schedule, it is important to evaluate algorithm skill. For this reason, a limited validation effort was performed. This minimal approach will include determinations of probability of detection (Section 8.3.1), false alarm ratio (Section 8.3.2), probability of missed detection (Section 8.3.3), and mean event detection latency (Section 7.4.1).

Algorithm validation results based on 576 of proxy irradiance data are summarized in Appendix C.

8.1 Data Considerations

The volume of available proxy irradiance data will limit the comprehensiveness of algorithm validation. The validation proxy data set incorporated into this study consists of 476 days, beginning with April 20, 2010 and ending with August 18, 2011.

8.2 Contingency Tables

Contingency tables, which are commonly utilized in the assessment of weather forecast models, are generally accepted as an objective basis from which to derive "skill scores" that quantify algorithm prediction and/or detection skill.

A contingency table is simply a 2x2 tabulation of the number of correct detections, false alarms, missed detections, and correct rejections. In the case of EUV event detection, the concept of a correct rejection is not meaningful.

Skill parameters determined from contingency tables that represent extensive periods of time are considerably more rigorous, objective and substantive than (invariably subjective) assessments based on the graphic presentation of limited selected results (e.g., a "visual verification" of cherry-picked results).

A contingency table is constructed as follows

	Observed	Not Observed
Detected	Correct Detection (Hit)	False Alarm
Not Detected	Missed Detection (Miss)	Correct Rejections

Table 4. Validation contingency table

A variety of simple skill scores, such as the probability of detection and false alarm rate, are derived from the contingency table.

8.3 Skill Scores

Skill scores are simple unidimensional measures of algorithm performance. They are derived directly from contingency table values.

Although skill scores are most meaningful when comparing the performance of one detection algorithm to another, the simplest skill scores do have absolute meaning. For example, the false alarm rate indicates the fraction of event detections that were invalid.

Because of their simplistic nature, skill scores are most meaningful when interpreted collectively, rather than individually. Also, skill scores represent reliable predictors of future algorithm behavior only when based on significant volumes of validation data.

8.3.1 Probability of Detection

Probability of detection refers to the fraction of legitimate events that were detected. A perfect score is 1 (no misses). A weakness of probability of detection, at least as a sole indicator of skill, is that it is not influenced by false alarms and therefore “rewarded” for over-prediction. For example, prediction of an event at every possible opportunity would result in a POD of 1, but such a “perfect” POD would be accompanied by a false alarm ratio that would also be very nearly equal to 1.

POD = Hits/(Hits + Misses)

8.3.2 False Alarm Ratio

The false alarm ratio refers to the fraction of “detected events” that did not actually occur. In other words, a false alarm ratio of 0.1 indicates that 10% of detections are actually false alarms. A perfect score is 0 (no false alarms). A weakness of false alarm ratio is that it is independent of misses and therefore “rewarded” for under-prediction. For example, an algorithm that did not predict a single event, which would, of course, be useless for event detection, would have a “perfect” false alarm ratio of 0.

FAR = False Alarms/(Hits + False Alarms)

8.3.3 Missed Detection Rate

Missed detection rate is a measure of the fraction of legitimate events that the algorithm fails to detect. A perfect score is 0 (no misses). Missed detection rate is independent of false alarms and therefore rewarded for overprediction.

MDR = Misses/(Hits + Misses)

8.3.4 Frequency Bias

Frequency bias is a measure of the tendency for the algorithm to either “over detect” or “under detect”. It is the ratio of detected events to observed events. Over detection is indicated by values greater than 1 and under detection is indicated by values less than 1. A value of 1 is a perfect score.

BIAS = (Hits + False Alarms)/(Hits + Misses)

8.3.5 Compound Skill Scores

The simplest skill scores, such as the probability of detection, probability of missed detection, and false alarm rate, are each based on only two contingency table values.

More complex skill scores exist that incorporate all contingency table statistics (hits, misses, false alarms, and correct rejections). The Gilbert Skill Score, the Heidke Skill Score, and the Pierce Skill Score are examples of such compound skill scores.

A disadvantage of compound skill scores is that their interpretation is not as straightforward as that of simple skill scores. Probability of detection, probability of missed detection, and false alarm ratio are intuitive measures of algorithm skill. In contrast, compound skill scores reduce multiple aspects of algorithm skill to a single single representation that is not necessarily intuitive.

Compound skill scores are most effective in the comparison of competing detection models or as quantitative measures of the improvement or degradation of a single model. Compound skill scores are not particularly useful as an absolute representation of algorithm skill.

For this reason, validation of the EUV event detection and characterization algorithm will be limited to simple skill scores including probability of detection, false alarm ratio, and probability of missed detection.

9 REFERENCES

Bewsher, D., R. A. Harrison, and D. S. Brown, The relationship between EUV dimming and coronal mass ejections, Astronomy & Astrophysics, 478, 897-906, 2008.

Chamberlin, P. C., T. N. Woods, and F. G. Eparvier, Flare Irradiance Spectral Model (FISM): Flare component algorithms and results, Space Weather, 6, S05001, doi:10.1029/2007SW000372, 2008.

Chamberlin, P. C., T. N. Woods, and F. G. Eparvier, Flare Irradiance Spectral Model (FISM): Daily component algorithms and results, Space Weather, 5, S07005, doi:10.1029/2007SW000316, 2007.

Viereck and Puga, The NOAA Mg II core-to-wing solar index: Construction of a 20-year time series of chromospheric variability from multiple satellites., JGR, 104, pp9995-10005, May 1999.

Viereck et al., The Mg II Index: A proxy for Solar EUV., GRL, 28, pp1343-1346, April 2001.

Bowman, B. R., Tobiska, W. K., et al., “A New Empirical Thermospheric Density Model JB2008 Using New Solar and Geomagnetic Indices”,AIAA 2008-6438, AIAA/AAS Astrodynamics Specialist Conference, 18-21 August 2008, Honolulu, Hawaii.

APPENDIX A

Days Used for Algorithm Development and Optimization

The following days were selected for algorithm development and optimization. They were chosen for the relatively wide range of event types represented, including potential false alarms (marginally below event definition threshold), small events (marginally above event definition threshold), large events, impulsive events, slow risers, brief events, extended duration events, and events superimposed on relatively noisy backgrounds. The number of events associated with each day is indicated in parentheses.

28.4 nm	30.4 nm	121.6 nm
June 12, 2010 (1)	June 12, 2010 (2)	August 7, 2010 (1)
July 19, 2010 (1)	August 1, 2010 (0)	November 6, 2010 (2)
August 1, 2010 (0)	August 7, 2010 (1)	November 11, 2010 (0)
August 7, 2010 (1)	August 14, 2010 (1)	February 13, 2011 (1)
August 14, 2010 (1)	November 6, 2010 (3)	February 14, 2011 (2)
November 3, 2010 (1)	February 13, 2011 (1)	February 15, 2011 (1)
November 5, 2010 (2)	February 14, 2011 (5)	February 16, 2011 (1)
November 6, 2010 (2)	February 16, 2011 (7)	February 18, 2011 (1)
February 14, 2011 (1)	March 7, 2011 (8)	March 7, 2011 (4)
February 15, 2011 (1)	March 8, 2011 (7)	July 30, 2011 (1)
March 8, 2011 (1)	March 12, 2011 (6)	August 4, 2011 (1)
August 9, 2011 (1)	August 9, 2011 (1)	August 9, 2011 (1)

APPENDIX B

Complete Preliminary Algorithm Results

Graphical representations of algorithm results for each of the dozen test and development days per spectral line are presented in this appendix. Refer to Appendix A for a complete list of days used for algorithm development and optimization.

There are 12 plots for the 28.4 nm emissions, 12 plots for the 30.4 nm emissions, and 12 plots for the 121.6 nm emissions. See Section 7.1 for an explanation of plot symbols.

28.4 nm June 12, 2010

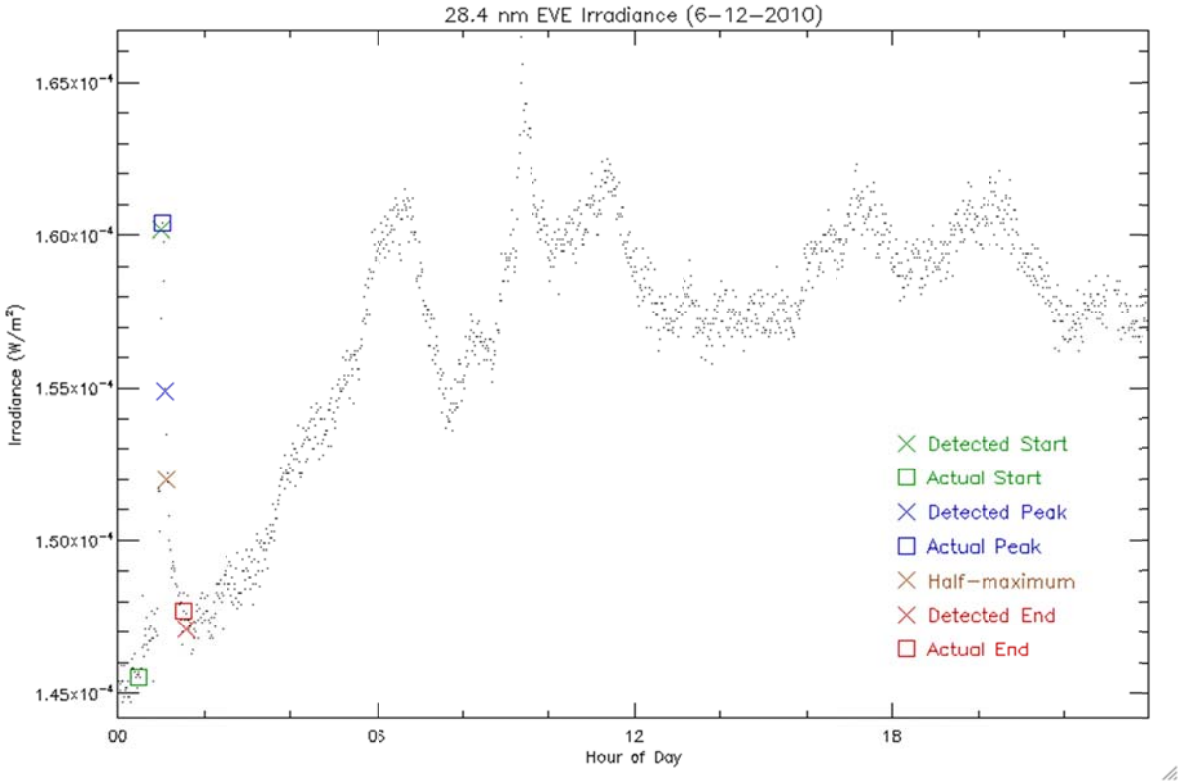

Detection of a single event with a maximum irradiance increase of 10.2%, a detection latency of 32 minutes, and an event duration of 62 minutes. Although the irradiance increases by slightly more than 13% after the event, the increase occurs over a period exceeding 7 hours and does not qualify as an event.

Summary: one correct detection, no missed detections or false alarms.

28.4 nm July 19, 2010

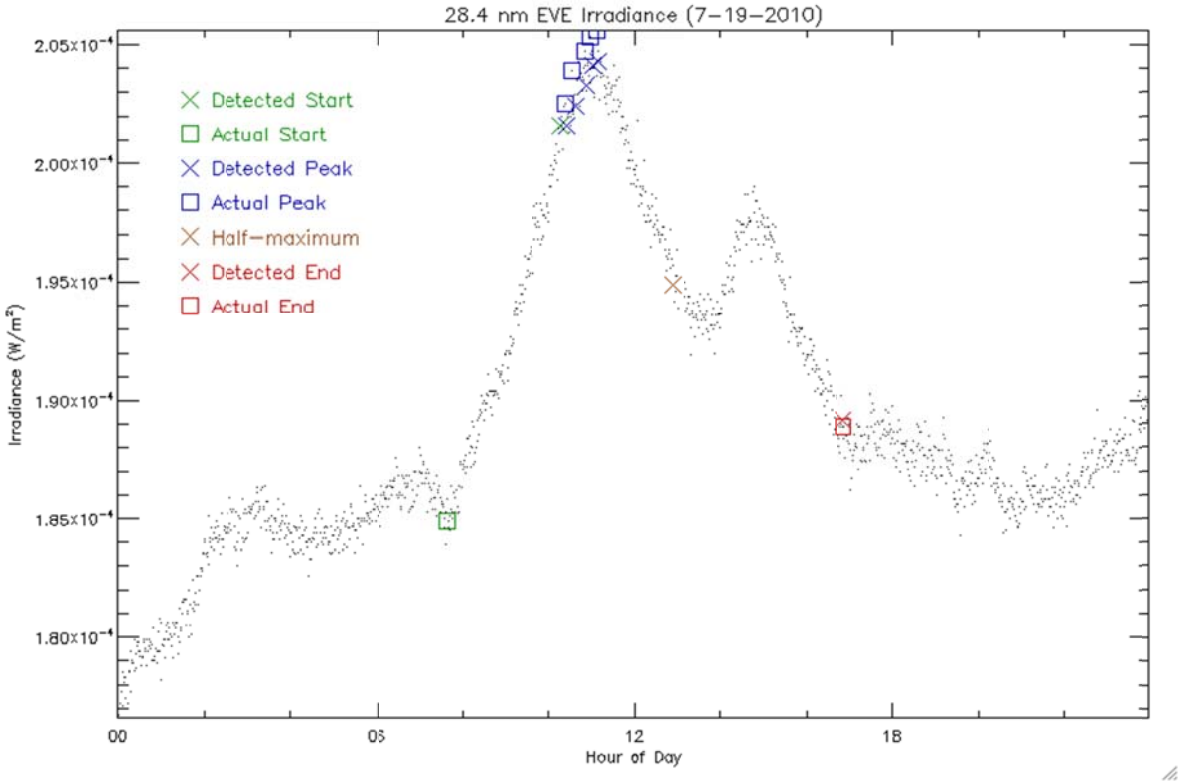

Detection of a single event with a maximum irradiance increase of 11.2%, a detection latency of 157 minutes, and an event duration of 552 minutes. Despite the sudden upward flux during the declining phase, the entire period is recognized as a single event.

Summary: one correct detection, no missed detections or false alarms.

28.4 nm August 1, 2010

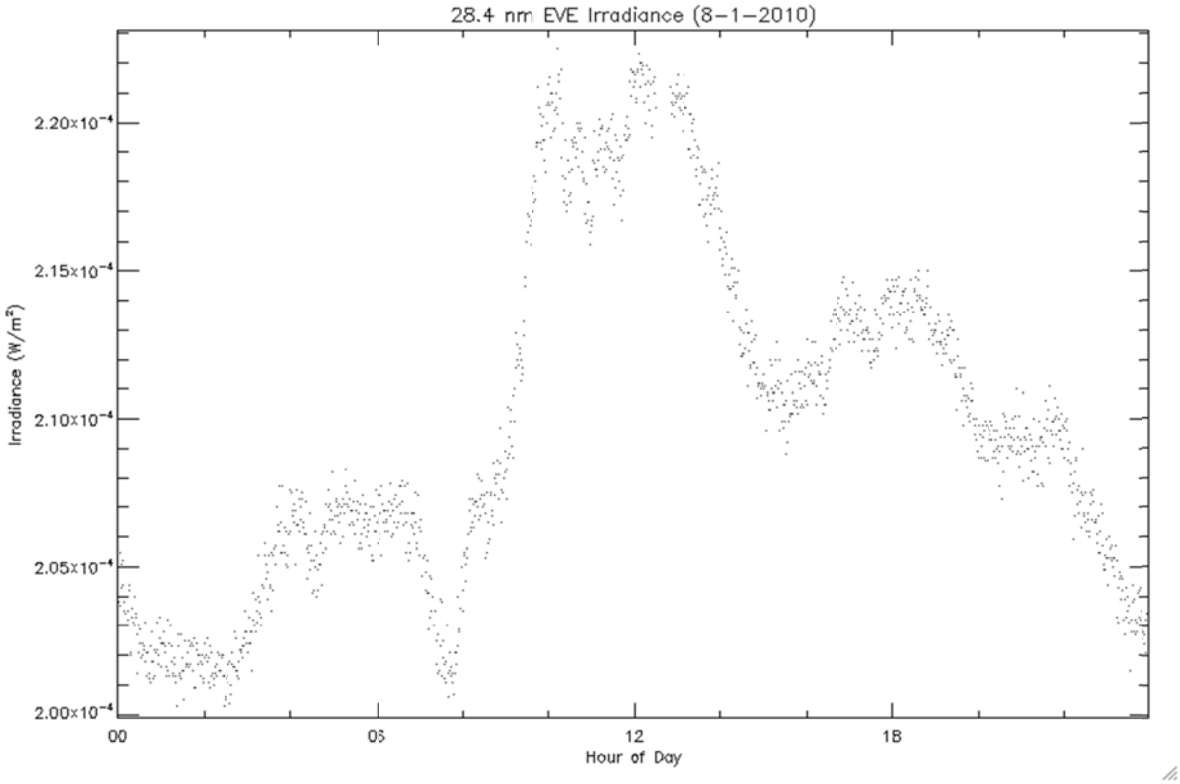

A missed detection – one of five total missed detections (of 476 processed days) identified for the 28.4 nm spectral line. The 10.9% irradiance increase occurs within 5 hours or less and thus qualifies as an event.

Summary: no detections, one missed detection, and no false alarms.

28.4 nm August 7, 2010

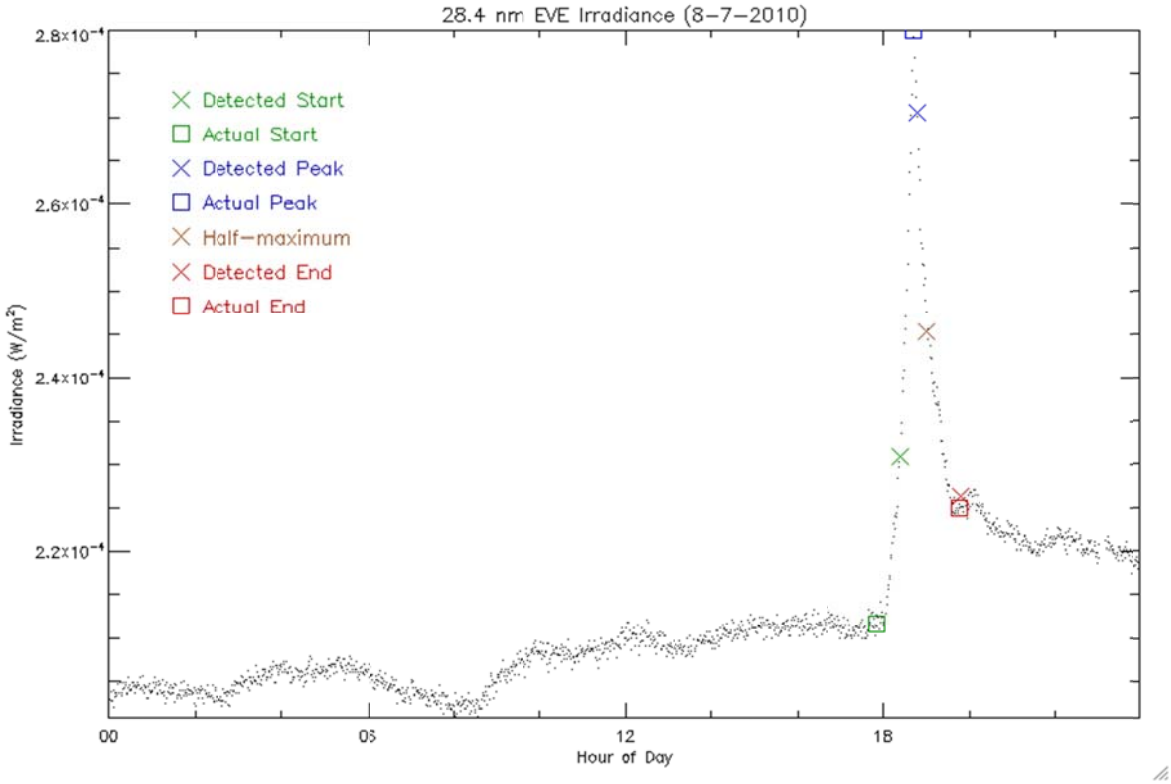

Detection of a single event with a maximum irradiance increase of 32.3%, a detection latency of 32 minutes, and an event duration of 114 minutes.

This plot is the same as Figure 28.

Summary: one correct detection, no missed detections or false alarms.

28.4 nm August 14, 2010

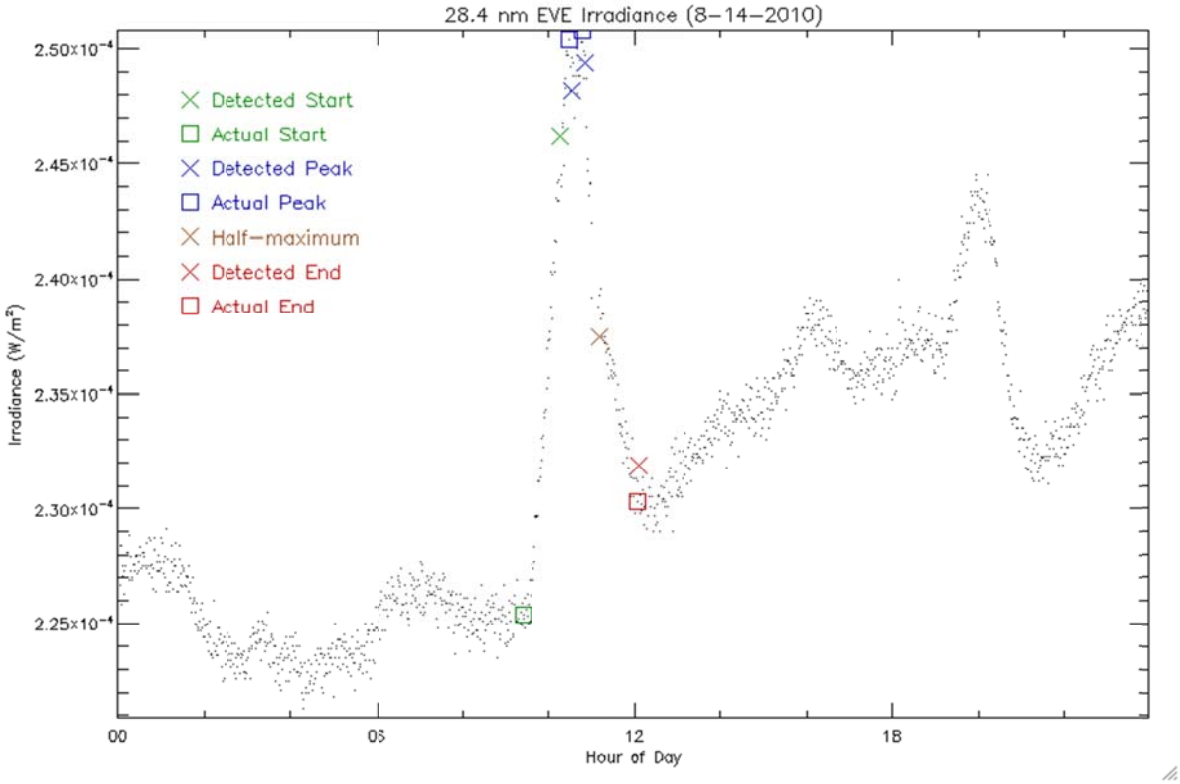

Detection of a single event with a maximum irradiance increase of 11.3%, a detection latency of 52 minutes, and an event duration of 161 minutes.

This plot is the same as Figure 30.

Summary: one correct detection, no missed detections or false alarms.

28.4 nm November 3, 2010

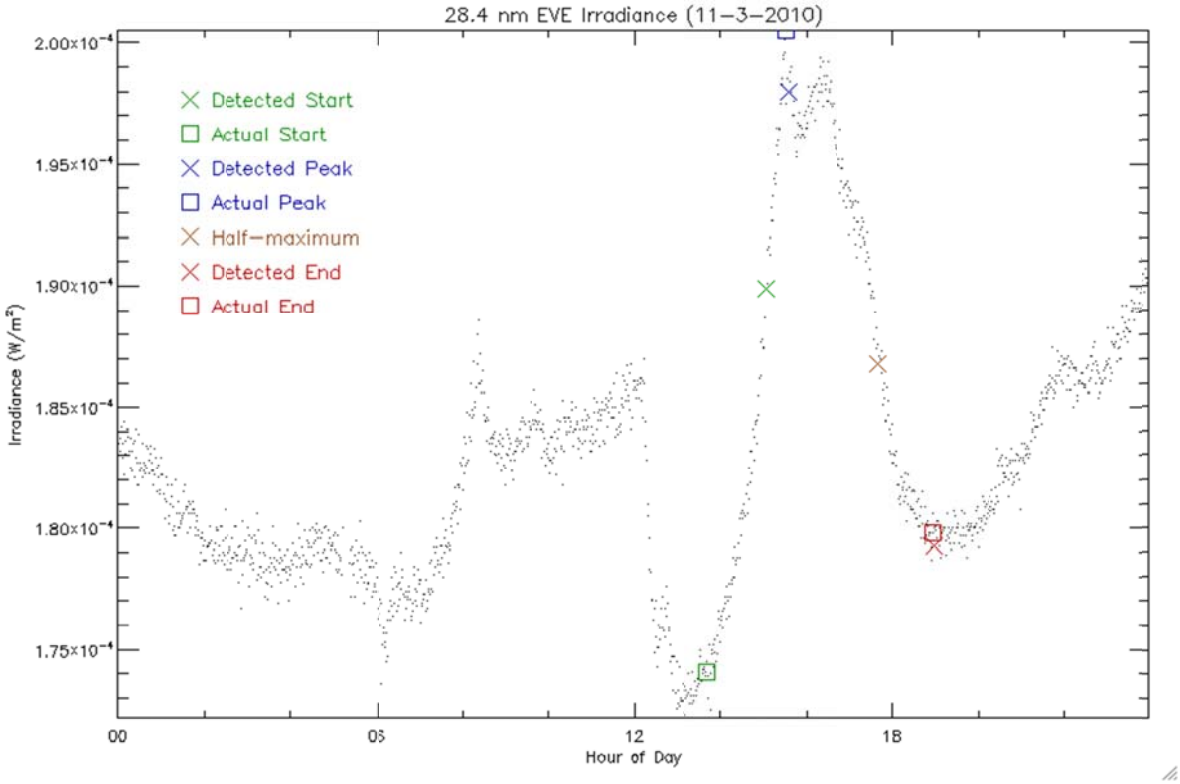

Detection of a single event with a maximum irradiance increase of 15.2%, a detection latency of 81 minutes, and an event duration of 314 minutes.

This plot is the same as Figure 31.

Summary: one correct detection, no missed detections or false alarms.

28.4 nm November 5, 2010

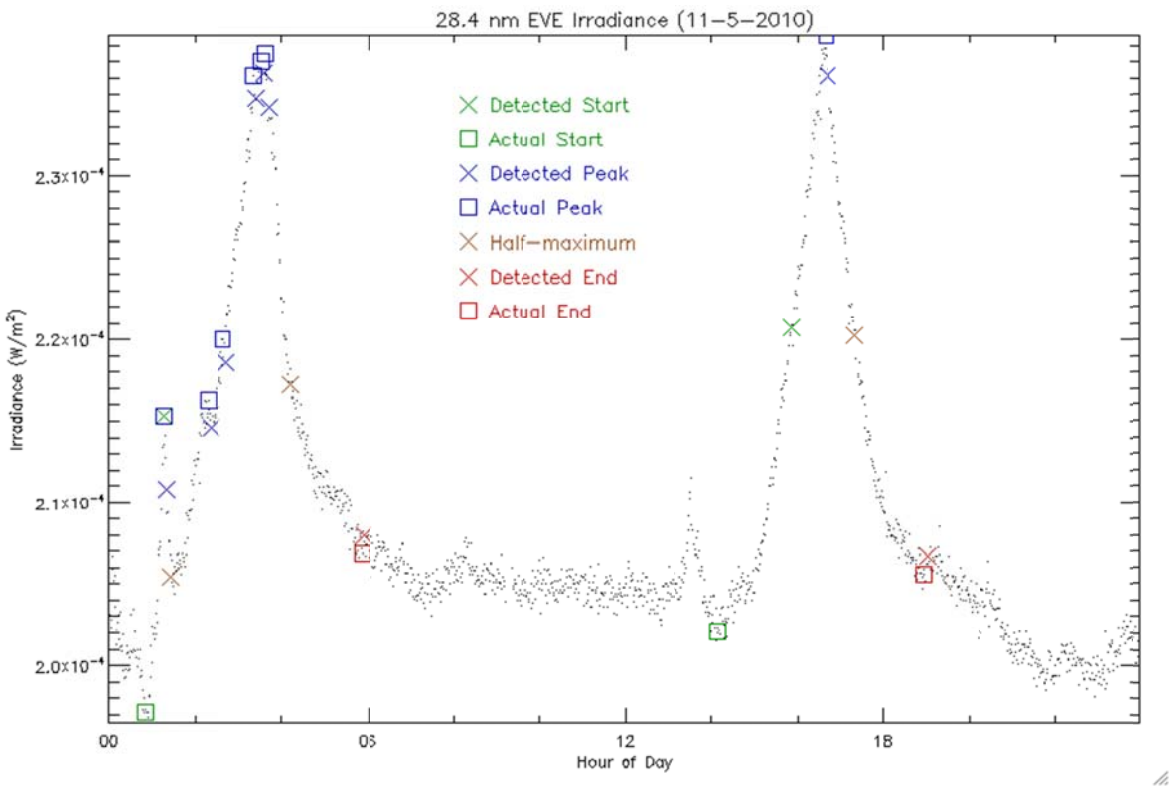

Detection of two events with maximum irradiance increases of 20.5% and 18.0%, detection latencies of 24 and 101 minutes, and event durations of 301 and 285 minutes. The spike that immediately precedes the first event is incorporated into that event, whereas the smaller spike that immediately precedes the second event is simply ignored.

This plot is the same as Figure 29.

Summary: two correct detections, no missed detections or false alarms.

28.4 nm November 6, 2010

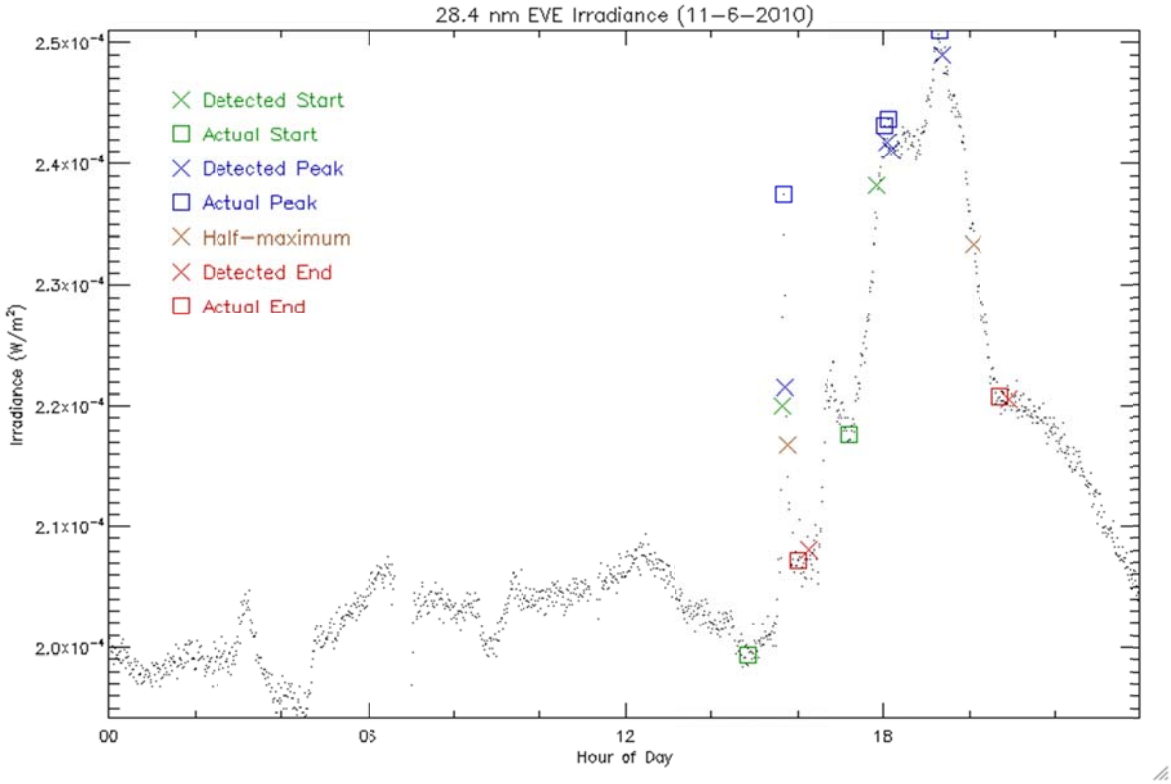

Detection of two immediately adjacent events with maximum irradiance increases of 19.0% and 15.4%, detection latencies of 46 and 38 minutes, and event durations of 69 and 209 minutes. With alternative event termination parameters, the algorithm might treat these as a single event.

Summary: two correct detections, no missed detections or false alarms.

28.4 nm February 14, 2011

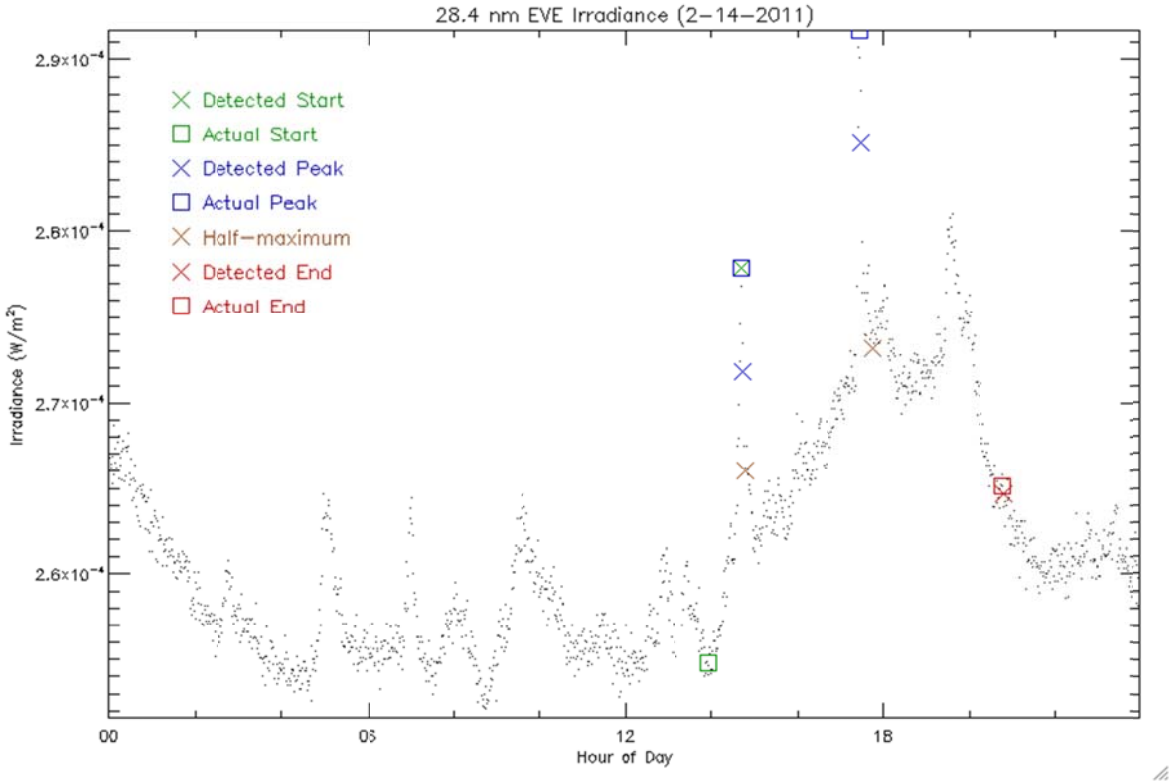

Detection of a single extended duration complex event with a maximum irradiance increase of 14.5%, a detection latency of 45 minutes, and an event duration of 412 minutes. Minor irradiance spikes preceding the event are appropriately ignored.

Summary: one correct detection, no missed detections or false alarms.

28.4 nm February 15, 2011

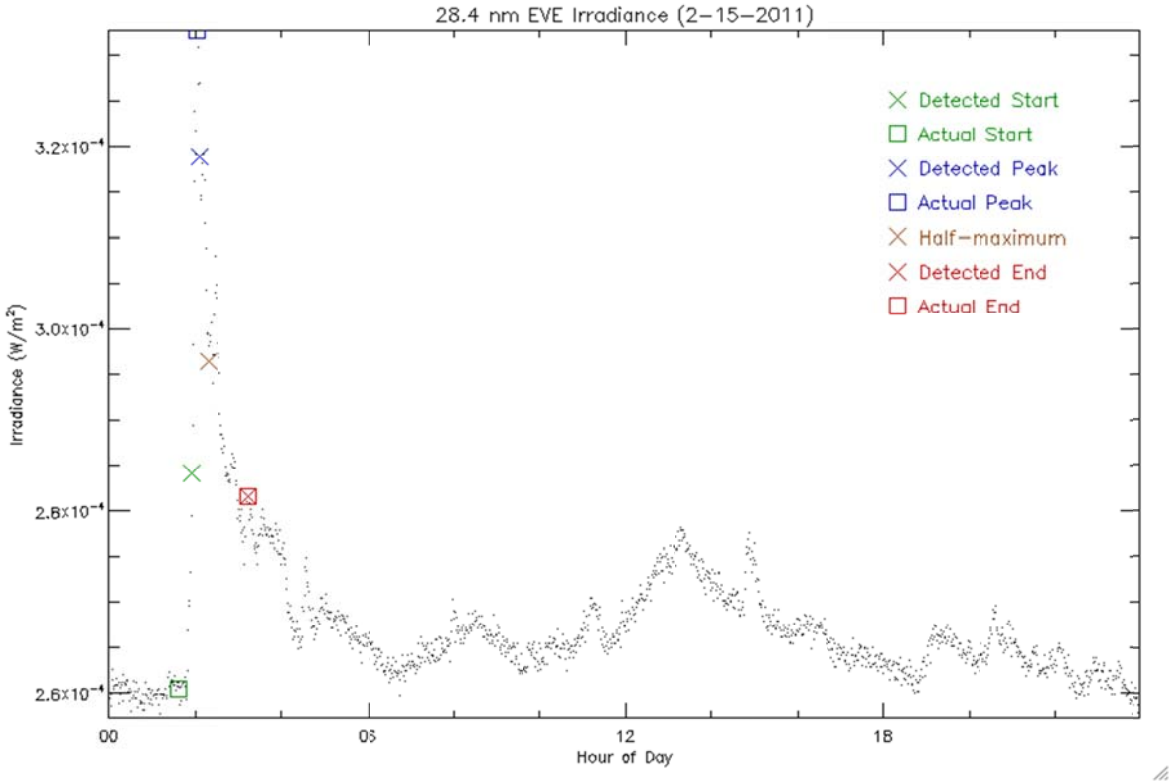

Detection of a single event with a maximum irradiance increase of 27.7%, a detection latency of 18 minutes, and an event duration of 98 minutes. Minor irradiance fluctuations following the event are appropriately ignored.

Summary: one correct detection, no missed detections or false alarms.

28.4 nm March 8, 2011

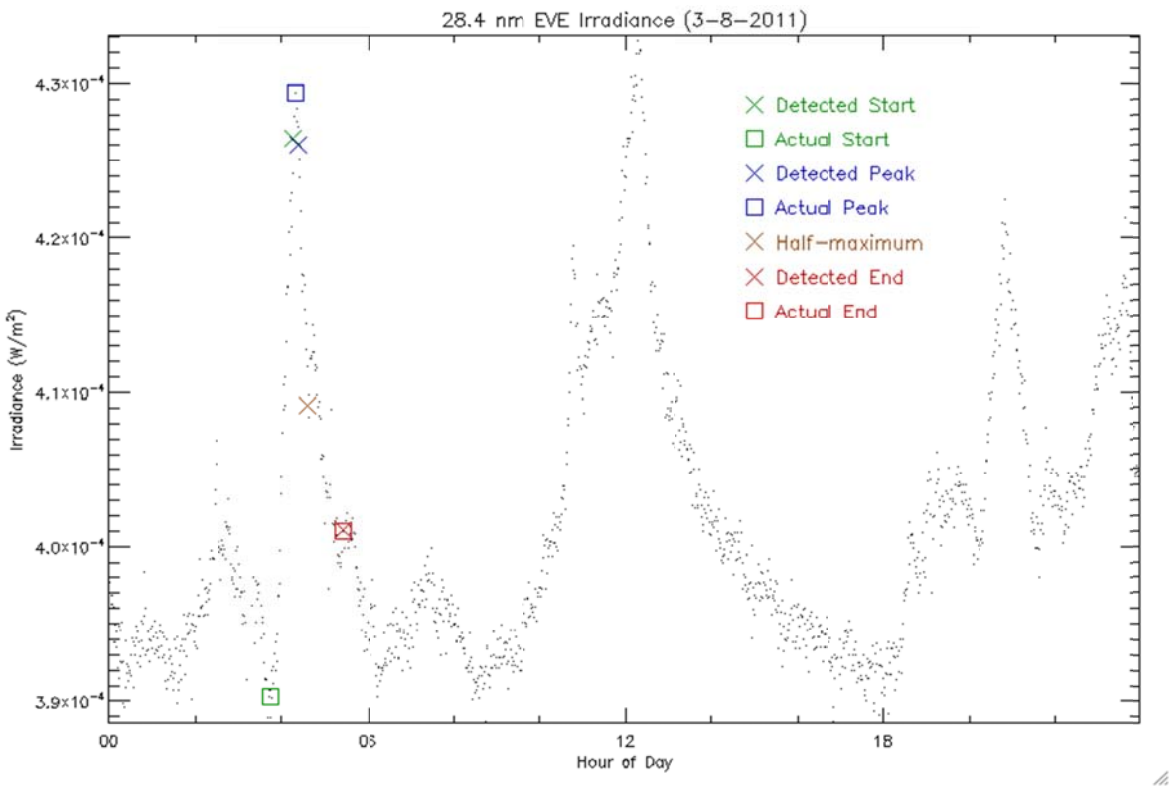

Detection of a single event, followed by a missed detection.

Detection of a single event characterized by a 10.0% irradiance increase, a detection latency of 31 minutes, and a duration of 100 minutes. This correct detection is followed by a missed detection of an 11.0% irradiance increase. This is one of five total missed detections (of 476 processed days) identified for the 28.4 nm spectral line.

This plot is the same as Figure 32.

Summary: one correct detection, one missed detection, and no false alarms.

28.4 nm August 9, 2011

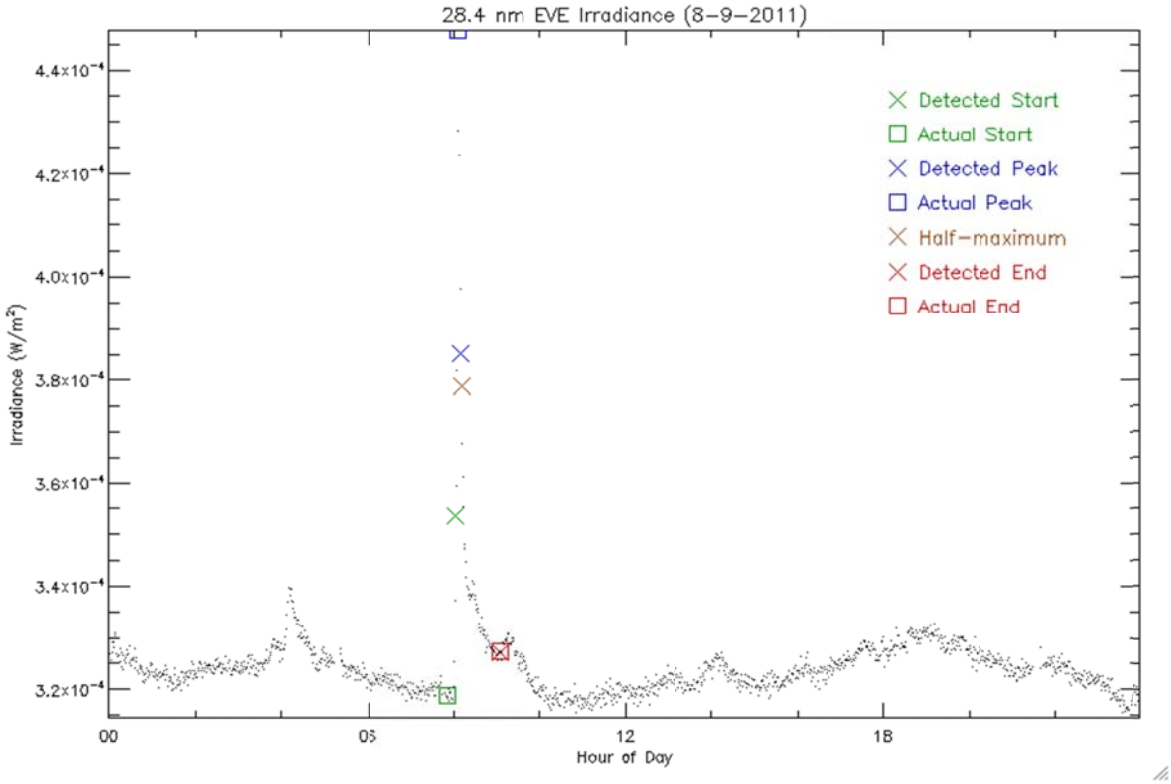

Detection of a single event with a maximum irradiance increase of 40.4%, a detection latency of 11 minutes, and an event duration of 73 minutes.

Summary: one correct detection, no missed detections or false alarms.

30.4 nm June 12, 2010

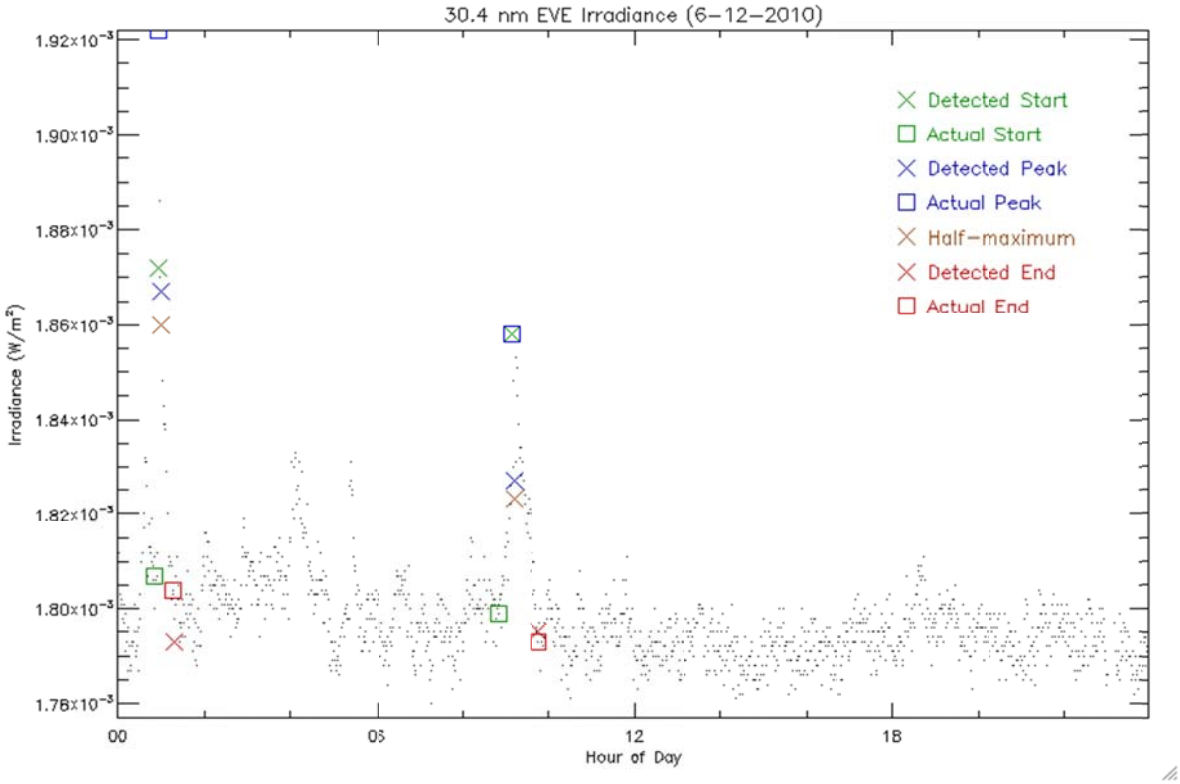

Detection of two events with maximum irradiance increases of 6.4% and 3.3%, detection latencies of 3 and 17 minutes, and event durations of 25 and 56 minutes. Noisy spikes between the two events are appropriately ignored.

Summary: two correct detections, no missed detections or false alarms.

30.4 nm August 1, 2010

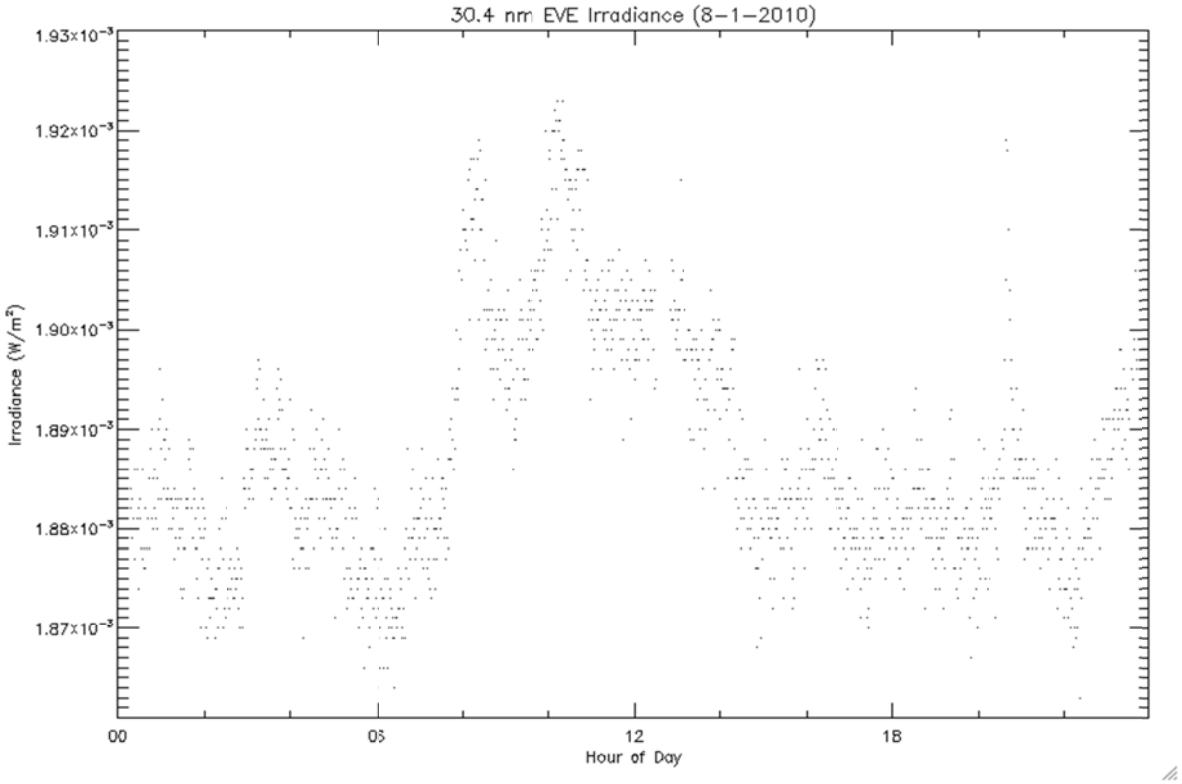

The algorithm correctly reports no alerts.

Summary: no detections, missed detections or false alarms.

30.4 nm August 7, 2010

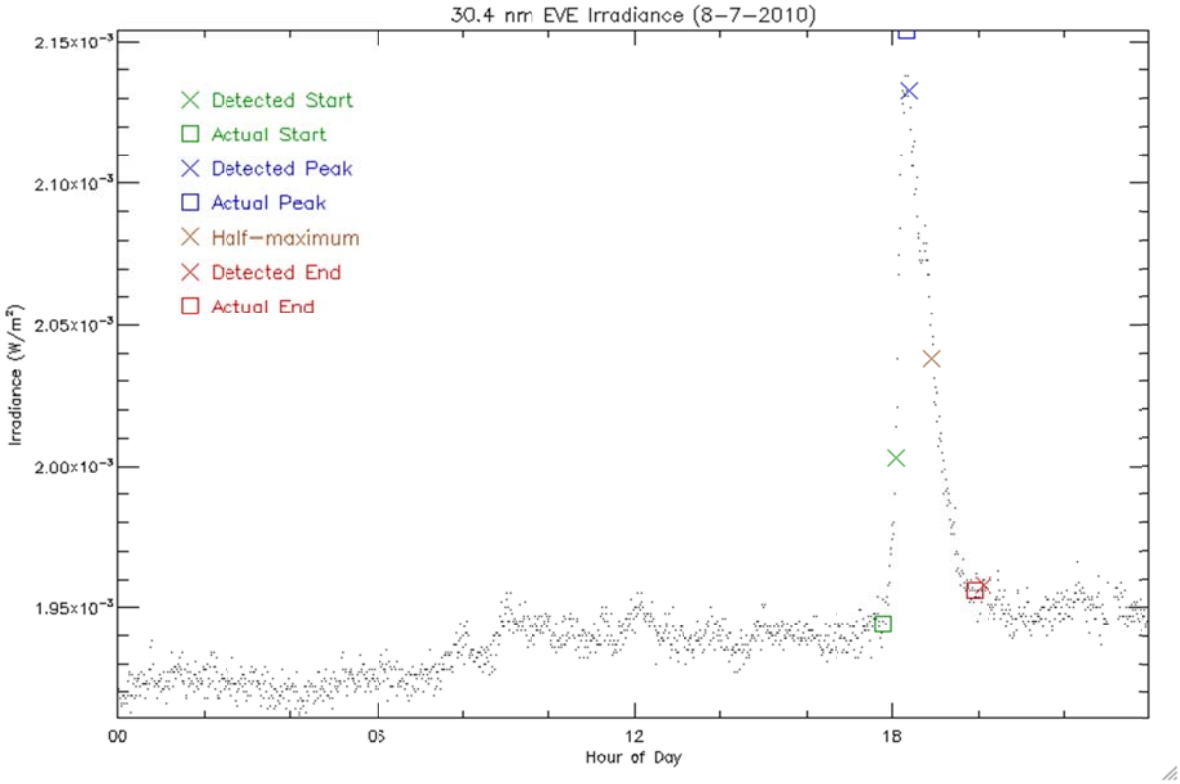

Detection of a single event with a maximum irradiance increase of 10.8%, a detection latency of 17 minutes, and an event duration of 128 minutes.

This plot is the same as Figure 26.

Summary: one correct detection, no missed detections or false alarms.

30.4 nm August 14, 2010

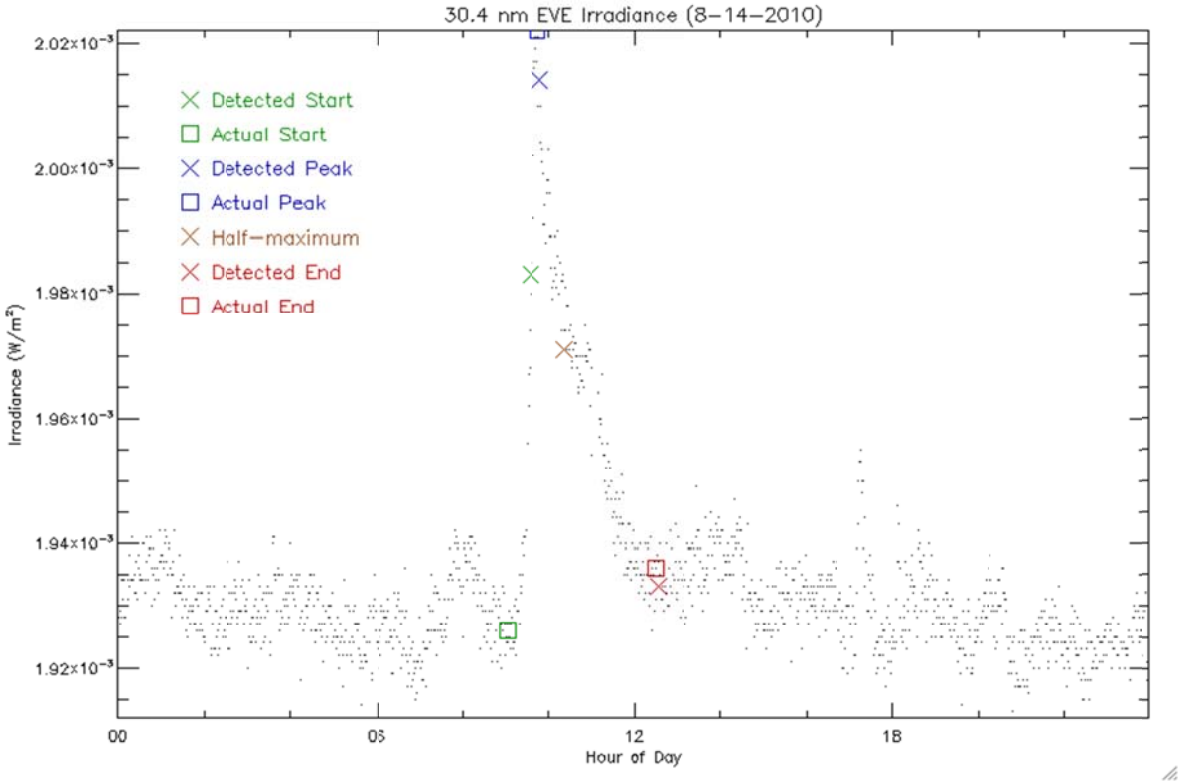

Detection of a single event with a maximum irradiance increase of 5.0%, a detection latency of 32 minutes, and an event duration of 207 minutes.

Summary: one correct detection, no missed detections or false alarms.

30.4 nm November 6, 2010

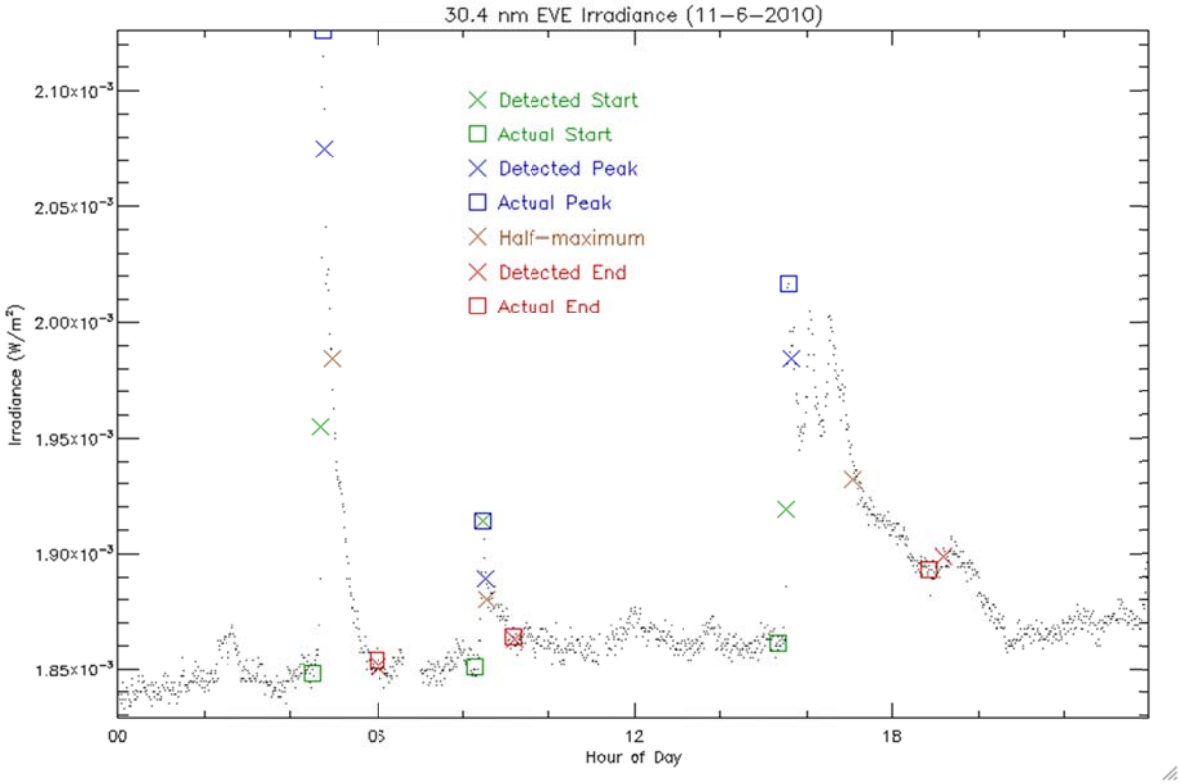

Correct detection of three events with maximum irradiance increases of 15.1%, 3.5% and 8.4%, detection latencies of 11, 11 and 11 minutes, and event durations of 92, 54 and 210 minutes.

Detection of three events, none of which are false alarms.
Maximum irradiance increases: 15.1%, 3.5% and 8.4%
Detection latencies: 11, 11 and 11 minutes
Event durations: 92, 54 and 210 minutes

Summary: three correct detections, no missed detections or false alarms.

30.4 nm February 13, 2011

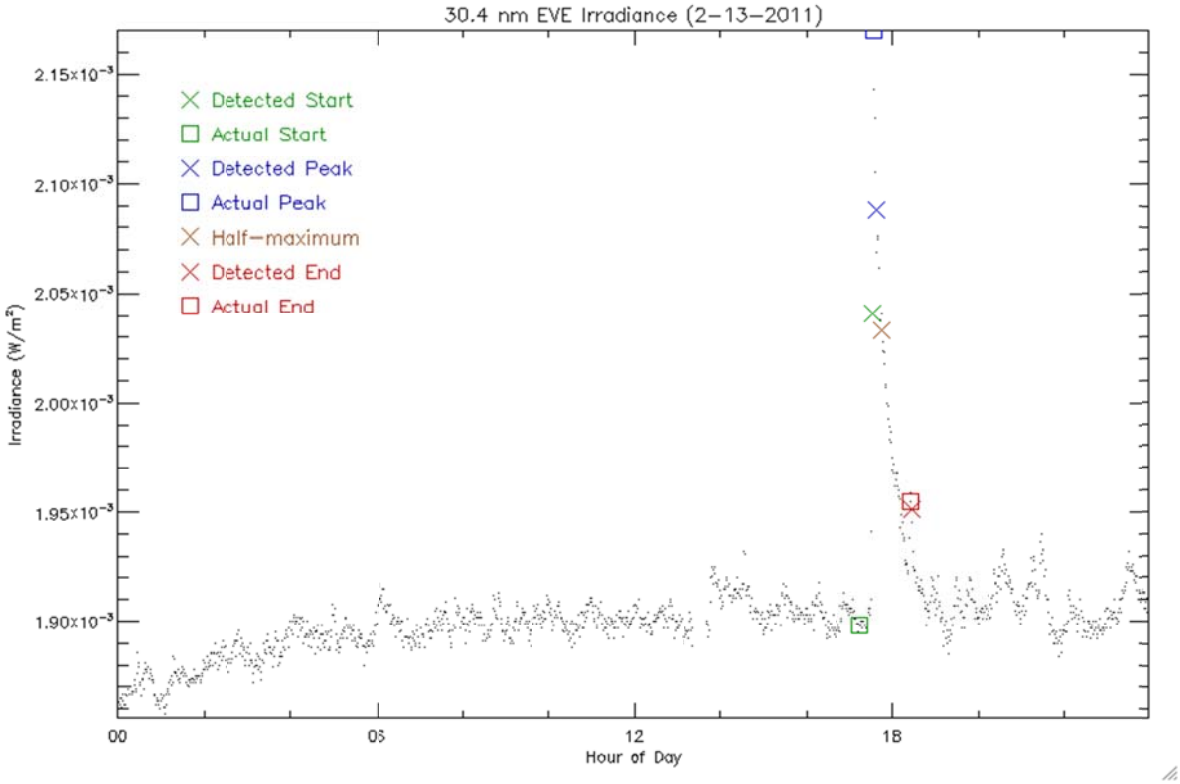

Detection of a single event with a maximum irradiance increase of 14.4%, a detection latency of 18 minutes, and an event duration of 70 minutes.

Summary: one correct detection, no missed detections or false alarms.

30.4 nm February 14, 2011

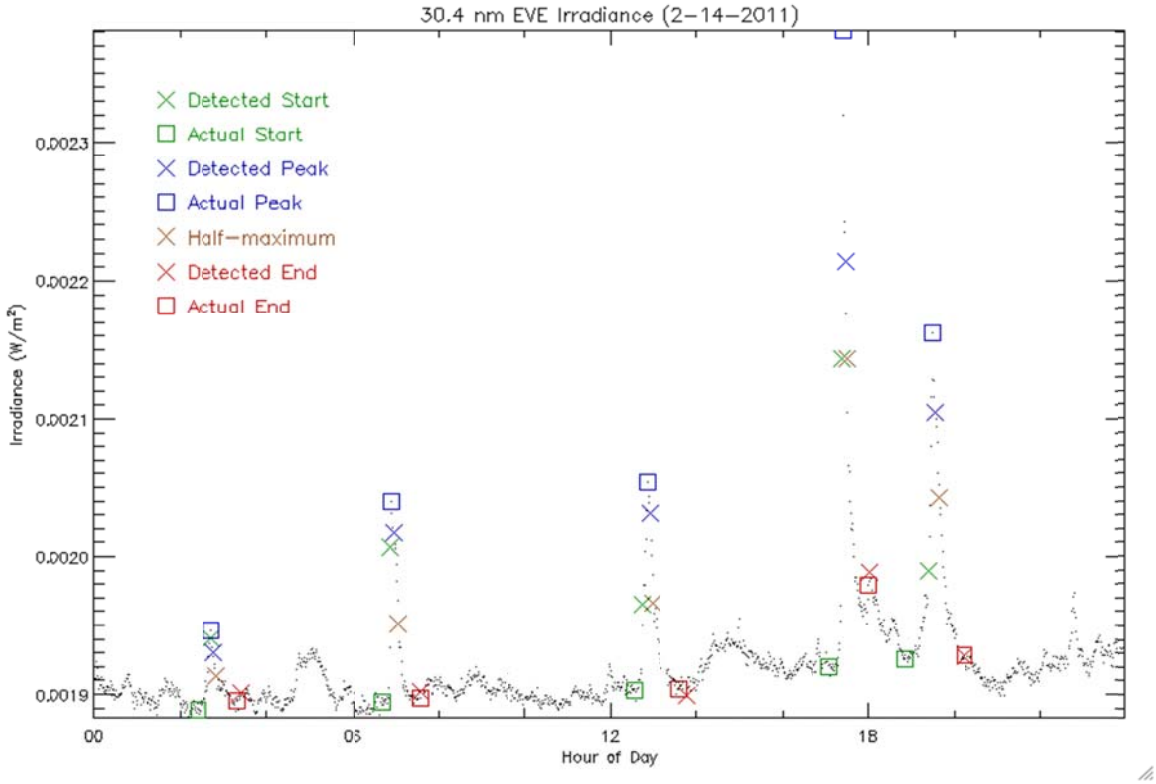

Detection of five events, none of which are false alarms.
Maximum irradiance increases: 3.0%, 7.7%, 8.0%, 24.0% and 12.3%
Detection latencies: 17, 11, 11, 18 and 31 minutes
Event durations: 54, 53, 63, 55, and 82 minutes

Summary: five correct detections, no missed detections or false alarms.

30.4 nm February 16, 2011

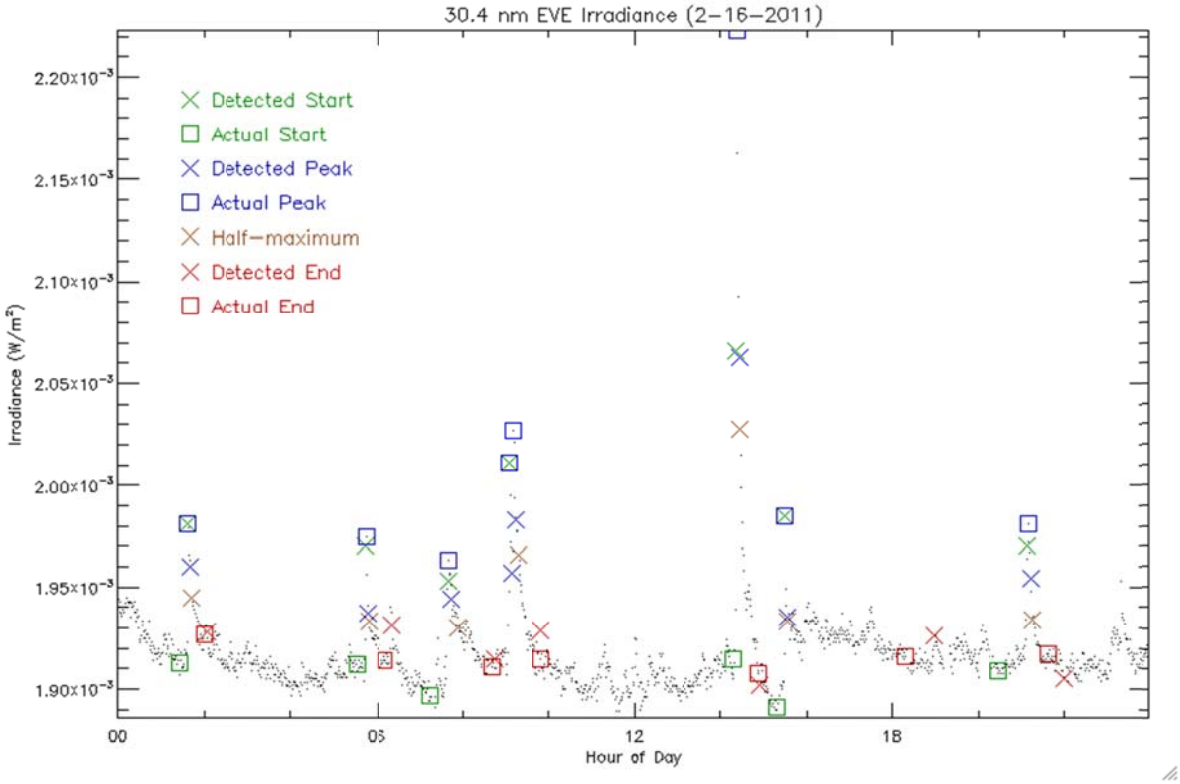

Detection of seven events, none of which are false alarms.
Maximum irradiance increases: 3.5%, 3.3% 3.5%, 6.0%, 16.1%, 5.0% and 3.7%
Detection latencies: 11, 10, 24, 24, 4, 11 and 38 minutes
Event durations: 35, 39, 85, 69, 36, 180 and 68 minutes

Summary: seven correct detections, no missed detections or false alarms.

30.4 nm March 7, 2011

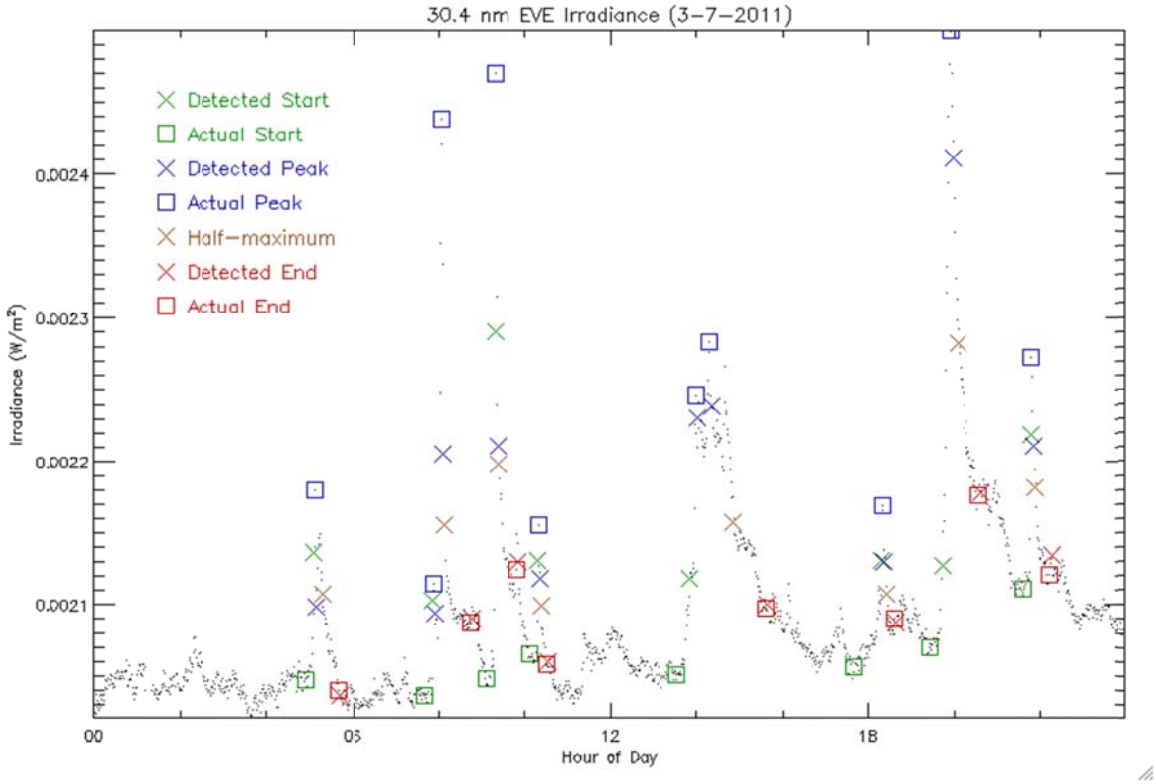

Detection of eight events, none of which are false alarms.
Maximum irradiance increases: 6.5%, 19.7%, 20.6%, 4.3%, 11.3%, 5.5%, 20.8% and 7.6%
Detection latencies: 11, 11, 11, 11, 17, 38, 17 and 11 minutes
Event durations: 46, 65, 43, 25, 123, 57, 69 and 37 minutes

Summary: eight correct detections, no missed detections or false alarms.

30.4 nm March 8, 2011

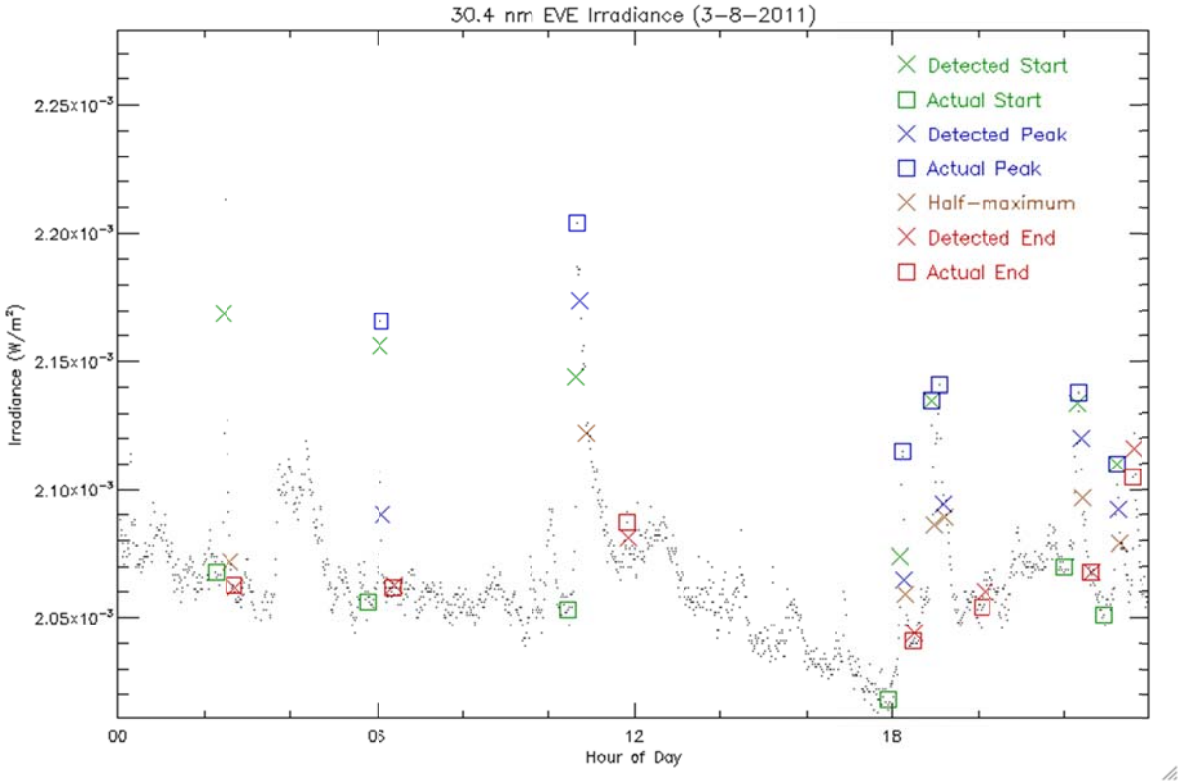

Detection of seven events, none of which are false alarms, and one missed detection.
Maximum irradiance increases: 10.2%, 3.0% (not detected), 5.3%, 7.3%, 4.8%, 4.9%, 3.3% and 3.4%
Detection latencies: 11, NA, 17, 11, 17, 24, 17 and 18 minutes
Event durations: 26, NA, 38, 81, 35, 96, 36 and 41 minutes

Summary: seven correct detections, one missed detection, and no false alarms.

30.4 nm March 12, 2011

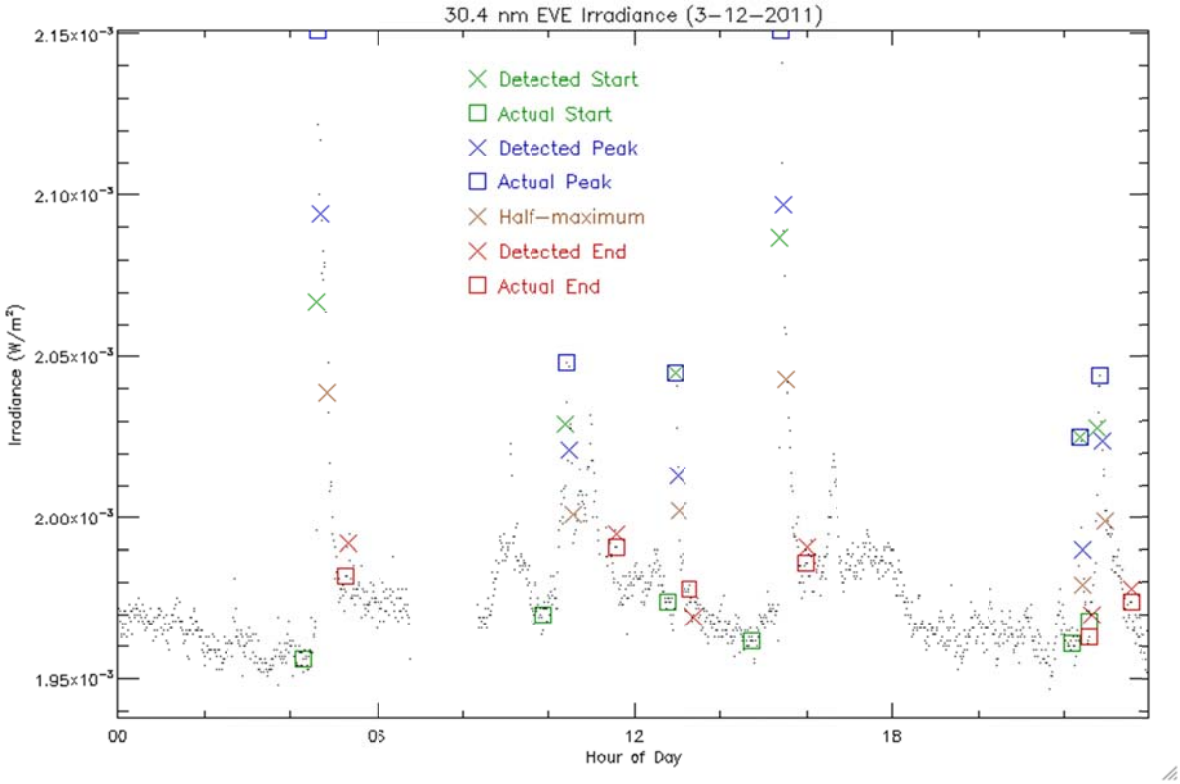

Detection of six events, none of which are false alarms.
Maximum irradiance increases: 10.0%, 4.0%, 3.6%, 9.7%, 3.3% and 3.8%
Detection latencies: 17, 31, 11, 38, 10 and 11 minutes
Event durations: 57, 102, 31, 73, 23 and 58 minutes

Summary: six correct detections, no missed detections, and one false alarm.

30.4 nm August 9, 2011

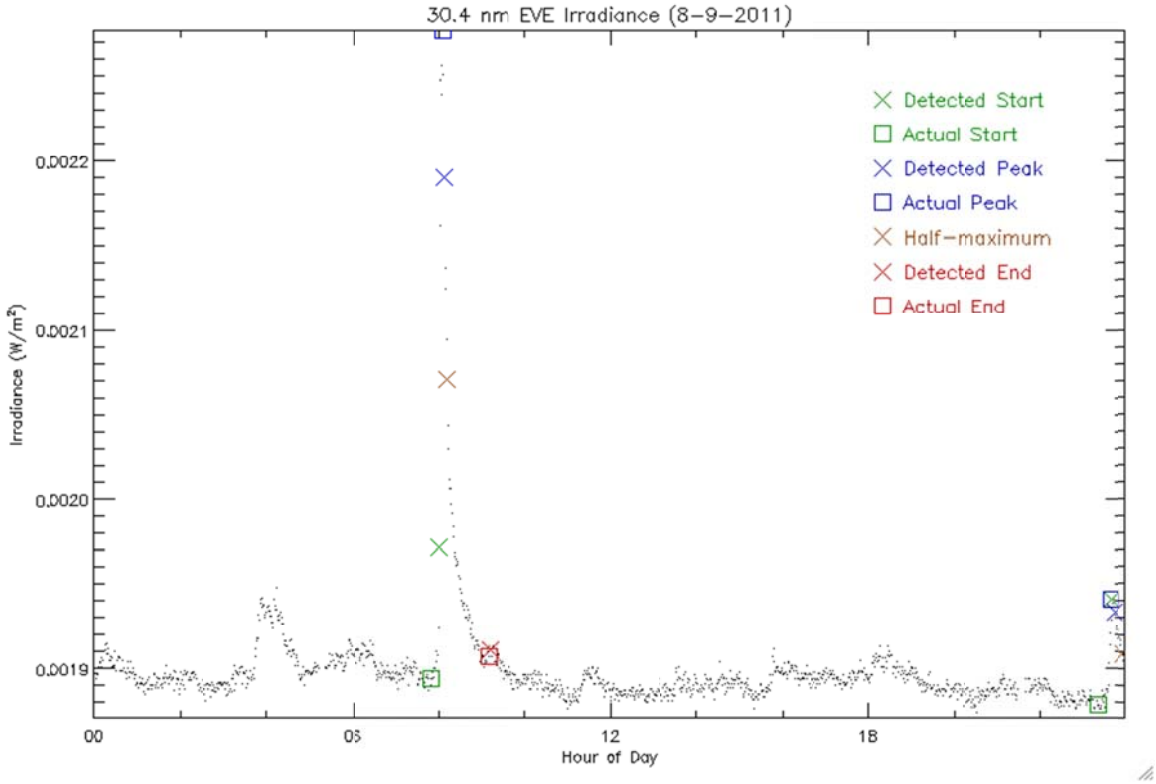

Detection of a single event with a maximum irradiance increase of 20.2%, a detection latency of 11 minutes, and an event duration of 81 minutes.

Summary: one correct detection, no missed detections or false alarms.

121.6 nm August 7, 2010

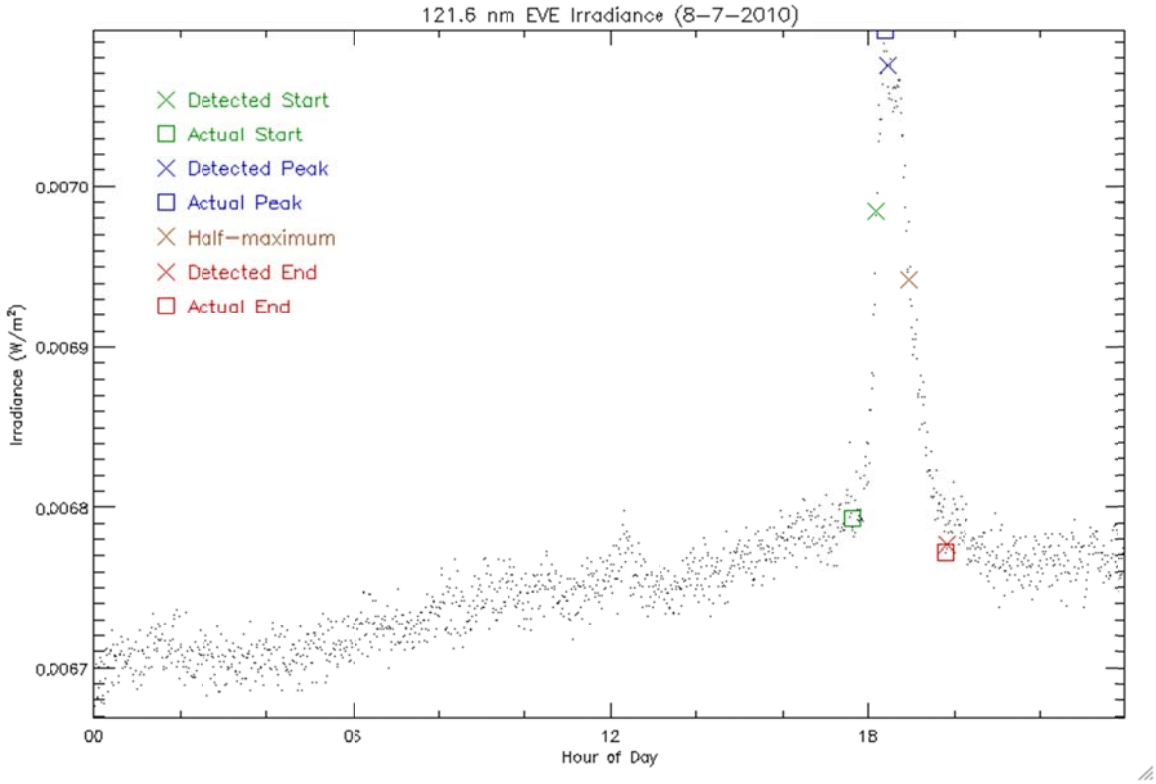

Detection of a single event with a maximum irradiance increase of 4.5%, a detection latency of 31 minutes, and an event duration of 129 minutes.

This plot is the same as Figure 27.

Summary: one correct detection, no missed detections or false alarms.

121.6 nm November 6, 2010

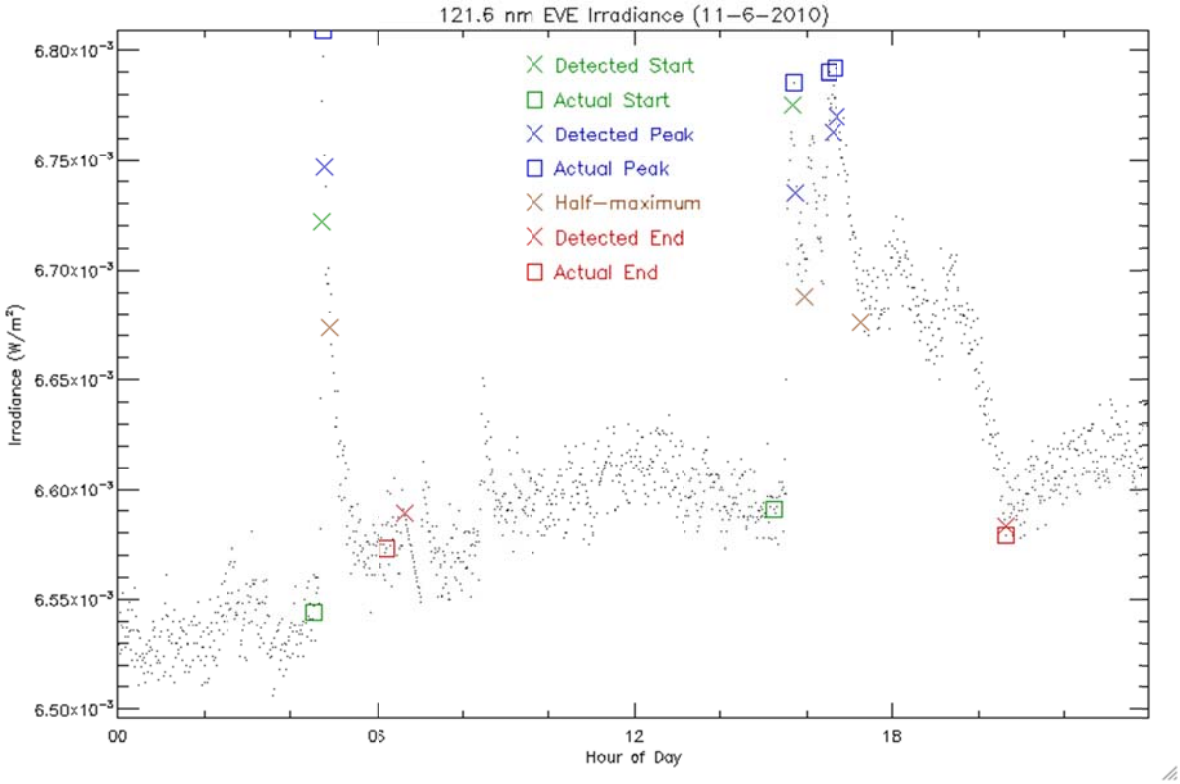

Detection of two events with maximum irradiance increases of 4.0% and 3.0%, detection latencies of 11 and 24 minutes, and event durations of 105 and 325 minutes.

Summary: two correct detections, no missed detections or false alarms.

121.6 nm November 11, 2010

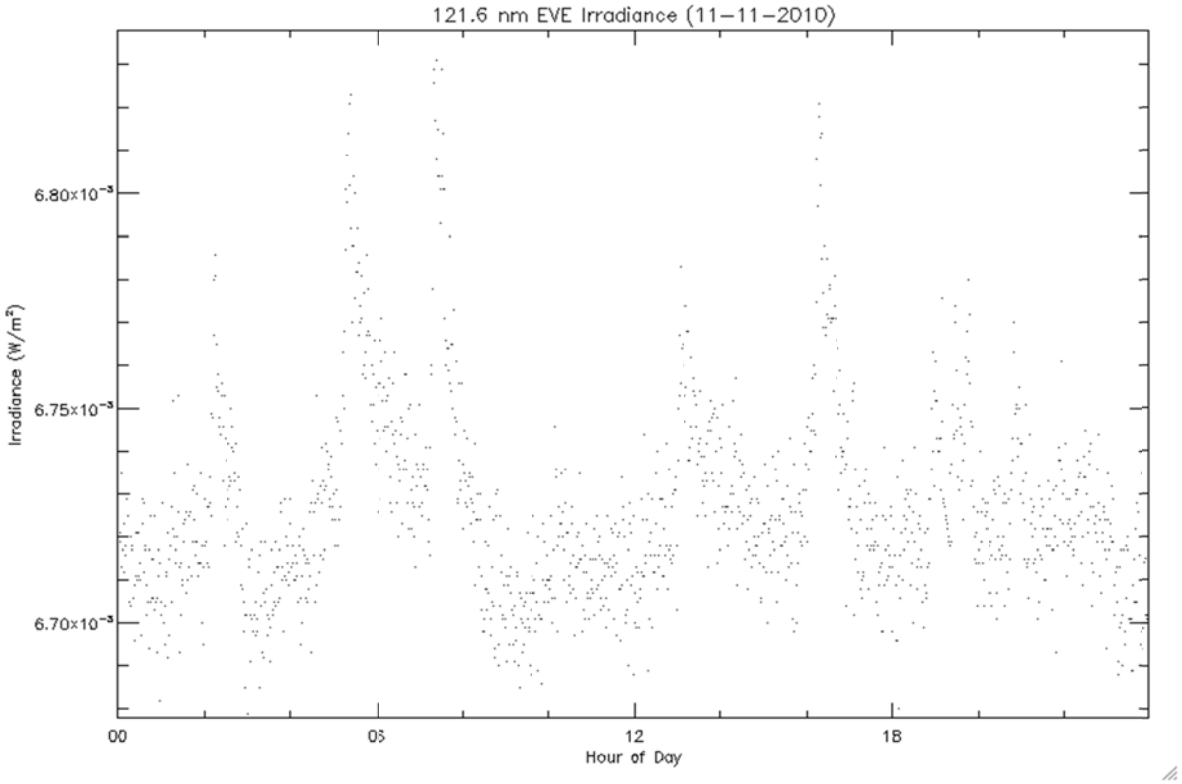

At no point is there a 3.0% or greater increase within a 2-hour period. The algorithm behaves correctly and does not alert.

Summary: no detections, missed detections or false alarms.

121.6 nm February 13, 2011

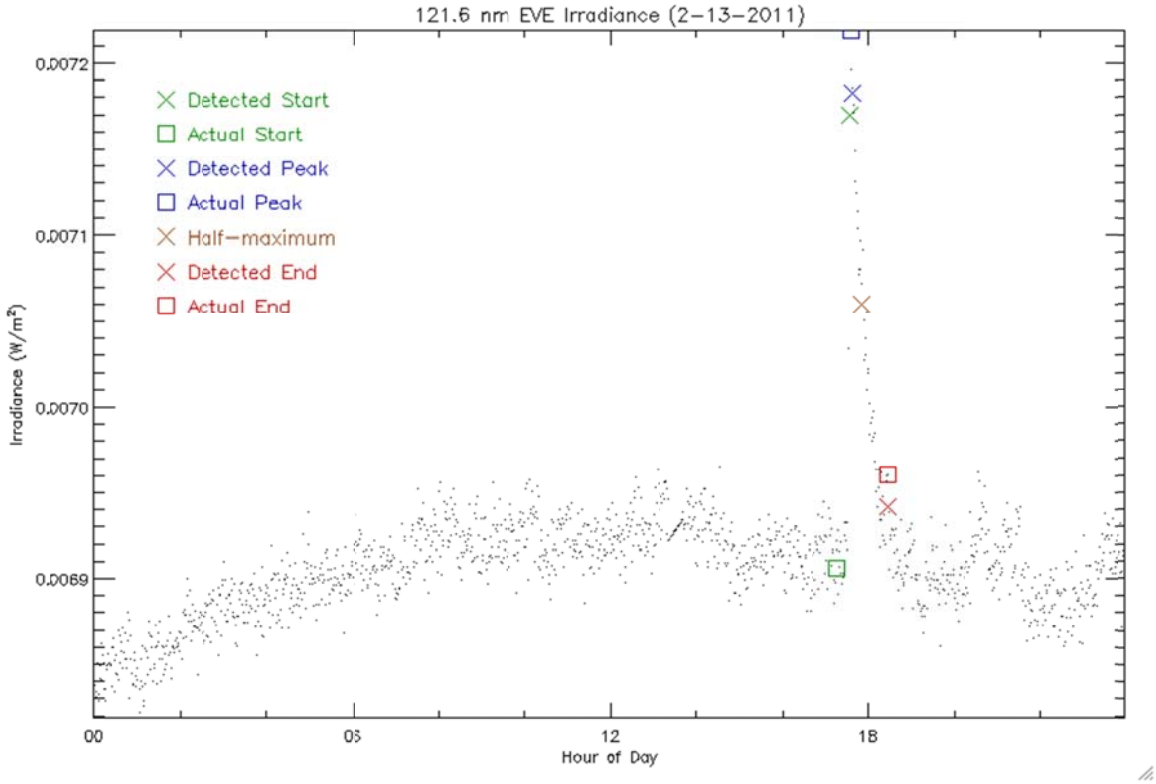

Detection of a single event with a maximum irradiance increase of 4.5%, a detection latency of 17 minutes, and an event duration of 71 minutes.

Summary: one correct detection, no missed detections or false alarms.

121.6 nm February 14, 2011

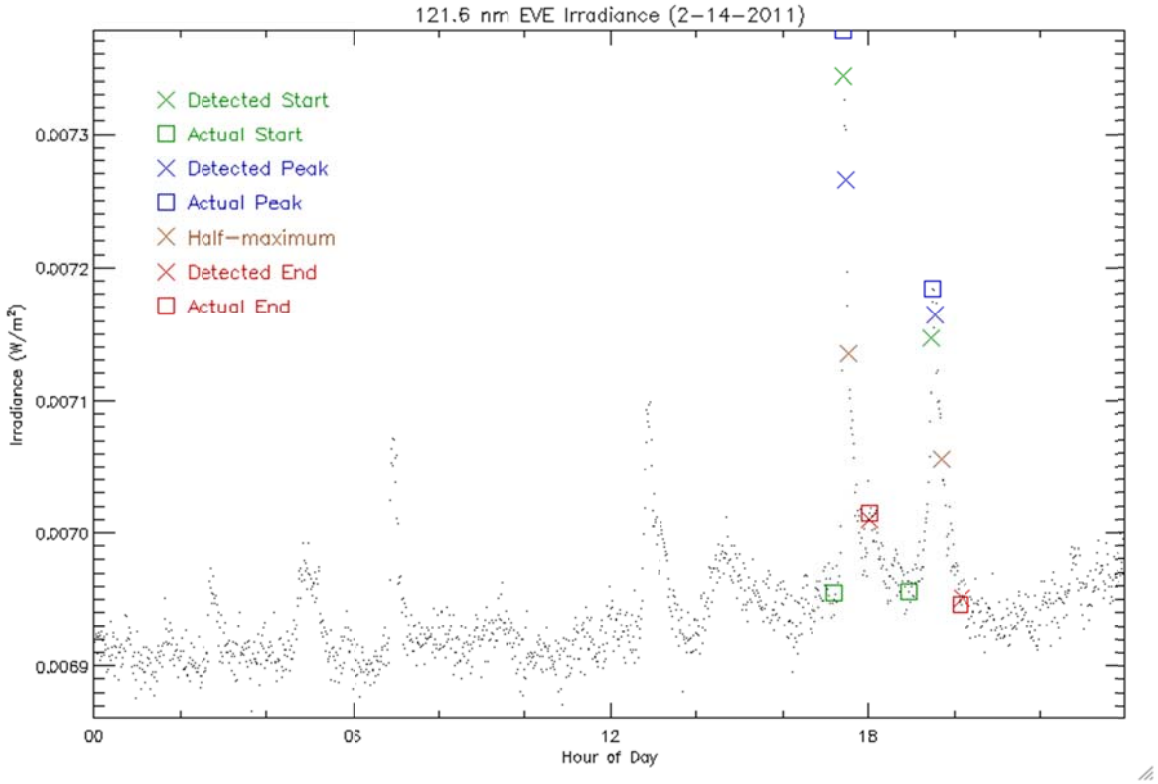

Detection of two events, neither of which is a false alarm.
Maximum irradiance increases: 6.1% and 3.3%
Detection latencies: 10 and 31 minutes
Event durations: 48 and 74 minutes

Summary: two correct detections, no missed detections or false alarms.

121.6 nm February 15, 2011

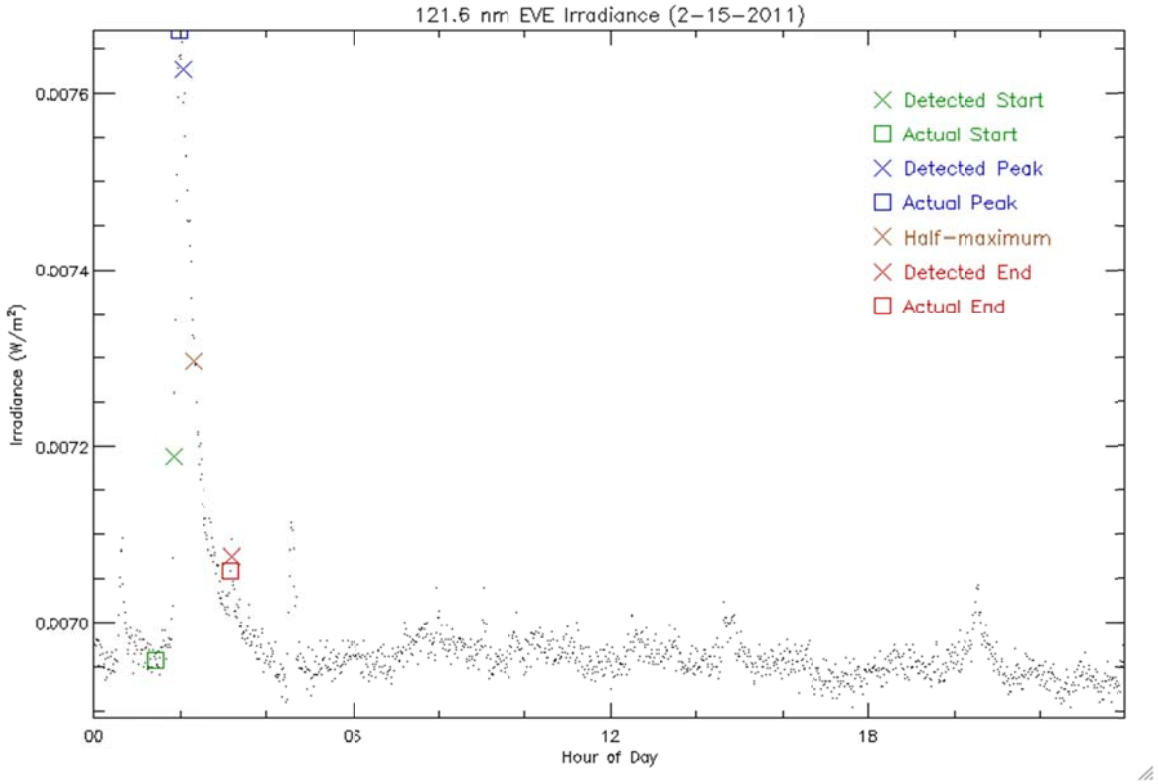

Detection of a single event with a maximum irradiance increase of 10.3%, a detection latency of 24 minutes, and an event duration of 104 minutes.

Summary: one correct detection, no missed detections or false alarms.

121.6 nm February 16, 2011

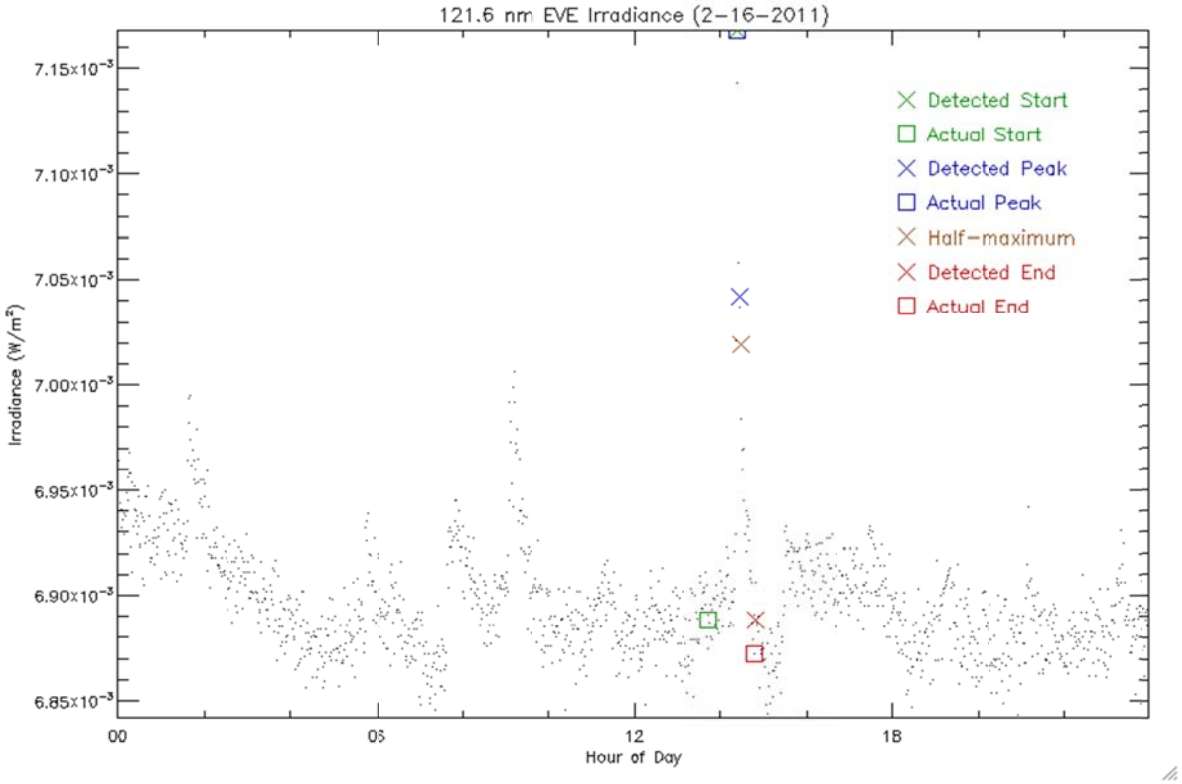

Detection of a single event with a maximum irradiance increase of 4.0%, a detection latency of 38 minutes, and an event duration of 63 minutes.

Summary: one correct detection, no missed detections or false alarms.

121.6 nm February 18, 2011

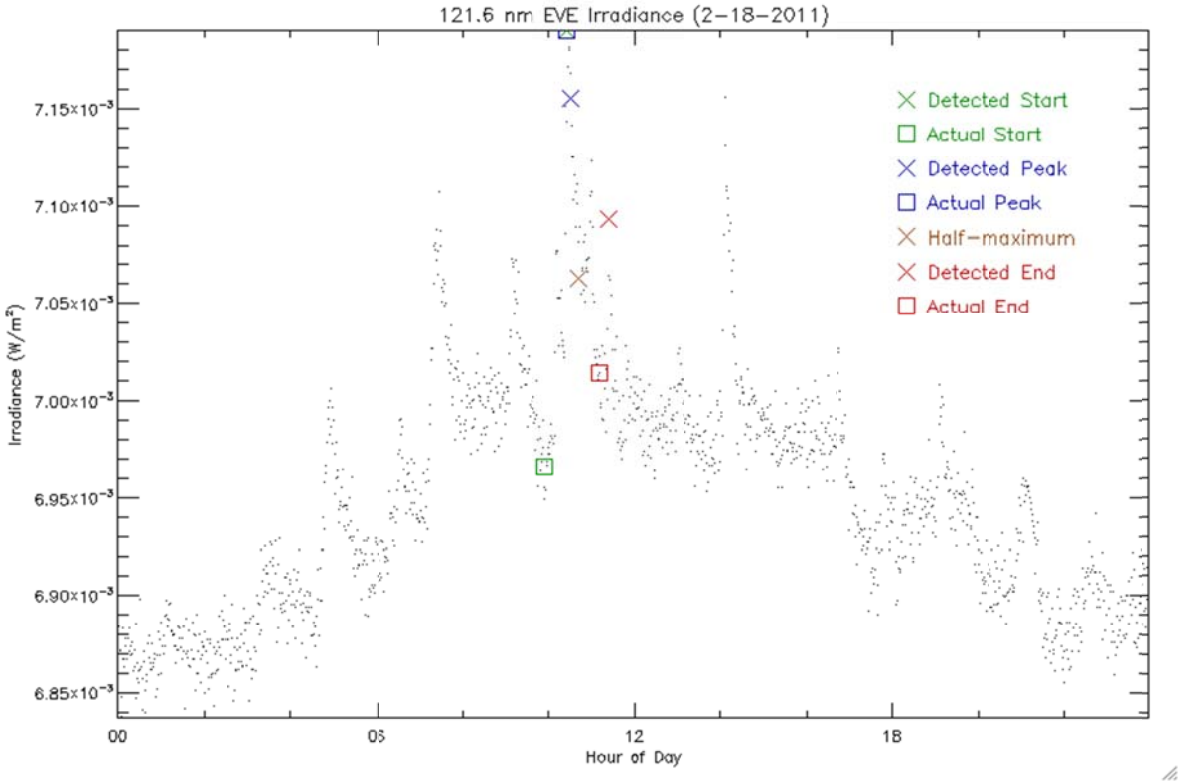

Detection of a single event with a maximum irradiance increase of 3.2%, a detection latency of 32 minutes, and an event duration of 77 minutes.

This plot is the same as Figure 33.

Summary: one correct detection, no missed detections or false alarms.

121.6 nm March 7, 2011

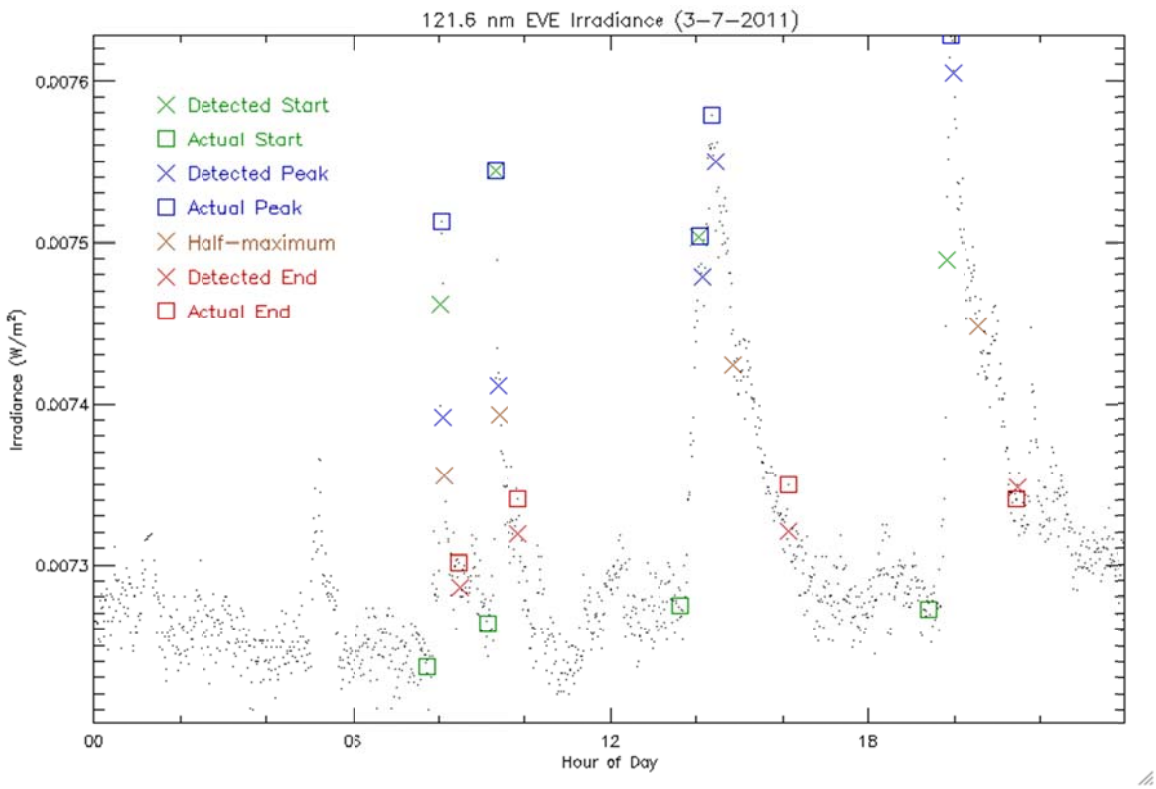

Detection of four events, none of which are false alarms.
Maximum irradiance increases: 3.8%, 3.9%, 4.2% and 4.9%
Detection latencies: 18, 10, 24 and 24 minutes
Event durations: 44, 43, 148 and 124 minutes

Summary: four correct detections, no missed detections or false alarms.

121.6 nm July 30, 2011

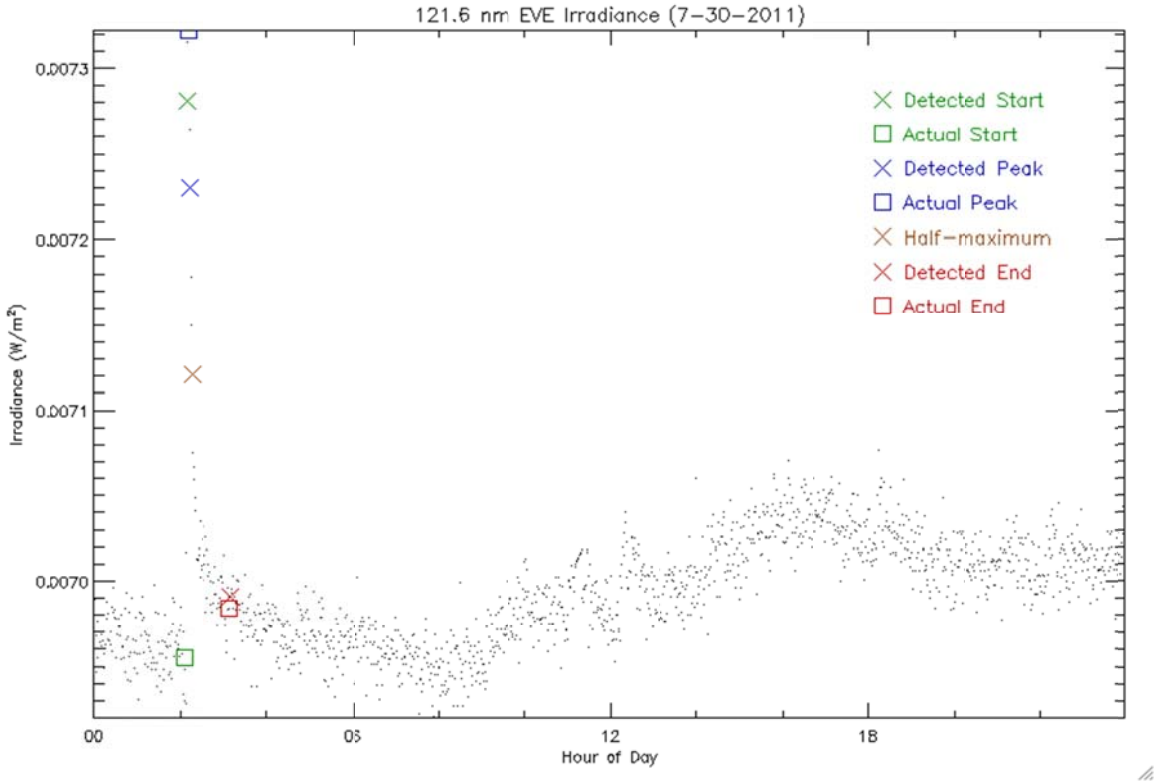

Detection of a single event with a maximum irradiance increase of 5.3%, a detection latency of 4 minutes, and an event duration of 66 minutes.

Summary: one correct detection, no missed detections or false alarms.

121.6 nm August 4, 2011

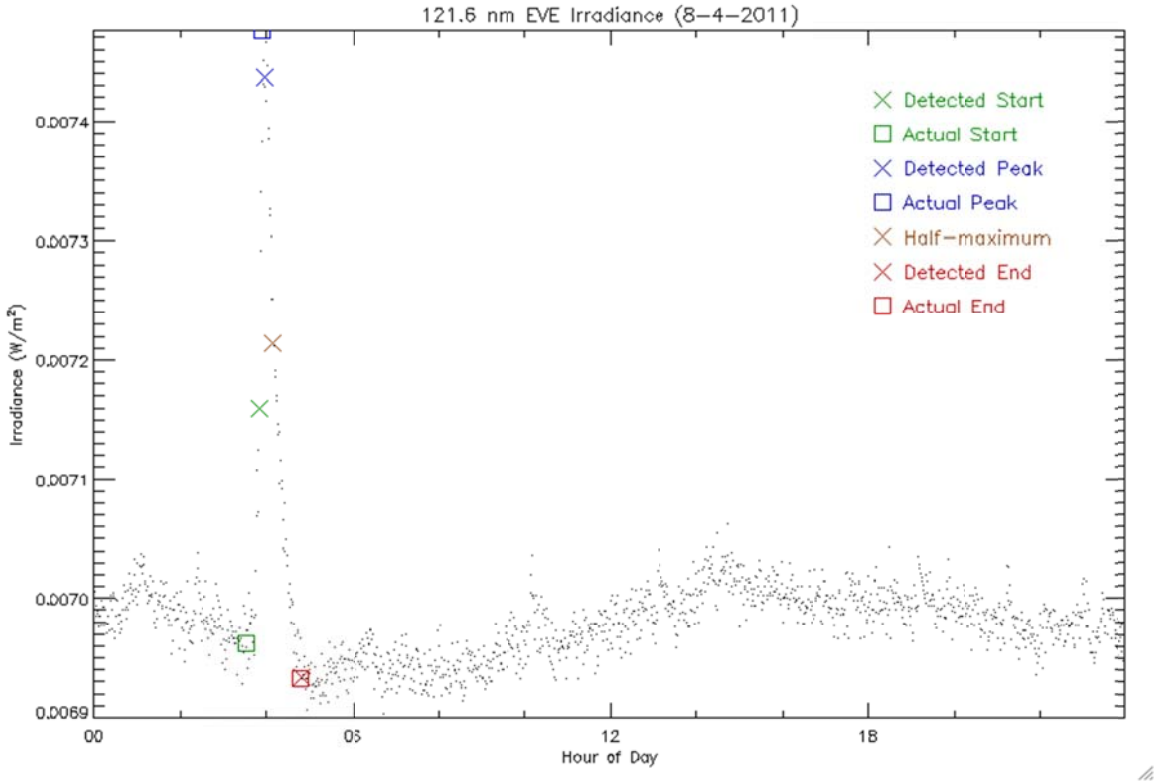

Detection of a single event with a maximum irradiance increase of 7.4%, a detection latency of 17 minutes, and an event duration of 75 minutes.

Summary: one correct detection, no missed detections or false alarms.

121.6 nm August 9, 2011

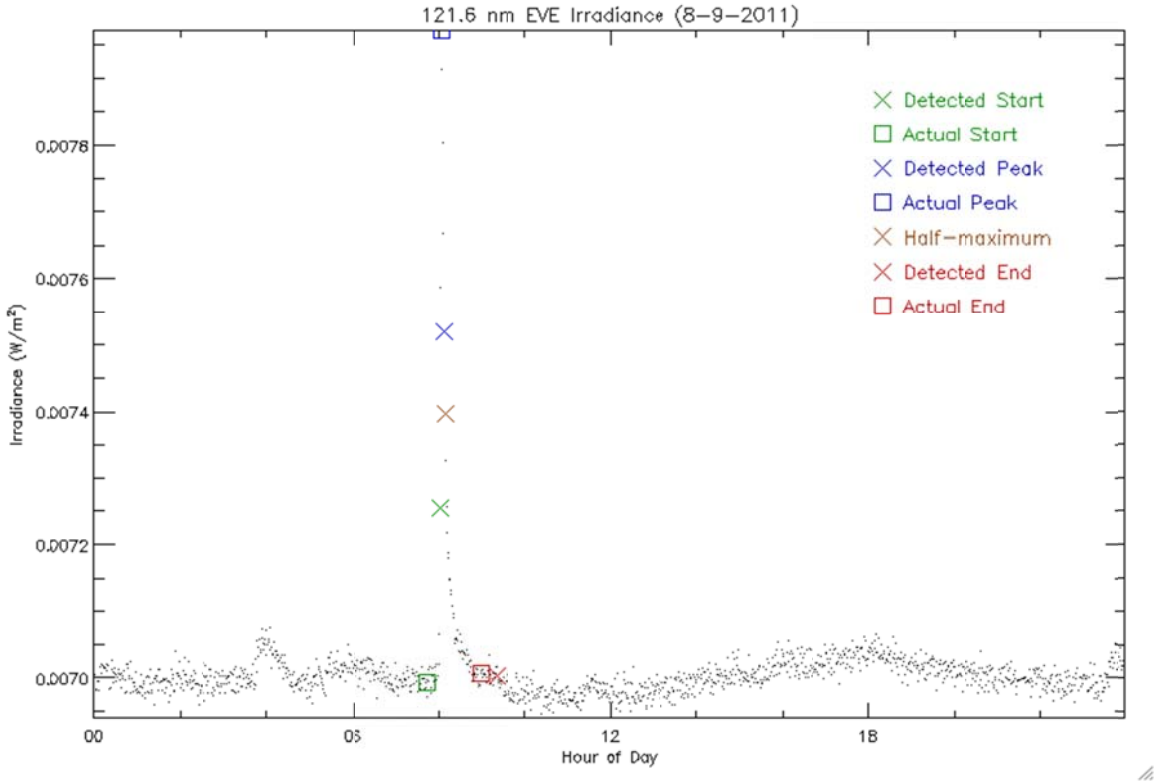

Detection of a single event with a maximum irradiance increase of 14.0%, a detection latency of 18 minutes, and an event duration of 75 minutes.

Summary: one correct detection, no missed detections or false alarms.

APPENDIX C

Algorithm Validation Statistics

Although not subjected to the same degree of scrutiny as the dozen test and development days assigned each of the spectral lines, all 476 days of available GOES-R proxy data were processed by the algorithm using the high false alarm suppression configuration (9.0% for 28.4 nm and 2.7% for 30.4 nm and 121.6 nm). This test data set inclusively spanned April 30, 2010 to August 18, 2011.

In addition, all 476 days were manually inspected for potential missed detections.

Note that

total events = total alerts + total missed detections – total false alarms

False alarms can be eliminated entirely by simply setting the false alarm suppression threshold to the event definition threshold. Note, however, that a detection latency penalty, which will be most severe for the 28.4 nm spectral line, will result.

As discussed in Section 7.4, there is a relationship between the false alarm suppression threshold and missed associated with EUV events that proceed erratically (i.e., increase in successively greater spikes). In these cases, missed detections can be reduced considerably by setting the false alarm suppression threshold to zero, but the one-minute updates would be dominated by a false alarm rate approaching 90%. One option would be to run a separate instance of the algorithm in which the false alarm suppression thresholds are set to zero, ignore the one-minute updates, and filter the post-event summary output by event magnitude to eliminate false alarms. Although this option would not provide meaningful alerts due to excessive false alarms, it would provide a more complete event catalog with fewer missed detections.

28.4 nm Validation Results

28.4 nm Contingency Table

	Observed	Not Observed
Detected	26	1
Not Detected	5	NA

Total Events: 31
Total Alerts: 27
Missed Detections: 5
Total False Alarms: 1
Mean Detection Latency: 41.3 Minutes
Minimum Detection Latency: 4 Minutes
Maximum Detection Latency: 157 Minutes
Mean Event Duration: 270.6 Minutes
Minimum Event Duration: 34 Minutes
Maximum Event Duration: 1441 Minutes
Probability of Detection: 83.9%
Missed Detection Rate: 16.1%
False Alarm Rate: 3.7%

Missed Detections:
August 1, 2010 (10.9% event)
February 18, 2011 (13.3% event)
March 6, 2011 (16.7% event)
March 8, 2011 (11.0% event)
August 2, 2011 (11.6% event)

All 28.4 nm missed detections were associated with erratic irradiance increases as discussed in Section.

There were 12 28.4 nm events associated with irradiance increases of 15% or greater. For these events, the algorithm probability of detection is 91.7%.

There were 6 28.4 nm events associated with irradiance increases of 20% or greater. For these events, the algorithm probability of detection is 100%.

30.4 nm Validation Results

30.4 nm Contingency Table

	Observed	Not Observed
Detected	193	21
Not Detected	2	NA

Total Events: 192
Total Alerts: 210
Missed Detections: 2
Total False Alarms: 20
Mean Detection Latency: 18.3 Minutes
Minimum Detection Latency: 3 Minutes
Maximum Detection Latency: 80 Minutes
Mean Event Duration: 77.5 Minutes
Minimum Event Duration: 18 Minutes
Maximum Event Duration: 1441 Minutes
Probability of Detection: 99.0%
Missed Detection Rate: 1.0%
False Alarm Rate: 9.5%

Missed Detections:
March 1, 2011 (3.0% event)
March 8, 2011 (3.0% event)

121.6 nm Validation Results

121.6 nm Contingency Table

	Observed	Not Observed
Detected	25	3
Not Detected	0	NA

Total Events: 25
Total Alerts: 28
Missed Detections: 0
Total False Alarms: 3
Mean Detection Latency: 21.8 Minutes
Minimum Detection Latency: 3 Minutes
Maximum Detection Latency: 74 Minutes
Mean Event Duration: 158.7 Minutes
Minimum Event Duration: 43 Minutes
Maximum Event Duration: 1441 Minutes
Probability of Detection: 100.0%
Missed Detection Rate: 0.0%
False Alarm Rate: 10.7%

Missed Detections:
None

APPENDIX D

Preliminary EUV Event Catalog

In this section, the post-event summaries for all GOES-R proxy data processed by the algorithm are presented. Note that false alarms are included and missed detections are not included.

```
# UNITS: Irradiance (W/m^2), Energy (J/m^2), Duration (minutes)
#
# Line    Start          Start      Peak           Peak        End            End          Mean         Event     Total       Max Irradiance
# ID      YYYYMMDDHHMM   Irradiance YYYYMMDDHHMM   Irradiance  YYYYMMDDHHMM   Irradiance   Irradiance   Duration  Energy      Increase (%)
# ------  ------------   ---------- ------------   ----------  ------------   ----------   ----------   --------- ----------  ---------------
30.4nm    201004301923   1.863e-03  201004301934   1.932e-03   201004301950   1.876e-03    1.762e-01    28        4.933e+00              3.69
30.4nm    201005010112   1.875e-03  201005010137   1.934e-03   201005010207   1.891e-03    1.137e-01    54        6.142e+00              3.14
30.4nm    201005051713   1.946e-03  201005051717   2.013e-03   201005051820   1.953e-03    1.244e-01    67        8.337e+00              3.41
30.4nm    201005070722   1.929e-03  201005070749   1.988e-03   201005070856   1.946e-03    1.172e-01    94        1.102e+01              3.06
30.4nm    201005080439   1.940e-03  201005080457   2.008e-03   201005080551   1.931e-03    1.171e-01    71        8.317e+00              3.50
30.4nm    201005081137   1.938e-03  201005081149   2.017e-03   201005081301   1.936e-03    1.176e-01    84        9.881e+00              4.04
30.4nm    201006120051   1.807e-03  201006120056   1.922e-03   201006120117   1.793e-03    1.100e-01    25        2.750e+00              6.35
28.4nm    201006120028   1.455e-04  201006120101   1.604e-04   201006120130   1.477e-04    9.519e-03    62        5.901e-01             10.22
30.4nm    201006120850   1.799e-03  201006120908   1.858e-03   201006120947   1.795e-03    1.091e-01    56        6.111e+00              3.30
30.4nm    201006140029   1.788e-03  201006140049   1.871e-03   201006140132   1.797e-03   -1.000e+05    63       -1.000e+05              4.66
30.4nm    201007091908   1.858e-03  201007091941   1.968e-03   201007092007   1.893e-03    1.138e-01    58        6.603e+00              5.92
28.4nm    201007091935   1.701e-04  201007092317   1.908e-04   201007100917   1.755e-04   -1.000e+05    822      -1.000e+05             12.17
30.4nm    201007141137   1.904e-03  201007141229   1.956e-03   201007142340   1.903e-03   -1.000e+05    170      -1.000e+05              2.77
30.4nm    201007171723   1.921e-03  201007171759   1.988e-03   201007171900   1.937e-03    1.220e-01    97        1.183e+01              3.46
28.4nm    201007190739   1.849e-04  201007191107   2.056e-04   201007191652   1.892e-04   -1.000e+05    552      -1.000e+05             11.16
30.4nm    201007310442   1.902e-03  201007310528   1.964e-03   201007310544   1.904e-03    1.631e-01    63        1.027e+01              3.28
30.4nm    201008062050   1.927e-03  201008062101   1.995e-03   201008062121   1.925e-03   -1.000e+05    30       -1.000e+05              3.53
28.4nm    201008071752   2.116e-04  201008071843   2.800e-04   201008071945   2.250e-04    1.443e-02    114       1.645e+00             32.29
121.6nm   201008071739   6.793e-03  201008071824   7.097e-03   201008071949   6.777e-03    4.147e-01    129       5.350e+01              4.48
30.4nm    201008071747   1.944e-03  201008071821   2.154e-03   201008071955   1.956e-03    1.313e-01    128       1.680e+01             10.80
28.4nm    201008140924   2.254e-04  201008141047   2.508e-04   201008141206   2.319e-04   -1.000e+05    161      -1.000e+05             11.27
30.4nm    201008140903   1.926e-03  201008140944   2.022e-03   201008141230   1.936e-03   -1.000e+05    207      -1.000e+05              4.99
30.4nm    201008180430   1.870e-03  201008180450   1.924e-03   201008180528   1.873e-03    1.130e-01    58        6.556e+00              2.87
30.4nm    201009061433   1.863e-03  201009061459   1.930e-03   201009061527   1.875e-03    1.126e-01    53        5.969e+00              3.63
30.4nm    201009170117   1.881e-03  201009170122   1.943e-03   201009170135   1.876e-03    1.136e-01    18        2.044e+00              3.32
28.4nm    201010161855   2.200e-04  201010161913   2.428e-04   201010161933   2.195e-04    1.343e-02    38        5.102e-01             10.37
30.4nm    201010161906   1.946e-03  201010161911   2.115e-03   201010162008   1.952e-03    1.182e-01    62        7.330e+00              8.68
30.4nm    201010181441   1.936e-03  201010181632   2.024e-03   201010182227   1.941e-03    1.192e-01    466       5.556e+01              4.54
30.4nm    201010231727   1.915e-03  201010231738   1.971e-03   201010231841   1.911e-03    1.163e-01    74        8.608e+00              2.97
30.4nm    201010252157   1.911e-03  201010252209   1.982e-03   201010252235   1.909e-03    1.186e-01    38        4.508e+00              3.66
30.4nm    201010310418   1.837e-03  201010310429   1.893e-03   201010310452   1.849e-03    1.110e-01    34        3.773e+00              3.03
28.4nm    201011031343   1.741e-04  201011031531   2.005e-04   201011031856   1.798e-04    1.135e-02    314       3.563e+00             15.17
28.4nm    201011050051   1.971e-04  201011050338   2.375e-04   201011050553   2.080e-04    1.297e-02    301       3.903e+00             20.49
28.4nm    201011051410   2.021e-04  201011051640   2.386e-04   201011051856   2.056e-04    1.318e-02    285       3.757e+00             18.05
30.4nm    201011060430   1.848e-03  201011060444   2.126e-03   201011060602   1.851e-03    1.145e-01    92        1.054e+01             15.07
121.6nm   201011060431   6.544e-03  201011060444   6.809e-03   201011060615   6.573e-03    4.850e-01    105       5.092e+01              4.05
30.4nm    201011060817   1.851e-03  201011060828   1.914e-03   201011060911   1.863e-03    1.125e-01    54        6.073e+00              3.45
28.4nm    201011061452   1.994e-04  201011061541   2.374e-04   201011061600   2.072e-04    1.483e-02    69        1.024e+00             19.02
30.4nm    201011061521   1.861e-03  201011061535   2.017e-03   201011061851   1.893e-03    1.268e-01    210       2.663e+01              8.40
121.6nm   201011061515   6.591e-03  201011061640   6.792e-03   201011062041   6.583e-03    4.014e-01    325       1.305e+02              3.06
28.4nm    201011061713   2.176e-04  201011061918   2.510e-04   201011062043   2.208e-04    1.508e-02    209       3.151e+00             15.37
30.4nm    201011062341   1.870e-03  201011070006   1.921e-03   201011070041   1.878e-03    1.173e-01    59        6.922e+00              2.72
30.4nm    201011070119   1.871e-03  201011070140   2.058e-03   201011070336   1.884e-03    1.315e-01    137       1.802e+01             10.05
30.4nm    201011110456   1.912e-03  201011110517   1.986e-03   201011110608   1.918e-03    1.348e-01    72        9.705e+00              3.89
30.4nm    201011110708   1.901e-03  201011110723   2.010e-03   201011110804   1.897e-03    1.159e-01    56        6.489e+00              5.70
30.4nm    201011111548   1.905e-03  201011111614   1.978e-03   201011111707   1.909e-03    1.156e-01    78        9.014e+00              3.81
30.4nm    201011120114   1.893e-03  201011120134   2.078e-03   201011120201   1.897e-03    1.202e-01    47        5.651e+00              9.77
30.4nm    201011160243   1.912e-03  201011160301   1.966e-03   201011160340   1.917e-03   -1.000e+05    57       -1.000e+05              2.83
30.4nm    201011170426   1.917e-03  201011170439   1.988e-03   201011170453   1.914e-03    1.161e-01    27        3.133e+00              3.70
30.4nm    201012141448   1.830e-03  201012141537   1.888e-03   201012141655   1.851e-03    1.203e-01    126       1.515e+01              3.12
28.4nm    201012141508   2.149e-04  201012141626   2.345e-04   201012142021   2.184e-04    1.349e-02    312       4.210e+00              9.08
30.4nm    201012150626   1.827e-03  201012150638   1.939e-03   201012150748   1.825e-03    1.107e-01    81        8.963e+00              6.14
30.4nm    201101210406   1.783e-03  201101210418   1.840e-03   201101210442   1.776e-03    1.078e-01    36        3.879e+00              3.21
30.4nm    201101211501   1.796e-03  201101211519   1.863e-03   201101211544   1.794e-03    1.086e-01    42        4.563e+00              3.74
30.4nm    201101262158   1.693e-03  201101262209   1.747e-03   201101262241   1.702e-03    1.230e-01    44        5.410e+00              3.18
30.4nm    201101271148   1.677e-03  201101271200   1.728e-03   201101271301   1.689e-03    1.013e-01    73        7.394e+00              3.05
30.4nm    201101280040   1.685e-03  201101280101   1.754e-03   201101280136   1.704e-03    1.459e-01    56        8.171e+00              4.08
30.4nm    201102081356   1.792e-03  201102081449   1.843e-03   201102081539   1.803e-03    1.115e-01    102       1.137e+01              2.86
30.4nm    201102081840   1.808e-03  201102081852   1.889e-03   201102081936   1.821e-03    1.310e-01    56        7.335e+00              4.51
30.4nm    201102082044   1.808e-03  201102082110   1.937e-03   201102082159   1.823e-03    1.096e-01    74        8.109e+00              7.11
30.4nm    201102090117   1.812e-03  201102090129   1.961e-03   201102090220   1.813e-03    1.096e-01    63        6.902e+00              8.25
30.4nm    201102131715   1.898e-03  201102131734   2.170e-03   201102131825   1.955e-03    1.218e-01    70        8.523e+00             14.35
121.6nm   201102131716   6.906e-03  201102131736   7.219e-03   201102131828   6.942e-03    4.205e-01    71        2.985e+01              4.53
28.4nm    201102131725   2.560e-04  201102131741   2.897e-04   201102131843   2.621e-04    1.601e-02    78        1.249e+00             13.15
30.4nm    201102140224   1.889e-03  201102140243   1.946e-03   201102140319   1.895e-03    1.268e-01    54        6.846e+00              2.98
30.4nm    201102140643   1.894e-03  201102140655   2.040e-03   201102140736   1.902e-03    1.156e-01    53        6.125e+00              7.72
30.4nm    201102141234   1.903e-03  201102141251   2.054e-03   201102141336   1.904e-03   -1.000e+05    63       -1.000e+05              7.97
30.4nm    201102141706   1.920e-03  201102141725   2.381e-03   201102141801   1.979e-03    1.246e-01    55        6.855e+00             24.00
121.6nm   201102141714   6.955e-03  201102141726   7.378e-03   201102141803   7.010e-03    4.238e-01    48        2.034e+01              6.08
121.6nm   201102141856   6.956e-03  201102141929   7.184e-03   201102142011   6.951e-03    4.210e-01    74        3.116e+01              3.27
30.4nm    201102141852   1.925e-03  201102141929   2.162e-03   201102142015   1.927e-03    1.185e-01    82        9.713e+00             12.34
28.4nm    201102141356   2.548e-04  201102141727   2.917e-04   201102142049   2.647e-04    1.614e-02    412       6.650e+00             14.49
30.4nm    201102150024   1.924e-03  201102150037   2.047e-03   201102150131   1.934e-03    1.167e-01    67        7.817e+00              6.38
30.4nm    201102150116   1.926e-03  201102150158   2.414e-03   201102150305   1.992e-03    1.269e-01    108       1.371e+01             25.30
121.6nm   201102150125   6.957e-03  201102150158   7.671e-03   201102150310   7.059e-03    4.388e-01    104       4.563e+01             10.25
```

28.4nm	201102150136	2.605e-04	201102150201	3.327e-04	201102150314	2.816e-04	1.739e-02	98	1.704e+00	27.69
30.4nm	201102150300	1.984e-03	201102150311	2.042e-03	201102150323	1.967e-03	1.197e-01	23	2.752e+00	2.95
30.4nm	201102150426	1.925e-03	201102150434	2.111e-03	201102150512	1.931e-03	1.178e-01	46	5.420e+00	9.66
30.4nm	201102150844	1.935e-03	201102150902	2.011e-03	201102150910	1.921e-03	1.165e-01	26	3.029e+00	3.94
30.4nm	201102152008	1.936e-03	201102152035	2.003e-03	201102152107	1.931e-03	1.171e-01	58	6.792e+00	3.47
30.4nm	201102160125	1.913e-03	201102160136	1.981e-03	201102160159	1.927e-03	1.224e-01	35	4.285e+00	3.53
30.4nm	201102160532	1.912e-03	201102160544	1.975e-03	201102160611	1.914e-03	1.474e-01	39	5.749e+00	3.32
30.4nm	201102160715	1.897e-03	201102160741	1.963e-03	201102160840	1.911e-03	1.205e-01	85	1.024e+01	3.48
30.4nm	201102160840	1.911e-03	201102160910	2.027e-03	201102160950	1.929e-03	1.161e-01	69	8.012e+00	6.04
121.6nm	201102161345	6.888e-03	201102161424	7.168e-03	201102161449	6.888e-03	4.155e-01	63	2.618e+01	4.06
30.4nm	201102161419	1.915e-03	201102161424	2.223e-03	201102161455	1.902e-03	1.181e-01	36	4.251e+00	16.13
30.4nm	201102161519	1.891e-03	201102161530	1.985e-03	201102161819	1.916e-03	1.406e-01	180	2.530e+01	4.98
30.4nm	201102162030	1.909e-03	201102162111	1.981e-03	201102162139	1.917e-03	1.502e-01	68	1.021e+01	3.74
30.4nm	201102172047	1.883e-03	201102172140	1.952e-03	201102172235	1.913e-03	1.353e-01	108	1.461e+01	3.66
30.4nm	201102180429	1.898e-03	201102180453	1.991e-03	201102180532	1.917e-03	1.160e-01	63	7.310e+00	4.91
30.4nm	201102180601	1.912e-03	201102180633	1.972e-03	201102180713	1.948e-03	1.161e-01	72	8.358e+00	3.18
30.4nm	201102180705	1.930e-03	201102180721	2.059e-03	201102180800	1.958e-03	1.502e-01	56	8.412e+00	6.70
30.4nm	201102180856	1.949e-03	201102180909	2.030e-03	201102180946	1.947e-03	1.186e-01	50	5.931e+00	4.14
30.4nm	201102181000	1.945e-03	201102181026	2.134e-03	201102181121	1.987e-03	1.214e-01	81	9.835e+00	9.70
121.6nm	201102180955	6.966e-03	201102181027	7.190e-03	201102181111	7.014e-03	4.935e-01	77	3.800e+01	3.23
30.4nm	201102181113	1.970e-03	201102181125	2.047e-03	201102181134	1.966e-03	1.192e-01	21	2.504e+00	3.91
30.4nm	201102181347	1.942e-03	201102181407	2.086e-03	201102181428	1.960e-03	1.305e-01	41	5.349e+00	7.46
30.4nm	201102181634	1.941e-03	201102181646	2.003e-03	201102181708	1.941e-03	1.174e-01	34	3.992e+00	3.18
30.4nm	201102181736	1.920e-03	201102181906	2.028e-03	201102182035	1.916e-03	1.170e-01	179	2.094e+01	5.64
30.4nm	201102190431	1.899e-03	201102190451	1.967e-03	201102190504	1.905e-03	1.365e-01	32	4.369e+00	3.59
30.4nm	201102190752	1.895e-03	201102190806	1.971e-03	201102190841	1.898e-03	1.439e-01	50	7.194e+00	4.06
30.4nm	201102210950	1.786e-03	201102211016	1.850e-03	201102211101	1.784e-03	1.113e-01	70	7.793e+00	3.58
30.4nm	201102211837	1.774e-03	201102211858	1.854e-03	201102211945	1.785e-03	1.079e-01	67	7.227e+00	4.48
28.4nm	201102240728	2.318e-04	201102240740	2.610e-04	201102240816	2.379e-04	1.542e-02	48	7.403e-01	12.62
30.4nm	201102240706	1.709e-03	201102240740	1.807e-03	201102240929	1.728e-03	-1.000e+05	142	-1.000e+05	5.73
30.4nm	201102281228	1.774e-03	201102281249	1.957e-03	201102281333	1.803e-03	-1.000e+05	65	-1.000e+05	10.33
30.4nm	201103031406	1.919e-03	201103031418	2.002e-03	201103031502	1.938e-03	-1.000e+05	56	-1.000e+05	4.38
30.4nm	201103032016	1.928e-03	201103032048	1.982e-03	201103032138	1.937e-03	-1.000e+05	83	-1.000e+05	2.80
30.4nm	201103050059	1.958e-03	201103050111	2.031e-03	201103050136	1.951e-03	1.183e-01	37	4.376e+00	3.74
30.4nm	201103050213	1.949e-03	201103050245	2.009e-03	201103050408	1.977e-03	1.185e-01	114	1.351e+01	3.07
30.4nm	201103051222	1.962e-03	201103051340	2.044e-03	201103051603	1.998e-03	-1.000e+05	221	-1.000e+05	4.20
30.4nm	201103060155	2.006e-03	201103060207	2.068e-03	201103060241	2.016e-03	1.211e-01	46	5.570e+00	3.09
30.4nm	201103060513	1.999e-03	201103060532	2.066e-03	201103060701	2.003e-03	1.234e-01	108	1.333e+01	3.35
30.4nm	201103060715	2.007e-03	201103060733	2.067e-03	201103060753	2.004e-03	1.210e-01	37	4.476e+00	2.97
30.4nm	201103061016	2.005e-03	201103061036	2.102e-03	201103061053	2.022e-03	1.216e-01	37	4.499e+00	4.85
30.4nm	201103061425	2.042e-03	201103061443	2.171e-03	201103061446	2.067e-03	1.236e-01	21	2.595e+00	6.32
30.4nm	201103061513	2.022e-03	201103061524	2.095e-03	201103061544	2.038e-03	1.263e-01	32	4.041e+00	3.60
30.4nm	201103061551	2.030e-03	201103061629	2.134e-03	201103061705	2.039e-03	1.236e-01	74	9.144e+00	5.14
30.4nm	201103061730	2.026e-03	201103061802	2.082e-03	201103061831	2.024e-03	1.224e-01	60	7.344e+00	2.76
30.4nm	201103070454	2.047e-03	201103070506	2.180e-03	201103070540	2.036e-03	1.250e-01	46	5.752e+00	6.48
121.6nm	201103070745	7.237e-03	201103070804	7.513e-03	201103070829	7.286e-03	4.388e-01	44	1.931e+01	3.81
30.4nm	201103070741	2.036e-03	201103070804	2.438e-03	201103070846	2.090e-03	1.267e-01	65	8.233e+00	19.72
30.4nm	201103070907	2.048e-03	201103070919	2.470e-03	201103070949	2.124e-03	1.341e-01	43	5.768e+00	20.58
121.6nm	201103070908	7.263e-03	201103070919	7.544e-03	201103070952	7.319e-03	4.407e-01	43	1.895e+01	3.87
30.4nm	201103071008	2.065e-03	201103071020	2.155e-03	201103071033	2.060e-03	1.249e-01	25	3.122e+00	4.32
30.4nm	201103071334	2.051e-03	201103071419	2.283e-03	201103071538	2.100e-03	1.297e-01	123	1.596e+01	11.27
121.6nm	201103071339	7.275e-03	201103071423	7.579e-03	201103071608	7.321e-03	4.450e-01	148	6.586e+01	4.19
30.4nm	201103071740	2.056e-03	201103071820	2.169e-03	201103071838	2.087e-03	1.251e-01	57	7.129e+00	5.51
30.4nm	201103071925	2.070e-03	201103071955	2.500e-03	201103072035	2.176e-03	1.409e-01	69	9.725e+00	20.79
121.6nm	201103071924	7.272e-03	201103071955	7.628e-03	201103072129	7.348e-03	4.456e-01	124	5.525e+01	4.90
28.4nm	201103071938	4.001e-04	201103072057	4.549e-04	201103072150	4.158e-04	2.536e-02	131	3.323e+00	13.70
30.4nm	201103072136	2.111e-03	201103072148	2.272e-03	201103072213	2.121e-03	1.425e-01	37	5.272e+00	7.63
30.4nm	201103080216	2.068e-03	201103080229	2.279e-03	201103080242	2.062e-03	-1.000e+05	26	-1.000e+05	10.17
28.4nm	201103080344	3.903e-04	201103080419	4.294e-04	201103080525	4.011e-04	-1.000e+05	100	-1.000e+05	10.02
30.4nm	201103080547	2.056e-03	201103080606	2.166e-03	201103080626	2.063e-03	-1.000e+05	38	-1.000e+05	5.32
30.4nm	201103081028	2.053e-03	201103081041	2.204e-03	201103081149	2.087e-03	-1.000e+05	81	-1.000e+05	7.33
30.4nm	201103081754	2.018e-03	201103081814	2.115e-03	201103081830	2.041e-03	-1.000e+05	35	-1.000e+05	4.81
30.4nm	201103081829	2.041e-03	201103081905	2.141e-03	201103082005	2.054e-03	-1.000e+05	96	-1.000e+05	4.90
30.4nm	201103082201	2.070e-03	201103082220	2.138e-03	201103082238	2.068e-03	1.253e-01	36	4.511e+00	3.27
30.4nm	201103082254	2.051e-03	201103082336	2.122e-03	201103082335	2.105e-03	1.302e-01	41	5.340e+00	3.44
30.4nm	201103091026	2.023e-03	201103091038	2.140e-03	201103091107	2.022e-03	1.227e-01	41	5.030e+00	5.77
30.4nm	201103091347	2.026e-03	201103091359	2.127e-03	201103091441	2.038e-03	1.234e-01	53	6.541e+00	5.00
30.4nm	201103092041	2.006e-03	201103092108	2.090e-03	201103092135	2.029e-03	1.267e-01	54	6.841e+00	4.15
30.4nm	201103092133	2.027e-03	201103092211	2.237e-03	201103092243	2.022e-03	1.244e-01	69	8.585e+00	10.36
28.4nm	201103092315	4.100e-04	201103092330	4.698e-04	201103092357	4.309e-04	2.629e-02	42	1.104e+00	14.59
121.6nm	201103092302	7.250e-03	201103092322	8.019e-03	201103100030	7.234e-03	-1.000e+05	87	-1.000e+05	10.61
30.4nm	201103092307	1.994e-03	201103092321	2.648e-03	201103100053	1.992e-03	-1.000e+05	106	-1.000e+05	32.77
30.4nm	201103100633	2.006e-03	201103100644	2.070e-03	201103100704	2.021e-03	1.337e-01	31	4.144e+00	3.20
30.4nm	201103110522	1.996e-03	201103110602	2.068e-03	201103110624	2.004e-03	1.205e-01	61	7.348e+00	3.62
30.4nm	201103111135	2.000e-03	201103111147	2.085e-03	201103111204	1.992e-03	1.209e-01	29	3.507e+00	4.24
30.4nm	201103120418	1.956e-03	201103120437	2.151e-03	201103120516	1.982e-03	1.267e-01	57	7.220e+00	9.97
30.4nm	201103120828	1.968e-03	201103120907	2.023e-03	201103121000	1.974e-03	1.214e-01	91	1.105e+01	2.77
30.4nm	201103120953	1.970e-03	201103121026	2.048e-03	201103121136	1.995e-03	-1.000e+05	102	-1.000e+05	3.98
30.4nm	201103121246	1.974e-03	201103121257	2.045e-03	201103121317	1.978e-03	1.492e-01	31	4.627e+00	3.64
30.4nm	201103121444	1.962e-03	201103121524	2.151e-03	201103121558	1.986e-03	1.230e-01	73	8.979e+00	9.65
30.4nm	201103122211	1.961e-03	201103122222	2.025e-03	201103122234	1.963e-03	1.387e-01	23	3.191e+00	3.26
30.4nm	201103122235	1.968e-03	201103122249	2.044e-03	201103122333	1.978e-03	1.195e-01	58	6.929e+00	3.84
30.4nm	201103141550	1.888e-03	201103141609	1.950e-03	201103141636	1.893e-03	-1.000e+05	46	-1.000e+05	3.30
30.4nm	201103141926	1.894e-03	201103141951	2.108e-03	201103142016	1.930e-03	-1.000e+05	49	-1.000e+05	11.32
30.4nm	201103142315	1.884e-03	201103142338	2.031e-03	201103142359	1.882e-03	-1.000e+05	44	-1.000e+05	7.79
30.4nm	201103150018	1.879e-03	201103150023	1.951e-03	201103150040	1.873e-03	1.136e-01	22	2.499e+00	3.80
30.4nm	201103151721	1.855e-03	201103151733	1.950e-03	201103151805	1.848e-03	1.124e-01	44	4.947e+00	5.09
30.4nm	201103230201	1.802e-03	201103230214	1.910e-03	201103230252	1.808e-03	1.161e-01	51	5.922e+00	5.97
30.4nm	201103241526	1.858e-03	201103241545	1.911e-03	201103241603	1.878e-03	1.520e-01	37	5.625e+00	2.82
121.6nm	201103241640	6.936e-03	201103241706	7.157e-03	201103241735	6.930e-03	4.190e-01	55	2.305e+01	3.19
30.4nm	201103241624	1.864e-03	201103241706	2.075e-03	201103241736	1.854e-03	1.137e-01	72	8.183e+00	11.32
30.4nm	201103241736	1.856e-03	201103241808	1.953e-03	201103241824	1.892e-03	1.184e-01	47	5.563e+00	5.27
30.4nm	201103241846	1.879e-03	201103241909	1.965e-03	201103241920	1.881e-03	1.277e-01	34	4.340e+00	4.55
30.4nm	201103242043	1.874e-03	201103242057	2.076e-03	201103242137	1.881e-03	1.208e-01	54	6.521e+00	10.75
121.6nm	201103242046	6.967e-03	201103242057	7.164e-03	201103242202	6.982e-03	4.416e-01	77	3.401e+01	2.83
30.4nm	201103250007	1.861e-03	201103250040	1.944e-03	201103250123	1.873e-03	1.129e-01	75	8.468e+00	4.43
30.4nm	201103252302	1.922e-03	201103252314	2.087e-03	201103252359	1.927e-03	1.236e-01	58	7.170e+00	8.62
30.4nm	201103262351	1.982e-03	201103270011	2.218e-03	201103270104	2.015e-03	1.220e-01	73	8.906e+00	11.90
121.6nm	201103262352	7.261e-03	201103270012	7.540e-03	201103270110	7.306e-03	-1.000e+05	77	-1.000e+05	3.85

30.4nm	201103290005	2.054e-03	201103290030	2.122e-03	201103290050	2.062e-03	1.402e-01	45	6.309e+00	3.32
30.4nm	201104010131	2.067e-03	201104010150	2.160e-03	201104010247	2.080e-03	1.254e-01	75	9.403e+00	4.50
30.4nm	201104010323	2.063e-03	201104010356	2.133e-03	201104010446	2.066e-03	1.309e-01	82	1.073e+01	3.36
121.6nm	201104060549	7.447e-03	201104060747	7.769e-03	201104061216	7.456e-03	4.583e-01	388	1.778e+02	4.32
30.4nm	201104112021	1.973e-03	201104112033	2.036e-03	201104112053	1.968e-03	1.192e-01	32	3.816e+00	3.21
30.4nm	201104141950	1.967e-03	201104142008	2.041e-03	201104142011	1.982e-03	1.188e-01	21	2.495e+00	3.76
30.4nm	201104151339	1.963e-03	201104151350	2.016e-03	201104151409	1.959e-03	1.182e-01	30	3.547e+00	2.71
30.4nm	201104151658	1.966e-03	201104151737	2.044e-03	201104151838	1.976e-03	1.193e-01	100	1.193e+01	3.96
30.4nm	201104180227	1.926e-03	201104180239	2.026e-03	201104180307	1.938e-03	1.713e-01	40	6.854e+00	5.23
30.4nm	201104201922	1.931e-03	201104201940	1.984e-03	201104202130	1.942e-03	1.191e-01	127	1.513e+01	2.75
30.4nm	201104210916	1.926e-03	201104210943	2.030e-03	201104211023	1.958e-03	1.298e-01	67	8.694e+00	5.39
30.4nm	201104220421	1.969e-03	201104220500	2.086e-03	201104220655	1.995e-03	1.244e-01	154	1.916e+01	5.94
121.6nm	201104220425	7.228e-03	201104220504	7.433e-03	201104220930	7.262e-03	4.392e-01	304	1.335e+02	2.84
30.4nm	201104220932	1.982e-03	201104220953	2.047e-03	201104221023	1.995e-03	1.203e-01	50	6.013e+00	3.29
30.4nm	201104221051	1.983e-03	201104221126	2.073e-03	201104221207	1.996e-03	-1.000e+05	76	-1.000e+05	4.54
30.4nm	201104221224	1.976e-03	201104221235	2.041e-03	201104221252	1.977e-03	1.273e-01	29	3.691e+00	3.30
30.4nm	201104221532	1.978e-03	201104221551	2.147e-03	201104221635	2.024e-03	1.220e-01	62	7.567e+00	8.55
30.4nm	201104221647	2.004e-03	201104221706	2.080e-03	201104221730	1.999e-03	1.214e-01	43	5.222e+00	3.79
30.4nm	201104270217	2.054e-03	201104270232	2.140e-03	201104270329	2.069e-03	1.251e-01	72	9.005e+00	4.17
30.4nm	201104292025	2.042e-03	201104292044	2.168e-03	201104292129	2.067e-03	-1.000e+05	65	-1.000e+05	6.17
30.4nm	201104292241	2.049e-03	201104292253	2.116e-03	201104292335	2.047e-03	1.238e-01	54	6.686e+00	3.29
30.4nm	201105010944	2.012e-03	201105010958	2.080e-03	201105011057	2.021e-03	1.219e-01	72	8.776e+00	3.36
28.4nm	201105030723	2.986e-04	201105040228	4.310e-04	201105040724	4.171e-04	-1.000e+05	1441	-1.000e+05	44.37
30.4nm	201105030728	1.343e-03	201105040148	2.082e-03	201105040707	2.035e-03	-1.000e+05	1441	-1.000e+05	55.01
121.6nm	201105030728	6.323e-03	201105030744	7.486e-03	201105040723	7.368e-03	-1.000e+05	1441	-1.000e+05	18.40
30.4nm	201105110156	1.968e-03	201105110228	2.023e-03	201105110418	1.982e-03	1.214e-01	141	1.712e+01	2.78
30.4nm	201105121148	1.913e-03	201105121229	2.152e-03	201105121340	1.932e-03	1.179e-01	111	1.308e+01	12.47
121.6nm	201105121155	7.038e-03	201105121228	7.256e-03	201105121329	7.072e-03	4.701e-01	94	4.419e+01	3.09
30.4nm	201105151709	1.873e-03	201105151742	1.940e-03	201105151854	1.872e-03	1.134e-01	105	1.191e+01	3.56
30.4nm	201105152325	1.870e-03	201105152331	1.970e-03	201105152356	1.856e-03	1.138e-01	31	3.529e+00	5.37
30.4nm	201105252042	1.830e-03	201105252102	1.898e-03	201105252152	1.835e-03	1.105e-01	70	7.738e+00	3.74
30.4nm	201105260044	1.840e-03	201105260109	1.898e-03	201105260153	1.849e-03	1.127e-01	68	7.664e+00	3.12
30.4nm	201105281001	1.890e-03	201105281028	1.952e-03	201105281109	1.913e-03	1.147e-01	67	7.686e+00	3.25
30.4nm	201105291002	1.935e-03	201105291138	2.040e-03	201105291235	1.958e-03	1.190e-01	152	1.809e+01	5.44
30.4nm	201105300558	1.976e-03	201105300602	2.045e-03	201105300639	1.976e-03	1.191e-01	41	4.884e+00	3.47
28.4nm	201105291007	3.496e-04	201105300802	3.926e-04	201105300936	3.854e-04	-1.000e+05	1441	-1.000e+05	12.30
30.4nm	201105310427	1.971e-03	201105310440	2.051e-03	201105310514	1.982e-03	1.220e-01	48	5.857e+00	4.06
30.4nm	201106010227	1.982e-03	201106010241	2.078e-03	201106010419	1.993e-03	1.229e-01	113	1.389e+01	4.86
30.4nm	201106010917	2.005e-03	201106010931	2.090e-03	201106011042	2.002e-03	1.217e-01	84	1.022e+01	4.25
30.4nm	201106011540	2.033e-03	201106011654	2.123e-03	201106011804	2.057e-03	1.245e-01	143	1.780e+01	4.47
30.4nm	201106020706	2.069e-03	201106020743	2.220e-03	201106020850	2.084e-03	-1.000e+05	105	-1.000e+05	7.29
121.6nm	201106070606	7.172e-03	201106070628	7.576e-03	201106070704	7.166e-03	4.385e-01	58	2.543e+01	5.64
30.4nm	201106070602	1.990e-03	201106070628	2.414e-03	201106070723	2.017e-03	1.329e-01	80	1.063e+01	21.27
28.4nm	201106070608	3.297e-04	201106070657	3.833e-04	201106072121	3.440e-04	-1.000e+05	912	-1.000e+05	16.26
30.4nm	201106142130	1.830e-03	201106142145	1.967e-03	201106142243	1.844e-03	1.125e-01	73	8.211e+00	7.48
30.4nm	201106161007	1.871e-03	201106161020	2.012e-03	201106161042	1.906e-03	1.152e-01	35	4.030e+00	7.54
30.4nm	201106190151	1.908e-03	201106190240	1.975e-03	201106190356	1.915e-03	1.157e-01	125	1.447e+01	3.51
30.4nm	201106210124	1.952e-03	201106210311	2.054e-03	201106210532	1.969e-03	1.202e-01	248	2.981e+01	5.25
28.4nm	201106210209	3.282e-04	201106210446	3.709e-04	201106210657	3.417e-04	2.083e-02	288	6.000e+00	13.01
30.4nm	201107031030	1.842e-03	201107031102	1.894e-03	201107031157	1.849e-03	1.138e-01	86	9.787e+00	2.81
30.4nm	201107081110	1.832e-03	201107081149	1.889e-03	201107081241	1.847e-03	1.110e-01	90	9.992e+00	3.09
30.4nm	201107081306	1.844e-03	201107081331	1.904e-03	201107081401	1.839e-03	1.113e-01	54	6.009e+00	3.24
30.4nm	201107081449	1.837e-03	201107081501	1.908e-03	201107081530	1.832e-03	1.112e-01	41	4.558e+00	3.88
30.4nm	201107111011	1.838e-03	201107111100	1.934e-03	201107111208	1.853e-03	1.125e-01	116	1.305e+01	5.27
30.4nm	201107270532	1.853e-03	201107270603	1.913e-03	201107270632	1.878e-03	1.183e-01	59	6.977e+00	3.24
30.4nm	201107270627	1.874e-03	201107270652	1.936e-03	201107270739	1.878e-03	1.169e-01	73	8.531e+00	3.34
30.4nm	201107271514	1.854e-03	201107271606	1.931e-03	201107271810	1.879e-03	1.142e-01	176	2.011e+01	4.13
30.4nm	201107281156	1.893e-03	201107281208	1.960e-03	201107281324	1.901e-03	1.151e-01	88	1.013e+01	3.54
30.4nm	201107281438	1.915e-03	201107281517	1.989e-03	201107281551	1.939e-03	1.196e-01	73	8.730e+00	3.85
30.4nm	201107281630	1.918e-03	201107281648	1.975e-03	201107281704	1.924e-03	1.646e-01	35	5.760e+00	3.00
30.4nm	201107281740	1.908e-03	201107281819	1.966e-03	201107281856	1.921e-03	1.153e-01	75	8.651e+00	3.06
30.4nm	201107290024	1.913e-03	201107290036	2.016e-03	201107290056	1.930e-03	1.165e-01	32	3.728e+00	5.36
30.4nm	201107290409	1.917e-03	201107290435	1.986e-03	201107290459	1.919e-03	1.251e-01	49	6.132e+00	3.63
30.4nm	201107290547	1.917e-03	201107290605	1.970e-03	201107290619	1.938e-03	1.157e-01	31	3.586e+00	2.73
30.4nm	201107291211	1.928e-03	201107291215	1.983e-03	201107291237	1.927e-03	1.163e-01	26	3.023e+00	2.84
30.4nm	201107291627	1.913e-03	201107291639	1.998e-03	201107291728	1.922e-03	-1.000e+05	62	-1.000e+05	4.48
28.4nm	201107300157	2.688e-04	201107300210	3.196e-04	201107300230	2.747e-04	1.780e-02	34	6.051e-01	18.89
30.4nm	201107300203	1.904e-03	201107300208	2.291e-03	201107300233	1.934e-03	1.198e-01	29	3.474e+00	20.29
121.6nm	201107300204	6.955e-03	201107300210	7.322e-03	201107300310	6.991e-03	4.218e-01	66	2.784e+01	5.28
30.4nm	201107311839	1.956e-03	201107311850	2.010e-03	201107311903	1.963e-03	1.368e-01	25	3.421e+00	2.74
30.4nm	201107312026	1.973e-03	201107312046	2.071e-03	201107312133	1.963e-03	1.201e-01	66	7.929e+00	4.94
30.4nm	201108010027	1.981e-03	201108010045	2.036e-03	201108010138	1.975e-03	1.202e-01	71	8.531e+00	2.80
30.4nm	201108010716	1.981e-03	201108010731	2.068e-03	201108010742	1.996e-03	1.483e-01	26	3.857e+00	4.36
30.4nm	201108020252	1.956e-03	201108020317	2.019e-03	201108020346	1.960e-03	1.502e-01	54	8.111e+00	3.25
30.4nm	201108020513	1.965e-03	201108020618	2.095e-03	201108020707	2.003e-03	1.648e-01	115	1.895e+01	6.64
121.6nm	201108020517	7.111e-03	201108020620	7.308e-03	201108020759	7.127e-03	4.553e-01	162	7.376e+01	2.77
30.4nm	201108021127	1.942e-03	201108021138	2.006e-03	201108021203	1.935e-03	1.173e-01	36	4.223e+00	3.28
30.4nm	201108030246	1.928e-03	201108030431	2.276e-03	201108030426	1.936e-03	1.243e-01	100	1.243e+01	18.02
30.4nm	201108030423	1.938e-03	201108030434	2.141e-03	201108030522	1.941e-03	1.229e-01	60	7.374e+00	10.48
121.6nm	201108030427	7.044e-03	201108030432	7.347e-03	201108030549	7.069e-03	4.259e-01	81	3.449e+01	4.29
28.4nm	201108031252	3.002e-04	201108031350	3.445e-04	201108031458	3.123e-04	1.931e-02	127	2.453e+00	14.78
30.4nm	201108031314	1.935e-03	201108031350	2.093e-03	201108031501	1.972e-03	1.272e-01	107	1.361e+01	8.20
121.6nm	201108031311	7.026e-03	201108031348	7.256e-03	201108031507	7.107e-03	4.274e-01	115	4.915e+01	3.29
30.4nm	201108040211	1.914e-03	201108040222	1.977e-03	201108040253	1.931e-03	1.158e-01	42	4.863e+00	3.29
30.4nm	201108040327	1.918e-03	201108040354	2.389e-03	201108040446	1.901e-03	1.229e-01	79	9.705e+00	24.57
121.6nm	201108040332	6.962e-03	201108040354	7.476e-03	201108040448	6.934e-03	4.271e-01	75	3.203e+01	7.38
28.4nm	201108040335	3.022e-04	201108040401	3.754e-04	201108040536	3.104e-04	2.279e-02	120	2.735e+00	24.24
30.4nm	201108040958	1.917e-03	201108041011	2.005e-03	201108041045	1.910e-03	1.160e-01	47	5.451e+00	4.59
30.4nm	201108042103	1.914e-03	201108042115	1.983e-03	201108042137	1.925e-03	1.259e-01	34	4.282e+00	3.61
30.4nm	201108081759	1.898e-03	201108081804	1.992e-03	201108081852	1.913e-03	1.677e-01	53	8.888e+00	4.99
28.4nm	201108090752	3.188e-04	201108090807	4.477e-04	201108090905	3.270e-04	2.042e-02	73	1.490e+00	40.43
30.4nm	201108090750	1.894e-03	201108090806	2.277e-03	201108090911	1.911e-03	1.181e-01	81	9.566e+00	20.22
121.6nm	201108090744	6.993e-03	201108090805	7.972e-03	201108090858	7.007e-03	5.478e-01	75	4.109e+01	14.00
30.4nm	201108092321	1.879e-03	201108092339	1.941e-03	201108100030	1.879e-03	1.139e-01	69	7.861e+00	3.34
30.4nm	201108101322	1.866e-03	201108101333	1.928e-03	201108101403	1.874e-03	1.179e-01	42	4.951e+00	3.35

APPENDIX E

Class Methods

In this section, all non-inline class methods are listed. Inline getters, setters and incrementors are excluded.

EuvEventAlgorithm class

```
EuvEventAlgorithm(string inputFile, string configFile)
~EuvEventAlgorithm()
void run()
void setDay(double julianDate)
string getPostEventOutputHeader()
vector<double> getData()
void newDayCheck(double dataTime)
void dataTimeConsistencyCheck(double dataTime)
void handleDataTimeRegression(double currentDataTime)
void handleNonFatalDataTimeInconsistency(double currentDataTime, double timeDiff)
void handleFatalDataTimeInconsistency(double currentDataTime, double timeDiff)
```

SpectralLine class

```
SpectralLine(spectral_line spectralLineId, Config* config, Logger* logger, ofstream*
      eventSummaryFile)
~SpectralLine()
void processNewData()
void setCurrentIrradiance()
void setCurrentTime()
void setSpectralLineName()
void updateIrradianceAndTimeDeques()
void updateDataMetricDeques()
void updateFiveMinuteMean()
void updateFiveMinuteSlope()
void updateTenMinuteSlope()
void updateTenMinuteStandardDeviation()
void updateThirtyMinuteStandardDeviation()
void updateMonotonicRank()
void updateMonotonicRankof5minMean()
void updateTenMinuteMaximumRelativeIncrease()
void updateSixtyMinute10thPercentile()
void updateConsecutiveValidDataCount()
void updateConsecutiveInvalidDataCount()
void updateThirtyMinuteInvalidDataCount()
void updateSixtyMinuteInvalidDataCount()
void updateImpairedStatus()
void handleImpairedStatus()
void checkEventInitiation()
void checkEventPeak()
void checkEventHalfMaximum()
void checkEventQuarterMaximum()
void checkEventTermination()
void terminateEvent()
void incrementDay(string yyyydoy)
void outputOneMinuteUpdate()
void setMonotonicRank()
string getOneMinuteOutputHeader()
string getOneMinuteUpdateOutput()
string getOneMinuteOutputFileName()
bool falseAlarmSuppression(double currentIrradiance, double startIrradiance)
pair<double, double> findEventStart(const deque<double>& data, const deque<double>& times,
int startupLookBackWindow, int invalidDataLimit)
bool checkStartupTimeConsistency()
```

Event class

```
Event(Config* config, Logger* logger, ofstream* eventSummaryFile, deque<double>&
      irradiance, deque<double>& times, deque<int>& monotonicRank)
~Event()
void setCurrentTime()
void initDuration()
void adjustDuration()
void initIntegratedEnergy()
void adjustIntegratedEnergy()
void updateMaxIrradiance()
void updateLastIrradianceDecline()
void updateIntegratedEnergy()
void updateIrradianceTrend()
void updateStatus()
void setStartDetectionLagTime()
void addPeakDetectionLagTime()
void outputPostEventSummary()
void setMeanIrradiance()
string getPostEventSummaryOutput()
```

AlgorithmUtilities “library”

```
string getYYYYDOYFromYYYYMMDD(string yyyymmdd)
string getYYYYMMDDFromYYYYDOY(string yyyydoy)
string getNextYYYYDOY(string currentYyyydoy)
string getYYYYMMDDFromJulianDate(double julianDate)
string getHHMMFromJulianDate(double julianDate)
string getYYYYDOYFromJulianDate(double julianDate)
string getYYYYMMDDFromYearMonthDayInts(int year, int month, int day)
string getHHMMFromHourMinuteInts(int hour, int minute)
string double2Str(double value, string format, int precision)
string int2Str(int value)
int    string2Int(string str)
string padStr(string inputStr, string padChar, int nbrPads)
int    getMonotonicRank(double newValue, double lastValue, int currentMonotonicRank)
double getMinimum(vector<double>& data)
double getMaximumRelativeIncrease(vector<double>& data)
double getMean(vector<double>& data)
double getStdDev(vector<double>& data)
double getMedian(vector<double>& data)
double getSlope(vector<double>& data, vector<double>& times)
double getNthPercentile(vector<double>& data, double percentile)
double getMidPointValue(vector<double>& data)
bool   isOdd(int nbr)
bool   isValid(double value)
vector<double> getValidData(vector<double>& data)
vector<double> getValidTimes(vector<double>& data, vector<double>& times)
vector<double> getVecFromDeque(const deque<double>& data, int indexStart, int indexEnd,
      Logger* logger)
pair<double, int> getMinimumWithBadDataCount(const deque<double>& data, int indexStart, int
      indexEnd, Logger* logger)
pair<double, int> getMaximumRelativeIncreaseWithBadDataCount(const deque<double>& data, int
      indexStart, int indexEnd, Logger* logger)
pair<double, int> getMeanWithBadDataCount(const deque<double>& data, int indexStart, int
      indexEnd, Logger* logger)
pair<double, int> getStdDevWithBadDataCount(const deque<double>& data, int indexStart, int
      indexEnd, Logger* logger)
pair<double, int> getMedianWithBadDataCount(const deque<double>& data, int indexStart, int
      indexEnd, Logger* logger)
pair<double, int> getSlopeWithBadDataCount(const deque<double>& data, const deque<double>&
      times, int indexStart, int indexEnd, Logger* logger)
pair<double, int> getNthPercentileWithBadDataCount(const deque<double>& data, double
      percentile, int indexStart, int indexEnd, Logger* logger)
pair<double, double> getMinimumWithTime(const deque<double>& data, const deque<double>&
      times, int indexStart, int indexEnd, Logger* logger)
pair<double, double> getMedianWithTime(const deque<double>& data, const deque<double>&
      times, int indexStart, int indexEnd, Logger* logger)
```

Config class

```
Config(string inputFile, string delimiterSym="=", string commentSym="#")
istream& operator>>(istream& is, Config& cfg)
int            getIntFromKey(const string& key)
double         getDblFromKey(const string& key)
bool           getBoolFromKey(const string& key)
string         getStrFromKey(const string& key)
vector<int>    getIntArrayFromKey(const string& key)
vector<double> getDblArrayFromKey(const string& key)
static void trim(string& str)
```

Logger class

```
Logger(string logFileWithPathStr, bool isTest = false)
~Logger()
void writeErrorMsg(string msgStr)
void writeWarningMsg(string msgStr)
void writeDiagnosticMsg(string msgStr)
void concludeMsg()
void handleError(string errorStr)
bool doesLogFileExist()
ofstream& getLogOutputFile()
```